

Correlated interaction effects in the three-dimensional semi-Dirac semimetal

Jing-Rong Wang,¹ Wei Li^{2,*} and Chang-Jin Zhang^{1,3,†}

¹High Magnetic Field Laboratory of Anhui Province, HFIPS, Chinese Academy of Sciences, Hefei 230031, China

²Key Laboratory of Materials Physics, Institute of Solid State Physics, HFIPS, Chinese Academy of Sciences, Hefei 230031, China

³Institute of Physical Science and Information Technology, Anhui University, Hefei 230601, China



(Received 1 May 2022; revised 29 March 2023; accepted 30 March 2023; published 13 April 2023)

Understanding the correlation effects in unconventional topological materials, in which the fermion excitations take unusual dispersion, is an important topic in recent condensed matter physics. We study the influence of short-range four-fermion interactions on three-dimensional semi-Dirac semimetal with an unusual fermion dispersion that is linear along two directions and quadratic along the third one. Based on renormalization group theory, we find all of 11 unstable fixed points including five quantum critical points, five bicritical points, and one tricritical point. The physical essences of the quantum critical points are determined by analyzing the susceptibility exponents for all of the source terms in particle-hole and particle-particle channels. We also verify phase diagrams of the system in the parameter space through numerically studying the flows of the four-fermion coupling parameters and behaviors of the susceptibility exponents. These results are helpful for us to understand the physical properties of candidate materials for three-dimensional semi-Dirac semimetal such as ZrTe₅.

DOI: [10.1103/PhysRevB.107.155125](https://doi.org/10.1103/PhysRevB.107.155125)

I. INTRODUCTION

In the past 15 years study about topological materials has become one of the most important fields in condensed matter physics [1–10]. Topological materials have wide potential implications as electronic devices due to their fascinating physical properties. In some topological materials, such as Dirac semimetal (DSM) including Cd₃As₂ and Na₃Bi and Weyl semimetal (WSM) including TaAs, TaP, NbAs, and NbP, the low-energy fermion excitations are Dirac fermions or Weyl fermions, which resemble the elementary particles in high energy physics. Thus these materials provide a platform to verify some important concepts in high energy physics.

Besides Dirac and Weyl fermions, there could be unconventional fermions with unusual dispersion in topological materials. In double (triple) WSM, the fermion dispersion is quadratic (cubic) along two directions and linear along the third one [11,12]. Semi-DSM emerges at the topological quantum critical point (QCP) between DSM and band insulator [13,14]. For two dimensional (2D) semi-DSM, the dispersion of fermion excitations is linear along one direction and quadratic along another one. For three dimensional (3D) semi-DSM, the fermion dispersion is linear along two directions and quadratic along the third one as shown in Fig. 1. Higher spin fermions with multiband crossing have also attracted a lot of interest recently [15–17]. Spin-1 chiral fermions characterized by a combination of a Dirac-like band and a flat band with three-bands crossing and spin-3/2 chiral fermions displaying a birefringent spectrum with two distinct fermion velocities have been observed recently [18–22].

The correlation effects in Dirac and Weyl fermion systems are extensively studied and are well understood relatively [23–34]. The influence of many-body interaction on unconventional fermion systems also attracted much interest and is an important topic. There have been studies about influence of long-range Coulomb interaction [35–51], short-range four-fermion interaction [52–57], and quantum fluctuation of order parameter [58–61] on some unconventional fermion systems. These studies revealed many novel behaviors, such as various quantum phase transitions, non-Fermi liquid behaviors, anisotropic screening effect, etc. These studies also showed that the correlation effects in unconventional fermion systems depend on the fermion dispersion subtly. For 2D semi-DSM, Isobe *et al.* showed that long-range Coulomb interaction results in non-Fermi liquid behaviors in a wide intermediate energy range and marginal Fermi liquid behaviors in the lowest energy regime [39]. However, for 3D semi-DSM, it was revealed that long-range Coulomb becomes irrelevant in the lowest energy regime and the system exhibits Fermi liquid behaviors [37,38].

There are still some important open questions about the correlation effects in unconventional fermion systems. An insightful study about the influence of short-range four-fermion interactions on 2D semi-DSM was performed by Roy and Foster [54]. However, the effects of short-range four-fermion interactions in 3D semi-DSM is an urgent question, which is yet to be resolved. In this article, we provide a comprehensive study for this question through renormalization group (RG) theory.

II. MODEL

The free action for 3D semi-DSM can be written as

$$S_0 = \int \frac{d\omega}{2\pi} \frac{d^3\mathbf{k}}{(2\pi)^3} \bar{\Psi}(\omega, \mathbf{k}) \gamma_0 [i\omega + \mathcal{H}(\mathbf{k})] \Psi(\omega, \mathbf{k}), \quad (1)$$

*Corresponding author: wliustc@theory.issp.ac.cn

†Corresponding author: zhangcj@hmfll.ac.cn

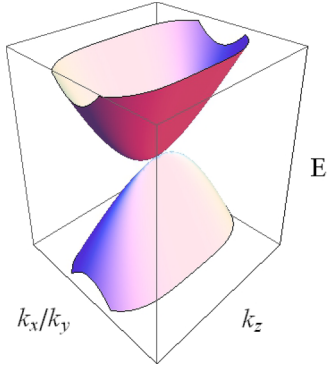


FIG. 1. Energy dispersion of fermions in 3D semi-DSM.

where the Hamiltonian density $\mathcal{H}(\mathbf{k})$ is given by

$$\mathcal{H}(\mathbf{k}) = \gamma_0(iv\gamma_1k_1 + ivk_2\gamma_2 + iAk_3^2\gamma_3), \quad (2)$$

with v and A being model parameters. Ψ is a four component spinor and $\bar{\Psi} = \Psi^\dagger\gamma_0$. The gamma matrices are defined as $\gamma_0 = \tau_3 \otimes \sigma_0$, $\gamma_1 = \tau_2 \otimes \sigma_1$, $\gamma_2 = \tau_2 \otimes \sigma_2$, $\gamma_3 = \tau_2 \otimes \sigma_3$, and $\gamma_5 = \tau_1 \otimes \sigma_0$, where $\tau_{1,2,3}$ and $\sigma_{1,2,3}$ are Pauli matrices. It is easy to verify that $\gamma_5 = \gamma_0\gamma_1\gamma_2\gamma_3$. The gamma matrices satisfy the anticommutation relation $\{\gamma_\mu, \gamma_\nu\} = 2\delta_{\mu\nu}$ for $\mu, \nu = 0, 1, 2, 3, 5$. The gamma matrices have the following properties:

$$\gamma_\mu^\dagger = \gamma_\mu, \quad (3)$$

$$\gamma_{0,2,5}^* = \gamma_{0,2,5}, \quad \gamma_{1,3}^* = -\gamma_{1,3}, \quad (4)$$

$$\gamma_{0,2,5}^T = \gamma_{0,2,5}, \quad \gamma_{1,3}^T = -\gamma_{1,3}. \quad (5)$$

The energy dispersion of fermions takes the form $E(\mathbf{k}) = \pm\sqrt{v^2k_\perp^2 + A^2k_3^4}$, where $k_\perp^2 = k_1^2 + k_2^2$. Density of states (DOS) is given by $\rho(\omega) \propto \omega^{3/2}/(v\sqrt{A})$, which vanishes at the Fermi level.

The fermion action S_0 is invariant under the discrete transformations including parity (\mathcal{P}), time reversal (\mathcal{T}), and charge conjugation (\mathcal{C}). Under parity transformation, the fermion spinor fields satisfy

$$\mathcal{P}\Psi_{\mathbf{k}}\mathcal{P}^{-1} = i\gamma_1\gamma_2\Psi_{-\mathbf{k}}, \quad (6)$$

$$\mathcal{P}\bar{\Psi}_{\mathbf{k}}\mathcal{P}^{-1} = -\bar{\Psi}_{-\mathbf{k}}i\gamma_2\gamma_1. \quad (7)$$

Utilizing time-reversal transformation, we have

$$\mathcal{T}\Psi_{\mathbf{k}}\mathcal{T}^{-1} = -i\gamma_1\gamma_5\Psi_{-\mathbf{k}}, \quad (8)$$

$$\mathcal{T}\bar{\Psi}_{\mathbf{k}}\mathcal{T}^{-1} = \bar{\Psi}_{-\mathbf{k}}i\gamma_5\gamma_1. \quad (9)$$

It should be noted that $\mathcal{T}i\mathcal{T}^{-1} = -i$. The realization of charge conjugation on spinor fields reads as

$$\mathcal{C}\Psi_{\mathbf{k}}\mathcal{C}^{-1} = -i\gamma_0\gamma_1\Psi_{\mathbf{k}}^* = -(\bar{\Psi}_{\mathbf{k}}i\gamma_1)^T, \quad (10)$$

$$\mathcal{C}\bar{\Psi}_{\mathbf{k}}\mathcal{C}^{-1} = -(i\gamma_1\Psi_{\mathbf{k}})^T. \quad (11)$$

The fermion action S_0 remains invariant under a continuous global $U(1)$ chiral rotation

$$\Psi_{\mathbf{k}} \rightarrow e^{i\theta\gamma_5}\Psi_{\mathbf{k}}, \quad (12)$$

$$\bar{\Psi}_{\mathbf{k}} \rightarrow \bar{\Psi}_{\mathbf{k}}e^{i\theta\gamma_5}. \quad (13)$$

The fermion action S_0 is also symmetric under a discrete Z_2 chiral transformation

$$\Psi_{\mathbf{k}} \rightarrow \gamma_5\Psi_{\mathbf{k}}, \quad (14)$$

$$\bar{\Psi}_{\mathbf{k}} \rightarrow -\bar{\Psi}_{\mathbf{k}}\gamma_5. \quad (15)$$

The $O(2)$ rotation about the z axis is generated by

$$R_z(\phi) = e^{\frac{i\phi\Gamma_{03}}{2}}, \quad (16)$$

where $\Gamma_{03} = \tau_0 \otimes \sigma_3$. We notice that Γ_{03} can also be expressed by $\Gamma_{03} = i\gamma_5\gamma_0\gamma_3$. Under the $O(2)$ transformation,

$$R_z(\phi)\hat{h}(\mathbf{k})R_z^{-1}(\phi) = \hat{h}(\mathbf{k}'), \quad (17)$$

where

$$k'_1 = k_1 \cos(\phi) + k_2 \sin(\phi), \quad (18)$$

$$k'_2 = -k_1 \sin(\phi) + k_2 \cos(\phi), \quad (19)$$

$$k'_3 = k_3. \quad (20)$$

Thus S_0 is invariant under the $O(2)$ rotation. For $\phi = \frac{\pi}{2}$,

$$R_z\left(\frac{\pi}{2}\right) = e^{\frac{i\pi\Gamma_{03}}{4}}, \quad (21)$$

which is just the C_4 rotation about the z axis.

If the four-fermion interaction is weak, it is irrelevant in 3D semi-DSM, due to the vanishing DOS. However, if the four-fermion interaction is strong enough, the system could be driven to a new phase. As shown in Appendix A, there are 12 kinds of four-fermion interactions. Due to the constraint by Fierz identity, five of them are linearly independent. Here, we consider the interacting Lagrangian as follows:

$$\begin{aligned} \mathcal{L}_{\text{int}} = & g_1(\bar{\Psi}\gamma_0\Psi)^2 + g_2(\bar{\Psi}\Psi)^2 + g_4(\bar{\Psi}\gamma_0\gamma_5\Psi)^2 \\ & + g_5(\bar{\Psi}i\gamma_5\Psi)^2 + g_{3z}(\bar{\Psi}\gamma_0\gamma_3\Psi)^2. \end{aligned} \quad (22)$$

In this article, we study the influence of four-fermion interactions on 3D semi-DSM through the RG method [62].

III. MEAN-FIELD RESULTS

In this section, taking the four-fermion interaction $g_2(\bar{\Psi}\Psi)^2$ as an example, we first show the results of mean-field analysis.

Under the influence of short-range four-fermion interaction $g_2(\bar{\Psi}\Psi)^2$, the expectation value

$$\Delta_2 = \langle \bar{\Psi}\Psi \rangle \quad (23)$$

could become finite. According to the derivation shown in Appendix B, we obtain the free energy density

$$f = -4T \int \frac{d^3\mathbf{k}}{(2\pi)^3} \ln \left[2 \cosh \left(\frac{E_{\mathbf{k}, \Delta_2}}{2T} \right) \right] + \frac{\Delta_2^2}{2g_2}, \quad (24)$$

where $E_{\mathbf{k}, \Delta_2} = \sqrt{v^2k_\perp^2 + A^2k_3^4 + \Delta_2^2}$.

Through

$$\frac{\partial f}{\partial \Delta_2} = 0, \quad (25)$$

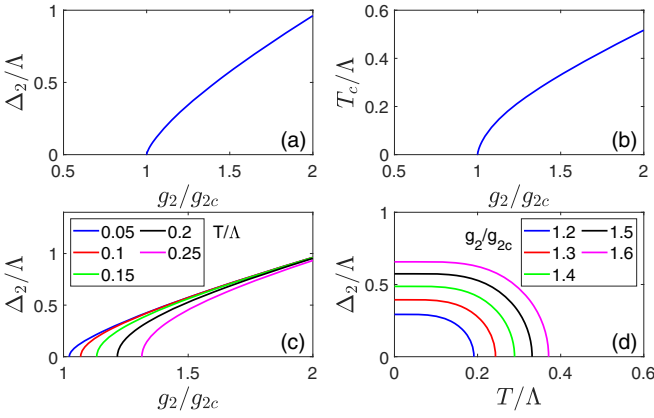


FIG. 2. Mean field results. (a) Dependence of Δ_2 on g_2 at zero temperature; (b) dependence of T_c on g_2 ; (c) dependence of Δ_2 on g_2 at different finite temperatures T/Λ ; (d) dependence of Δ_2 on temperature T with different values of g_2/g_{2c} .

we get the self-consistent equation for Δ_2 as follows:

$$1 = 2g_2 \int \frac{d^3\mathbf{k}}{(2\pi)^3} \tanh\left(\frac{E_{\mathbf{k},\Delta_2}}{2T}\right) \frac{1}{E_{\mathbf{k},\Delta_2}}. \quad (26)$$

At zero temperature, the equation becomes

$$1 = 2g_2 \int \frac{d^3\mathbf{k}}{(2\pi)^3} \frac{1}{E_{\mathbf{k},\Delta_2}}. \quad (27)$$

Based on analytical calculation for Eq. (27), we find that Δ_2 is given by

$$\Delta_2 \approx c_1 \Lambda \frac{(g_2 - g_{2c})^{\frac{2}{3}}}{g_2^{\frac{2}{3}}}, \quad (28)$$

if g_2 is close to g_{2c} , where

$$g_{2c} = \frac{3\pi^2 v^2 \sqrt{A}}{2\Lambda^{\frac{3}{2}}}. \quad (29)$$

and $c_1 \approx 0.662596$. Taking $\Delta_2 = 0$ for Eq. (26), we notice that the critical temperature T_c satisfies

$$T_c \approx c_2 \Lambda \frac{(g_2 - g_{2c})^{\frac{2}{3}}}{g_2^{\frac{2}{3}}}, \quad (30)$$

if g_2 is close to g_{2c} , where $c_2 = 1/(2\sqrt{2}a)^{\frac{2}{3}} \approx 0.622863$.

Numerical results are shown in Figs. 2(a)–2(d). In Fig. 2(a), dependence of Δ_2 on g_2 at zero temperature is depicted. Dependence of critical temperature T_c on g_2 is displayed in Fig. 2(b). The behaviors of Δ_2 at finite temperature are shown in Figs. 2(c) and 2(d).

IV. RG RESULTS

As shown in Appendix C, we first calculate all of the corrections from the one-loop Feynman diagrams, by employing a momentum shell $b\Lambda < \sqrt{v^2 k_{\perp}^2 + A^2 k_3^2} < \Lambda$, where $b = e^{-\ell}$, with ℓ being the RG running parameter. Then, we consider these corrections and perform RG transformations to restore the original form of the actions. Accordingly, we

obtain the RG equations for g_a , which can be written as

$$\frac{dg_a}{d\ell} = -\frac{3}{2}g_a + F_a(g_1, g_2, g_4, g_5, g_{3z}), \quad (31)$$

where $a = 1, 2, 4, 5, 3z$. The concrete expressions of F_a can be found in Appendix C.

Solving the equations

$$\left. \frac{dg_a}{d\ell} \right|_{(g_1, g_2, g_4, g_5, g_{3z}) = (g_1^*, g_2^*, g_4^*, g_5^*, g_{3z}^*)} = 0, \quad (32)$$

we get 12 fixed points, including the trivial Gaussian fixed point $(g_1^*, g_2^*, g_4^*, g_5^*, g_{3z}^*) = (0, 0, 0, 0, 0)$ and 11 nontrivial fixed points

$$\text{FP}i: (g_1^*, g_2^*, g_4^*, g_5^*, g_{3z}^*) = (g_{1,i}^*, g_{2,i}^*, g_{4,i}^*, g_{5,i}^*, g_{3z,i}^*), \quad (33)$$

with $i = 1, 2, \dots, 11$.

Expanding the RG equations of g_a in the vicinity of a fixed point, we obtain

$$\frac{d\delta g_a}{d\ell} = \sum_b M_{ab} \delta g_b, \quad (34)$$

where $\delta g_a = g_a - g_a^*$. M is a five dimension square matrix and the matrix elements are expressions of $g_1^*, g_2^*, g_4^*, g_5^*, g_{3z}^*$. From eigenvalues of M at a fixed point $(g_1^*, g_2^*, g_4^*, g_5^*, g_{3z}^*)$, we can get the properties of the fixed point. A negative (positive) eigenvalue is corresponding to a stable (unstable) eigendirection [32,34]. There is one unstable direction for QCP, and there are two and three unstable directions for bicritical point (BCP) and tricritical point (TCP), respectively. Substituting the values of g_a^* at each fixed point into the expression of M , we calculate the corresponding eigenvalues of M . We find that FP1, FP2, FP3, FP4, and FP5 are QCPs, FP6, FP7, FP8, FP9, and FP10 are BCPs, and FP11 is a TCP. The detailed calculations are presented in Appendix E.

For a QCP, the correlation length exponent ν is determined by the inverse of the corresponding positive eigenvalue of M . For the five QCPs, ν always satisfies

$$\nu^{-1} = 1.5. \quad (35)$$

In order to determine the physical essences of the QCPs, we analyze the RG flows of all the fermion bilinear source terms in particle-hole and particle-particle channels. The source terms in particle-hole channels can be written as

$$S_s = \Delta_X \int \frac{d\omega}{2\pi} \frac{d^3\mathbf{k}}{(2\pi)^3} \bar{\Psi}(\omega, \mathbf{k}) \Gamma_X \Psi(\omega, \mathbf{k}). \quad (36)$$

There are 12 choices for the matrix Γ_X , which corresponds to 12 different order parameters in particle-hole channels. The source terms in particle-particle channels take the form

$$S_s = \Delta_Y \int \frac{d\omega}{2\pi} \frac{d^3\mathbf{k}}{(2\pi)^3} \Psi^\dagger(\omega, \mathbf{k}) \Gamma_Y \Psi^*(\omega, \mathbf{k}). \quad (37)$$

There are six choices for the matrix Γ_Y , which are corresponding to six different superconducting pairings.

As presented in Appendix D, we calculate the one-loop order corrections to the source terms as shown in Eqs. (36) and (37) induced by the four-fermion interactions as shown in Eq. (22). Then, we include these corrections and perform RG transformations to restore the original forms of the source

terms. Accordingly, through the RG transformations, we obtain the equations

$$\bar{\beta}_{X,Y} = H_{X,Y}(g_1, g_2, g_4, g_5, g_{3z}), \quad (38)$$

where

$$\bar{\beta}_{X,Y} = \frac{d \ln(\Delta_{X,Y})}{d\ell} - 1. \quad (39)$$

$\bar{\beta}_{X,Y}$ are termed as susceptibility exponents or anomalous dimensions for the fermion-bilinear source terms. $H_{X,Y}$ are functions of g_a with $a = 1, 2, 4, 5, 3z$. The concrete expressions of $H_{X,Y}$ are shown in Appendix D. For a QCP, substituting the values of g_a at the QCP into Eq. (38), and finding the largest one among all of $\bar{\beta}_{X,Y}$, we can determine the physical meaning of the QCP.

For FP1, $\bar{\beta}_2$ takes the largest value. It represents that this fixed point is corresponding to the QCP to a state in which the order parameter $\Delta_2 = \langle \bar{\Psi} \Psi \rangle$ acquires finite value. The physical meaning of Δ_2 is scalar mass. Δ_2 breaks the continuous $U(1)$ chiral symmetry, but preserves \mathcal{P} , \mathcal{T} , \mathcal{C} symmetries. If Δ_2 becomes finite, the fermion dispersion becomes $E_{\mathbf{k},\Delta_2} = \sqrt{v^2 k_{\perp}^2 + A^2 k_3^4 + \Delta_2^2}$, which is gapped.

For FP2, $\bar{\beta}_5$ is the largest one. It means that this fixed point stands for the QCP to a state in which the order parameter $\Delta_5 = \langle \bar{\Psi} i \gamma_5 \Psi \rangle$ becomes finite. The physical meaning of Δ_5 corresponds to pseudoscalar mass. Δ_5 breaks continuous $U(1)$ chiral symmetry and \mathcal{C} symmetry, but preserves \mathcal{P} and \mathcal{T} symmetries. Once Δ_5 becomes finite, the corresponding fermion dispersion can be written as $E_{\mathbf{k},\Delta_5} = \sqrt{v^2 k_{\perp}^2 + A^2 k_3^4 + \Delta_5^2}$.

For FP3, $\bar{\beta}_2$ and $\bar{\beta}_5$ are largest simultaneously. It indicates that the fixed point corresponds to the QCP to a phase in which both Δ_2 and Δ_5 become finite. The parameter of this phase can be written as $\langle \bar{\Psi} [\cos(\theta) + i \gamma_5 \sin(\theta)] \Psi \rangle$. In the axionic insulating phase, the continuous $U(1)$ chiral symmetry is broken. This phase represents an axionic insulator [33]. In this case, the fermion dispersion takes the form $E_{\mathbf{k},\Delta_2,\Delta_5} = \sqrt{v^2 k_{\perp}^2 + A^2 k_3^4 + \Delta_2^2 + \Delta_5^2}$.

If the order parameters Δ_2 and Δ_5 are generated by four-fermion interactions, the continuous $U(1)$ chiral symmetry is broken. There will be a gapless Goldstone boson accompanied with breaking of continuous $U(1)$ chiral symmetry. In real solid-state materials, some higher-order gradient terms such as $\bar{\Psi} k^2 \mathbb{1}_{4 \times 4} \Psi$, $\bar{\Psi} k^4 \mathbb{1}_{4 \times 4} \Psi$, etc. could appear in the action of free 3D semi-DSM. In this case, the action of free 3D semi-DSM breaks the continuous $U(1)$ chiral symmetry, but still satisfies the discrete symmetries including \mathcal{P} , \mathcal{T} , and \mathcal{C} symmetries. Correspondingly, if Δ_2 and Δ_5 are generated by four-fermion interactions, we notice that the discrete symmetry \mathcal{C} is broken. Breaking of discrete symmetry will not lead to a gapless Goldstone mode.

For FP4, $\bar{\beta}_{7z}$ takes the largest value. It signifies that this fixed point is corresponding to the QCP to a state in which the order parameter $\Delta_{7z} = \langle \bar{\Psi} i \gamma_5 \gamma_3 \Psi \rangle$ becomes finite. Δ_{7z} stands for axial magnetization along the z axis. Δ_{7z} breaks \mathcal{T} symmetry, but preserves \mathcal{P} , \mathcal{C} , and $U(1)$ chiral symmetries. If $\Delta_{7z} > 0$, the original fermion dispersion becomes two dispersions $E_{\mathbf{k},\Delta_2}^{\pm}$, which can be written as $E_{\mathbf{k},\Delta_{7z}}^{\pm} =$

TABLE I. There are five QCPs among the 11 nontrivial unstable fixed points. The corresponding order parameters for the five QCPs are shown in the second rows.

	FP1	FP2	FP3	FP4	FP5
Order parameter	Δ_2	Δ_5	Δ_2/Δ_5	Δ_{7z}	Δ_{8z}

$\sqrt{v^2 k_{\perp}^2 + (Ak_3^2 \pm \Delta_{7z})^2}$. It is easy to find that one dispersion $E_{\mathbf{k},\Delta_{7z}}^+$ is gapped, but another dispersion $E_{\mathbf{k},\Delta_{7z}}^-$ is gapless at two points $\mathbf{k}_a = (0, 0, \sqrt{\frac{\Delta_{7z}}{A}})$ and $\mathbf{k}_b = (0, 0, -\sqrt{\frac{\Delta_{7z}}{A}})$. At these two gapless points, the fermion dispersion takes the form $E_{\mathbf{K},\Delta_{7z}} = \sqrt{v^2 K_{\perp}^2 + v_z^2 K_z^2}$, with $v_z = 2\sqrt{A\Delta_{7z}}$ and \mathbf{K} being the momentum relative to the point \mathbf{k}_a or \mathbf{k}_b . It is obvious that this fermion dispersion is linear within the xy plane and also linear along the z axis.

For FP5, $\bar{\beta}_{8z}$ is the largest one. It suggests that this fixed point represents the QCP to a state with finite order parameter $\Delta_{8z} = \langle \bar{\Psi} i \gamma_3 \Psi \rangle$. Δ_{8z} does not break the symmetries of the free semi-DSM. The physical meaning of Δ_{8z} is current along the z axis. If $\Delta_{8z} > 0$, the fermion dispersion becomes $E_{\mathbf{k},\Delta_{8z}} = \sqrt{v^2 k_{\perp}^2 + (Ak_3^2 + \Delta_{8z})^2}$, which is gapped.

For convenience, we summarize the corresponding order parameters for the five QCPs in Table I.

For general given initial conditions that are decided by $(g_{1,0}, g_{2,0}, g_{4,0}, g_{5,0}, g_{3z,0})$, we determine the corresponding phase through the flows of four-fermion coupling parameters g_a and flows of susceptibility exponents $\bar{\beta}_{X,Y}$. We show the flows of g_1, g_2, g_4, g_5 , and g_{3z} under several initial conditions in Fig. 3. If g_a with $a = 1, 2, 4, 5, 3z$ approaches zero, it represents that the system is still in SM phase. If $|g_a|$ flows to infinity at a finite running parameter ℓ_c , the system becomes unstable to a new phase.

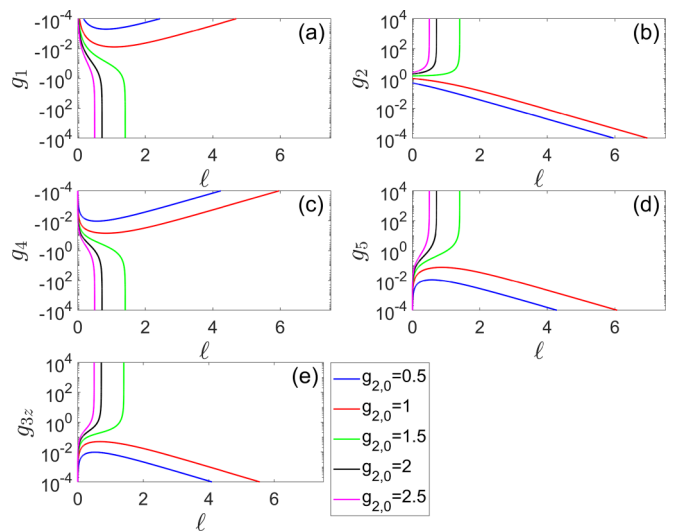


FIG. 3. (a)–(e) Flows of g_1, g_2, g_4, g_5 , and g_{3z} with different initial conditions $g_{2,0}$: 0.5 (blue), 1.0 (red), 1.5 (green), 2.0 (black), and 2.5 (magenta). $g_{1,0} = 0, g_{4,0} = 0, g_{5,0} = 0$, and $g_{3z,0} = 0$ are taken.

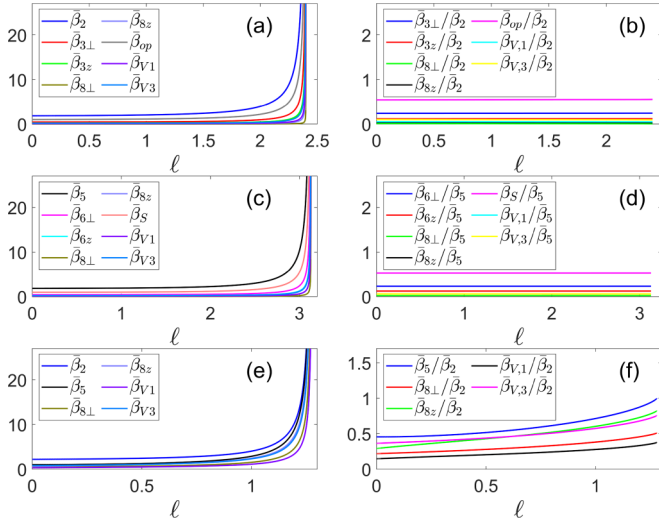


FIG. 4. Flows of $\bar{\beta}_{X,Y}$ which approach to positive infinity and ratios between $\bar{\beta}_{X,Y}$. (a),(b) $g_{1,0} = 0.15$, $g_{2,0} = 1.3$, $g_{4,0} = 0.46$, $g_{5,0} = -0.56$, and $g_{3z,0} = 0.055$ are taken; (c),(d) $g_{2,0} = 0.14$, $g_{2,0} = -0.59$, $g_{4,0} = 0.42$, $g_{5,0} = 1.36$, and $g_{3z,0} = 0.07$ are taken; (e),(f) $g_{1,0} = 0$, $g_{2,0} = 1.4$, $g_{3,0} = 0$, $g_{5,0} = 0.2$, and $g_{3z,0} = 0$ are taken.

In order to determine the physical essence of the new phase, we calculate the flows of the susceptibility exponents $\bar{\beta}_{X,Y}$ and compare them. For three general initial conditions, the flows of $\bar{\beta}_{X,Y}$ and the ratio between them are presented in Figs. 4(a)–4(f). Here we only show the susceptibility exponents that approach positive infinity in Figs. 4(a), 4(c), and 4(e), respectively. For the initial condition corresponding to Figs. 4(a) and 4(b), we find that $\bar{\beta}_2$ approaches positive

infinity most quickly. It means that scalar mass Δ_2 is generated in the new phase. For the initial condition corresponding to Figs. 4(c) and 4(d), $\bar{\beta}_5$ flows to positive infinity with the largest speed. It indicates that pseudoscalar mass Δ_5 becomes finite in the new phase. For the initial condition corresponding to Figs. 4(e) and 4(f), we notice that $\bar{\beta}_2$ and $\bar{\beta}_5$ approach positive infinity most quickly and $\bar{\beta}_5/\bar{\beta}_2 \rightarrow 1$. It represents that the system becomes a new phase where Δ_2 and Δ_5 acquire finite values simultaneously. Namely, the system becomes an axionic insulating phase.

The phase diagrams on the planes composed by initial values of two four-fermion coupling parameters are shown in Fig. 5. Different phases are marked by different colors. In Figs. 5(a)–5(j), we show all 10 phase diagrams on the planes composed by initial values of two coupling parameters chosen from the five linearly independent coupling parameters. The initial values of rest of three coupling parameters are taken as zero. Taking Fig. 5(a) composed by $g_{2,0}$ and $g_{5,0}$ as an example, we can notice that there are five phases: SM, insulator with scalar mass Δ_2 , insulator characterized by pseudoscalar mass Δ_5 , axionic insulating phase, and a phase with current along z axis Δ_{8z} . In Fig. 5(k), we present the phase diagram composed by $g_{5,0}$ and $g_{3z,0}$. In this phase diagram, $g_{1,0}$, $g_{2,0}$, and $g_{4,0}$ are taken as proper values so that the phase with axial magnetization along z axis Δ_{7z} appears in the phase diagram.

The behaviors in the vicinity of a QCP are generally consistent with those indicated by Sur and Roy [60]. In 3D semi-DSM, the Yukawa coupling between quantum fluctuation of order parameter and fermion excitations becomes irrelevant in the low energy regime. Thus the fermions should take Fermi liquid behaviors in the vicinity of a QCP between SM phase and a symmetry breaking phase in 3D semi-DSM.

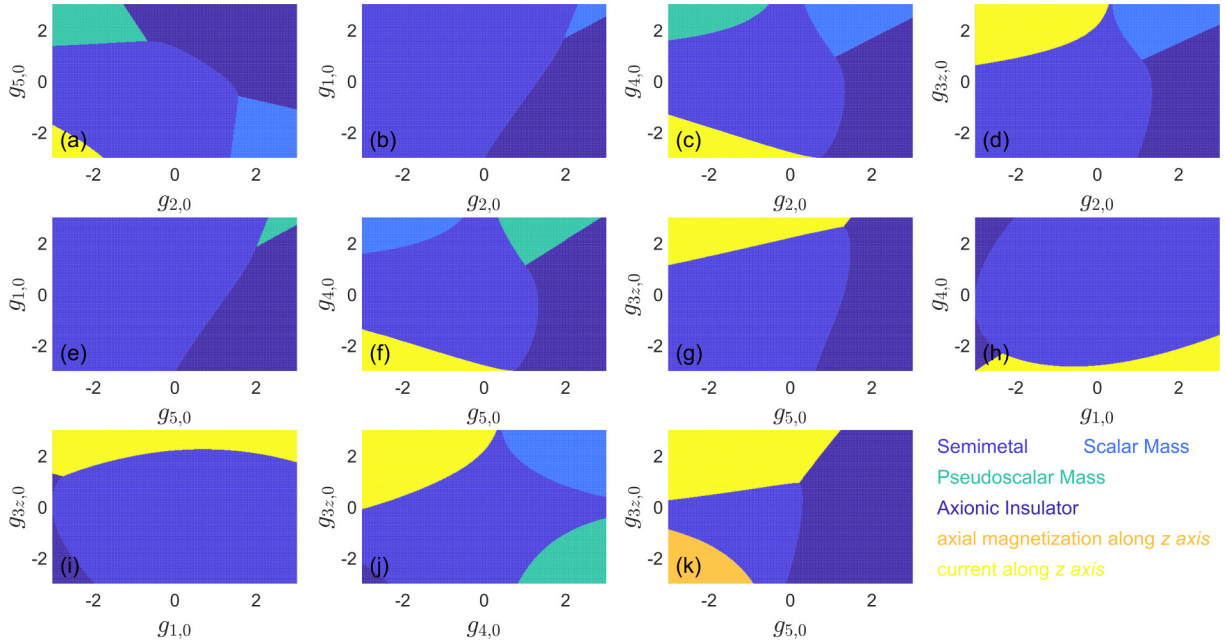


FIG. 5. Phase diagrams on the planes of two initial values of four-fermion coupling strength. (a) $g_{2,0}$ and $g_{5,0}$; (b) $g_{2,0}$ and $g_{1,0}$; (c) $g_{2,0}$ and $g_{4,0}$; (d) $g_{2,0}$ and $g_{3z,0}$; (e) $g_{5,0}$ and $g_{1,0}$; (f) $g_{5,0}$ and $g_{4,0}$; (g) $g_{5,0}$ and $g_{3z,0}$; (h) $g_{1,0}$ and $g_{4,0}$; (i) $g_{1,0}$ and $g_{3z,0}$; (j) $g_{4,0}$ and $g_{3z,0}$; (k) $g_{5,0}$ and $g_{3z,0}$. In (a)–(j), the initial values of rest four-fermion coupling parameters are taken as zero. For example, $g_{1,0} = 0$, $g_{4,0} = 0$, and $g_{3z,0} = 0$ are taken in (a). In (k), $g_{1,0} = -2.3$, $g_{2,0} = 0$, and $g_{4,0} = -0.61$ are taken.

Concretely, the residue of fermions Z_f approaches a finite constant value in the lowest energy limit and the Landau damping rate of fermions $\Gamma(\omega)$ satisfies

$$\lim_{\omega \rightarrow 0} \frac{\Gamma(\omega)}{\omega} \rightarrow 0. \quad (40)$$

Additionally, under the influence of quantum fluctuation of order parameter, the observable quantities DOS ρ , specific heat C_v , compressibility κ , and optical conductivities within the xy plane and along z axis $\sigma_{\perp\perp}$ and σ_{zz} should respectively still take the behaviors

$$\begin{aligned} \rho(\omega) &\sim \omega^{3/2}, & C_v(T) &\sim T^{5/2}, & \kappa(T) &\sim T^{3/2}, \\ \sigma_{\perp\perp}(\omega) &\sim \omega^{1/2}, & \sigma_{zz}(\omega) &\sim \omega^{3/2}, \end{aligned} \quad (41)$$

which are qualitatively the same as the ones for free fermions.

V. INTERPLAY WITH COULOMB INTERACTION

In 3D semi-DSM, the long-range Coulomb interaction becomes irrelevant in the low energy regime [37,38]. Considering the interplay of short-range four-fermion interactions and long-range Coulomb interaction, we find that the flow of Coulomb interaction is not changed and still becomes irrelevant in the low energy regime, whereas the flows of four-fermion interactions are modified by Coulomb interaction. It is shown that Coulomb interaction tends to enhance the instabilities in particle-hole channels. For the case that all the initial values of four-fermion coupling strength vanish, if the Coulomb interaction is strong enough, the four-fermion interactions are generated and become divergent finally driven by the Coulomb interaction. We notice that the system is driven into an axionic insulating phase in this case. The detailed derivation and numerical results are shown in Appendix F.

VI. SUMMARY

To conclude, we perform comprehensive studies about the influence of four-fermion interactions on 3D semi-DSM through RG theory. We find 11 unstable fixed points and show that five of them are QCPs, five are BCPs, and the remaining one is a TCP. The physical essence of the QCPs are determined by analyzing the scalings of fermion bilinear source terms. The phase diagrams for general initial conditions are also presented through detailed numerical calculations of flows of four-fermion couplings and susceptibility exponents.

According to the theoretical study by Yang and Nagaosa [14], the 3D semi-DSM state can be realized at the topological QCP between 3D DSM and band insulator. Through magneto-optics and magnetotransport, Yuan *et al.* observed the evidence of a 3D semi-DSM phase in ZrTe₅ [63]. The subsequent study about magnetotransport properties of ZrTe₅ under hydrostatic pressure also supports the existence of a 3D semi-DSM phase [64]. Recent measurements of optical spectroscopy in ZrTe₅ are also consistent with a 3D semi-DSM phase [65,66]. A 3D semi-DSM state was also realized in pressured Cd₃As₂ [67]. Recently, Monhanta *et al.* showed that nonmagnetic tetragonal perovskite oxides with $I4/mcm$ symmetry, e.g., SrNbO₃, CaNbO₃, and SrMoO₃, host 3D semi-Dirac fermions which are protected by a nonsymmorphic symmetry [68]. The present RG calculation results are

helpful for understanding the physical properties of these candidate materials for 3D semi-DSM.

ACKNOWLEDGMENTS

J.R.W. is grateful to Professor G.-Z. Liu for the valuable discussions. We acknowledge the support from the National Natural Science Foundation of China under Grants No. 11974356, No. 12164005, No. 12274414, and No. U1832209. A portion of this work was supported by the High Magnetic Field Laboratory of Anhui Province under Grant No. AHHM-FX-2020-01.

APPENDIX A: FIERZ IDENTITY

1. Fierz identity for 3D DSM

The four-fermion interactions can be generally written as form $(\bar{\Psi}M\Psi)(\bar{\Psi}N\Psi)$, where M and N are four dimensional matrices. There are 16 independent four-by-four matrices. Accordingly, there are a possible $16 + 16 \times 15/2 = 136$ kinds of four-fermion interactions. However, the number of four-fermion interactions can be drastically reduced by the symmetries of the system [31–34,52]. The action of free fermions satisfies the symmetries including parity symmetry, time-reversal symmetry, charge conjugation symmetry, rotation symmetry, etc. We could reduce the number of four-fermion interactions by these symmetries of action of free fermions [31–34,52]. The four-fermion interactions $(\bar{\Psi}M\Psi)(\bar{\Psi}N\Psi)$ with $M = N$ respect these symmetries, but the four-fermion interactions $(\bar{\Psi}M\Psi)(\bar{\Psi}N\Psi)$ with $M \neq N$ cannot fulfill these symmetries. Therefore, we do not consider the four-fermion interactions $(\bar{\Psi}M\Psi)(\bar{\Psi}N\Psi)$ with $M \neq N$ which are not allowed by the symmetries.

For 3D DSM, the interacting Lagrangian density can be written as [33]

$$\begin{aligned} \mathcal{L}_{\text{int}} &= g_1(\bar{\Psi}\gamma_0\Psi)^2 + g_2(\bar{\Psi}\Psi)^2 + g_3 \sum_{j=1}^3 (\bar{\Psi}\gamma_0\gamma_j\Psi)^2 \\ &+ g_4(\bar{\Psi}\gamma_0\gamma_5\Psi)^2 + g_5(\bar{\Psi}i\gamma_5\Psi)^2 \\ &+ g_6 \sum_{(lk)} (\bar{\Psi}i\gamma_l\gamma_k\Psi)^2 + g_7 \sum_{j=1}^3 (\bar{\Psi}i\gamma_5\gamma_j\Psi)^2 \\ &+ g_8 \sum_{j=1}^3 (\bar{\Psi}i\gamma_j\Psi)^2, \end{aligned} \quad (A1)$$

where

$$\begin{aligned} \sum_{(lk)} (\bar{\Psi}i\gamma_l\gamma_k\Psi)^2 &= [(\bar{\Psi}i\gamma_2\gamma_3\Psi)^2 + (\bar{\Psi}i\gamma_3\gamma_1\Psi)^2 \\ &+ (\bar{\Psi}i\gamma_1\gamma_2\Psi)^2]. \end{aligned} \quad (A2)$$

There are eight kinds of four-fermion couplings. However, not all of them are linearly independent, due to the constraint by Fierz identity [31,33,34].

The Fierz identity indicates that [31,33,34]

$$\begin{aligned} &[\bar{\Psi}(x)M\Psi(x)][\bar{\Psi}(y)N\Psi(y)] \\ &= -\frac{1}{16} \text{Tr}[M\Gamma_a N\Gamma_b][\bar{\Psi}(x)\Gamma_a\Psi(y)][\bar{\Psi}(y)\Gamma_b\Psi(x)]. \end{aligned} \quad (A3)$$

For local interaction, we have $x = y$. Thus

$$\begin{aligned} & [\bar{\Psi}(x)M\Psi(x)][\bar{\Psi}(x)N\Psi(x)] \\ &= -\frac{1}{16}\text{Tr}[M\Gamma_a N\Gamma_b][\bar{\Psi}(x)\Gamma_a\Psi(x)][\bar{\Psi}(x)\Gamma_b\Psi(x)]. \end{aligned} \quad (\text{A4})$$

Repeat of indexes a and b in Eqs. (A3) and (A4) represents summation. Substituting each four-fermion coupling in Eq. (A1) into Eq. (A4), we could get eight equations, which can be compactly expressed by

$$FX = 0, \quad (\text{A5})$$

where

$$X = \begin{pmatrix} (\bar{\Psi}\gamma_0\Psi)^2 \\ (\bar{\Psi}\Psi)^2 \\ \sum_{j=1}^3(\bar{\Psi}\gamma_0\gamma_j\Psi)^2 \\ (\bar{\Psi}\gamma_0\gamma_5\Psi)^2 \\ (\bar{\Psi}i\gamma_5\Psi)^2 \\ \sum_{(lk)}(\bar{\Psi}i\gamma_l\gamma_k\Psi)^2 \\ \sum_{j=1}^3(\bar{\Psi}i\gamma_5\gamma_j\Psi)^2 \\ \sum_{j=1}^3(\bar{\Psi}i\gamma_j\Psi)^2 \end{pmatrix} \quad (\text{A6})$$

and

$$F = \begin{pmatrix} 5 & 1 & 1 & 1 & 1 & 1 & 1 & 1 \\ 1 & 5 & -1 & -1 & -1 & 1 & 1 & -1 \\ 3 & -3 & 3 & -3 & 3 & 1 & -1 & 1 \\ 1 & -1 & -1 & 5 & -1 & -1 & 1 & 1 \\ 1 & -1 & 1 & -1 & 5 & -1 & 1 & -1 \\ 3 & 3 & 1 & -3 & -3 & 3 & -1 & 1 \\ 3 & 3 & -1 & 3 & 3 & -1 & 3 & -1 \\ 3 & -3 & 1 & 3 & -3 & 1 & -1 & 3 \end{pmatrix}. \quad (\text{A7})$$

It is easy to verify that rank of F is 4, namely

$$\text{Rank}(F) = 4. \quad (\text{A8})$$

Then, the number of linearly independent couplings is

$$8 - \text{Rank}(F) = 4. \quad (\text{A9})$$

For convenience, we take the four couplings

$$(\bar{\Psi}\gamma_0\Psi)^2, \quad (\bar{\Psi}\Psi)^2, \quad (\bar{\Psi}\gamma_0\gamma_5\Psi)^2, \quad (\bar{\Psi}i\gamma_5\Psi)^2 \quad (\text{A10})$$

as linearly independent couplings. The other couplings

$$\begin{aligned} & \sum_{j=1}^3(\bar{\Psi}\gamma_0\gamma_j\Psi)^2, \quad \sum_{(lk)}(\bar{\Psi}i\gamma_l\gamma_k\Psi)^2, \\ & \sum_{j=1}^3(\bar{\Psi}i\gamma_5\gamma_j\Psi)^2, \quad \sum_{j=1}^3(\bar{\Psi}i\gamma_j\Psi)^2 \end{aligned} \quad (\text{A11})$$

can be expressed by the four independent couplings shown in Eq. (A10). In order to obtain the concrete expressions for

other couplings, we define

$$\tilde{X} = \begin{pmatrix} \sum_{j=1}^3(\bar{\Psi}\gamma_0\gamma_j\Psi)^2 \\ \sum_{(lk)}(\bar{\Psi}i\gamma_l\gamma_k\Psi)^2 \\ \sum_{j=1}^3(\bar{\Psi}i\gamma_5\gamma_j\Psi)^2 \\ \sum_{j=1}^3(\bar{\Psi}i\gamma_j\Psi)^2 \\ (\bar{\Psi}\gamma_0\Psi)^2 \\ (\bar{\Psi}\Psi)^2 \\ (\bar{\Psi}\gamma_0\gamma_5\Psi)^2 \\ (\bar{\Psi}i\gamma_5\Psi)^2 \end{pmatrix}. \quad (\text{A12})$$

It is easy to find that

$$\tilde{F}\tilde{X} = 0, \quad (\text{A13})$$

where

$$\tilde{F} = \begin{pmatrix} 1 & 1 & 1 & 1 & 5 & 1 & 1 & 1 \\ -1 & 1 & 1 & -1 & 1 & 5 & -1 & -1 \\ 3 & 1 & -1 & 1 & 3 & -3 & -3 & 3 \\ -1 & -1 & 1 & 1 & 1 & -1 & 5 & -1 \\ 1 & -1 & 1 & -1 & 1 & -1 & -1 & 5 \\ 1 & 3 & -1 & 1 & 3 & 3 & -3 & -3 \\ -1 & -1 & 3 & -1 & 3 & 3 & 3 & 3 \\ 1 & 1 & -1 & 3 & 3 & -3 & 3 & -3 \end{pmatrix}. \quad (\text{A14})$$

Performing a series of similarity transformations for \tilde{F} ,

$$\tilde{F} \rightarrow \tilde{F}', \quad (\text{A15})$$

we obtain

$$\tilde{F}'\tilde{X} = 0, \quad (\text{A16})$$

where

$$\tilde{F}' = \begin{pmatrix} 1 & 0 & 0 & 0 & 1 & -1 & -1 & 2 \\ 0 & 1 & 0 & 0 & 1 & 2 & -1 & -1 \\ 0 & 0 & 1 & 0 & 2 & 1 & 1 & 1 \\ 0 & 0 & 0 & 1 & 1 & -1 & 2 & -1 \\ 0 & 0 & 0 & 0 & 0 & 0 & 0 & 0 \\ 0 & 0 & 0 & 0 & 0 & 0 & 0 & 0 \\ 0 & 0 & 0 & 0 & 0 & 0 & 0 & 0 \\ 0 & 0 & 0 & 0 & 0 & 0 & 0 & 0 \end{pmatrix}. \quad (\text{A17})$$

Equation (A16) can be equivalently expressed by

$$\begin{aligned} \sum_{j=1}^3(\bar{\Psi}\gamma_0\gamma_j\Psi)^2 &= -(\bar{\Psi}\gamma_0\Psi)^2 + (\bar{\Psi}\Psi)^2 \\ &+ (\bar{\Psi}\gamma_0\gamma_5\Psi)^2 - 2(\bar{\Psi}i\gamma_5\Psi)^2, \end{aligned} \quad (\text{A18})$$

$$\begin{aligned} \sum_{(lk)}(\bar{\Psi}i\gamma_l\gamma_k\Psi)^2 &= -(\bar{\Psi}\gamma_0\Psi)^2 - 2(\bar{\Psi}\Psi)^2 \\ &+ (\bar{\Psi}\gamma_0\gamma_5\Psi)^2 + (\bar{\Psi}i\gamma_5\Psi)^2, \end{aligned} \quad (\text{A19})$$

$$\begin{aligned} \sum_{j=1}^3(\bar{\Psi}i\gamma_5\gamma_j\Psi)^2 &= -2(\bar{\Psi}\gamma_0\Psi)^2 - (\bar{\Psi}\Psi)^2 \\ &- (\bar{\Psi}\gamma_0\gamma_5\Psi)^2 - (\bar{\Psi}i\gamma_5\Psi)^2, \end{aligned} \quad (\text{A20})$$

TABLE II. Transformation properties of various fermion bilinears under parity (\mathcal{P}), time-reversal (\mathcal{T}), charge conjugation (\mathcal{C}), Z_2 chiral, $U(1)$ chiral, and $O(2)$ rotation transformations. Notice that $j = 1, 2$ and $lk = 23, 31$. Here, + (−) represents that the fermion bilinear is even (odd) under a transformation. In the sixth column, \checkmark represents that the bilinear is a scalar under the $U(1)$ chiral transformation. Fermion bilinears which transform as components of a chiral $U(1)$ vector under the $U(1)$ chiral transformation are marked by circles with the same color. The colors red, green, and blue correspond to three different chiral $U(1)$ vectors. In the seventh column, 0 (1) stands for the fact that the bilinear transforms as a scalar (vector) under the $O(2)$ rotation about the z axis.

Bilinear	\mathcal{P}	\mathcal{T}	\mathcal{C}	Z_2	$U(1)$	$O(2)$
$\bar{\Psi}\gamma_0\Psi$	+	+	−	+	\checkmark	0
$\bar{\Psi}\Psi$	+	+	+	−	•	0
$\bar{\Psi}\gamma_0\gamma_j\Psi$	−	+	−	−	•	1
$\bar{\Psi}\gamma_0\gamma_3\Psi$	+	−	+	−	•	0
$\bar{\Psi}\gamma_0\gamma_5\Psi$	+	−	−	+	\checkmark	0
$\bar{\Psi}i\gamma_5\Psi$	+	+	−	−	•	0
$\bar{\Psi}i\gamma_l\gamma_k\Psi$	−	+	+	−	•	1
$\bar{\Psi}i\gamma_1\gamma_2\Psi$	+	−	−	−	•	0
$\bar{\Psi}i\gamma_5\gamma_j\Psi$	−	+	−	+	\checkmark	1
$\bar{\Psi}i\gamma_5\gamma_3\Psi$	+	−	+	+	\checkmark	0
$\bar{\Psi}i\gamma_j\Psi$	−	−	−	+	\checkmark	1
$\bar{\Psi}i\gamma_3\Psi$	+	+	+	+	\checkmark	0

$$\sum_{j=1}^3 (\bar{\Psi}i\gamma_j\Psi)^2 = -(\bar{\Psi}\gamma_0\Psi)^2 + (\bar{\Psi}\Psi)^2 - 2(\bar{\Psi}\gamma_0\gamma_5\Psi)^2 + (\bar{\Psi}i\gamma_5\Psi)^2. \quad (\text{A21})$$

2. Fierz identity for 3D semi-DSM

For 3D semi-DSM, the interacting Lagrangian density is described by

$$\begin{aligned} \mathcal{L}_{\text{int}} = & g_1(\bar{\Psi}\gamma_0\Psi)^2 + g_2(\bar{\Psi}\Psi)^2 + g_{3\perp} \sum_{j=1}^2 (\bar{\Psi}\gamma_0\gamma_j\Psi)^2 \\ & + g_{3z}(\bar{\Psi}\gamma_0\gamma_3\Psi)^2 + g_4(\bar{\Psi}\gamma_0\gamma_5\Psi)^2 + g_5(\bar{\Psi}i\gamma_5\Psi)^2 \\ & + g_{6\perp} \sum_{\langle\langle lk \rangle\rangle} (\bar{\Psi}i\gamma_l\gamma_k\Psi)^2 + g_{6z}(\bar{\Psi}i\gamma_1\gamma_2\Psi)^2 \\ & + g_{7\perp} \sum_{j=1}^2 (\bar{\Psi}i\gamma_5\gamma_j\Psi)^2 + g_{7z}(\bar{\Psi}i\gamma_5\gamma_3\Psi)^2 \\ & + g_{8\perp} \sum_{j=1}^2 (\bar{\Psi}i\gamma_j\Psi)^2 + g_{8z}(\bar{\Psi}i\gamma_3\Psi)^2, \end{aligned} \quad (\text{A22})$$

where

$$\sum_{\langle\langle lk \rangle\rangle} (\bar{\Psi}i\gamma_l\gamma_k\Psi)^2 = [(\bar{\Psi}i\gamma_2\gamma_3\Psi)^2 + (\bar{\Psi}i\gamma_3\gamma_1\Psi)^2]. \quad (\text{A23})$$

As shown in Eq. (A1), there are eight four-fermion couplings for 3D DSM. However, we consider 12 kinds of four-fermion couplings as shown in Eq. (A22) for 3D semi-DSM, due to the anisotropy of the fermion dispersion.

After careful derivation, as shown in Table II, we obtain the properties of each fermion bilinear under the parity (\mathcal{P}),

time-reversal (\mathcal{T}), charge conjugation (\mathcal{C}), and Z_2 chiral, $U(1)$ chiral, and $O(2)$ rotation transformations. We reduce 136 possible four-fermion interactions $(\bar{\Psi}M\Psi)(\bar{\Psi}N\Psi)$ by imposing discrete transformations including \mathcal{P} , \mathcal{T} , \mathcal{C} , and Z_2 chiral symmetries. It is easy to find that both $(\bar{\Psi}M\Psi)$ and $(\bar{\Psi}N\Psi)$ should be either even or odd under \mathcal{P} , \mathcal{T} , \mathcal{C} , and Z_2 transformations, such that the four-fermion interaction is invariant under all these four individual discrete symmetries. We can find that there are no two identical rows under these four symmetry transformations in Table II. Therefore, there exists no interaction term $(\bar{\Psi}M\Psi)(\bar{\Psi}N\Psi)$ with $M \neq N$ that mixes any two different fermion bilinears.

Substituting each four-fermion coupling in Eq. (A22) into Eq. (A4), we could get 12 equations, which can be compactly expressed by

$$FX = 0, \quad (\text{A24})$$

where

$$X = \begin{pmatrix} (\bar{\Psi}\gamma_0\Psi)^2 \\ (\bar{\Psi}\Psi)^2 \\ \sum_{j=1}^2 (\bar{\Psi}\gamma_0\gamma_j\Psi)^2 \\ (\bar{\Psi}\gamma_0\gamma_3\Psi)^2 \\ (\bar{\Psi}\gamma_0\gamma_5\Psi)^2 \\ (\bar{\Psi}i\gamma_5\Psi)^2 \\ \sum_{\langle\langle lk \rangle\rangle} (\bar{\Psi}i\gamma_l\gamma_k\Psi)^2 \\ (\bar{\Psi}i\gamma_1\gamma_2\Psi)^2 \\ \sum_{j=1}^2 (\bar{\Psi}i\gamma_5\gamma_j\Psi)^2 \\ (\bar{\Psi}i\gamma_5\gamma_3\Psi)^2 \\ \sum_{j=1}^2 (\bar{\Psi}i\gamma_j\Psi)^2 \\ (\bar{\Psi}i\gamma_3\Psi)^2 \end{pmatrix} \quad (\text{A25})$$

and

$$F = \begin{pmatrix} 5 & 1 & 1 & 1 & 1 & 1 & 1 & 1 & 1 & 1 & 1 & 1 \\ 1 & 5 & -1 & -1 & -1 & -1 & 1 & 1 & 1 & 1 & -1 & -1 \\ 1 & -1 & 2 & -1 & -1 & 1 & 0 & 1 & 0 & -1 & 0 & 1 \\ 1 & -1 & -1 & 5 & -1 & 1 & 1 & -1 & -1 & 1 & 1 & -1 \\ 1 & -1 & -1 & -1 & 5 & -1 & -1 & -1 & 1 & 1 & 1 & 1 \\ 1 & -1 & 1 & 1 & -1 & 5 & -1 & -1 & 1 & 1 & -1 & -1 \\ 1 & 1 & 0 & 1 & -1 & -1 & 2 & -1 & 0 & -1 & 0 & 1 \\ 1 & 1 & 1 & -1 & -1 & -1 & -1 & 5 & -1 & 1 & 1 & -1 \\ 1 & 1 & 0 & -1 & 1 & 1 & 0 & -1 & 2 & -1 & 0 & -1 \\ 1 & 1 & -1 & 1 & 1 & 1 & -1 & 1 & -1 & 5 & -1 & 1 \\ 1 & -1 & 0 & 1 & 1 & -1 & 0 & 1 & 0 & -1 & 2 & -1 \\ 1 & -1 & 1 & -1 & 1 & -1 & 1 & -1 & -1 & 1 & -1 & 5 \end{pmatrix}. \quad (\text{A26})$$

It is easy to find that

$$\text{Rank}(F) = 7. \quad (\text{A27})$$

Then the number of linearly independent couplings is

$$12 - \text{Rank}(F) = 5. \quad (\text{A28})$$

For convenience, we take the five couplings

$$\begin{aligned} &(\bar{\Psi}\gamma_0\Psi)^2, \quad (\bar{\Psi}\Psi)^2, \quad (\bar{\Psi}\gamma_0\gamma_5\Psi)^2, \\ &(\bar{\Psi}i\gamma_5\Psi)^2, \quad (\bar{\Psi}\gamma_0\gamma_3\Psi)^2 \end{aligned} \quad (\text{A29})$$

as linearly independent couplings. The other couplings

$$\begin{aligned} &\sum_{j=1}^2 (\bar{\Psi}\gamma_0\gamma_j\Psi)^2, \quad \sum_{\langle\langle lk \rangle\rangle} (\bar{\Psi}i\gamma_l\gamma_k\Psi)^2, \quad (\bar{\Psi}i\gamma_1\gamma_2\Psi)^2, \\ &\sum_{j=1}^2 (\bar{\Psi}i\gamma_5\gamma_j\Psi)^2, \quad (\bar{\Psi}i\gamma_5\gamma_3\Psi)^2, \\ &\sum_{j=1}^2 (\bar{\Psi}i\gamma_j\Psi)^2, \quad (\bar{\Psi}i\gamma_3\Psi)^2 \end{aligned} \quad (\text{A30})$$

can be expressed by the five independent couplings shown in Eq. (A29). In order to obtain the concrete expressions for other couplings, we define

$$\tilde{X} = \begin{pmatrix} \sum_{j=1}^2 (\bar{\Psi}\gamma_0\gamma_j\Psi)^2 \\ \sum_{\langle\langle lk \rangle\rangle} (\bar{\Psi}i\gamma_l\gamma_k\Psi)^2 \\ (\bar{\Psi}i\gamma_1\gamma_2\Psi)^2 \\ \sum_{j=1}^2 (\bar{\Psi}i\gamma_5\gamma_j\Psi)^2 \\ (\bar{\Psi}i\gamma_5\gamma_3\Psi)^2 \\ \sum_{j=1}^2 (\bar{\Psi}i\gamma_j\Psi)^2 \\ (\bar{\Psi}i\gamma_3\Psi)^2 \\ (\bar{\Psi}\gamma_0\Psi)^2 \\ (\bar{\Psi}\Psi)^2 \\ (\bar{\Psi}\gamma_0\gamma_5\Psi)^2 \\ (\bar{\Psi}i\gamma_5\Psi)^2 \\ (\bar{\Psi}\gamma_0\gamma_3\Psi)^2 \end{pmatrix}. \quad (\text{A31})$$

It is easy to get that

$$\tilde{F}\tilde{X} = 0, \quad (\text{A32})$$

where

$$\tilde{F} = \begin{pmatrix} 1 & 1 & 1 & 1 & 1 & 1 & 1 & 1 & 5 & 1 & 1 & 1 & 1 \\ -1 & 1 & 1 & 1 & 1 & -1 & -1 & 1 & 1 & 5 & -1 & -1 & -1 \\ 2 & 0 & 1 & 0 & -1 & 0 & 1 & 1 & -1 & -1 & -1 & 1 & -1 \\ -1 & 1 & -1 & -1 & 1 & 1 & -1 & 1 & -1 & -1 & 1 & 1 & 5 \\ -1 & -1 & -1 & 1 & 1 & 1 & 1 & 1 & -1 & -1 & 5 & -1 & -1 \\ 1 & -1 & -1 & 1 & 1 & -1 & -1 & 1 & -1 & -1 & 5 & 1 & 1 \\ 0 & 2 & -1 & 0 & -1 & 0 & 1 & 1 & 1 & -1 & -1 & -1 & 1 \\ 1 & -1 & 5 & -1 & 1 & 1 & -1 & 1 & 1 & -1 & -1 & -1 & -1 \\ 0 & 0 & -1 & 2 & -1 & 0 & -1 & 1 & 1 & 1 & 1 & 1 & -1 \\ -1 & -1 & 1 & -1 & 5 & -1 & 1 & 1 & 1 & 1 & 1 & 1 & 1 \\ 0 & 0 & 1 & 0 & -1 & 2 & -1 & 1 & -1 & 1 & -1 & -1 & 1 \\ 1 & 1 & -1 & -1 & 1 & -1 & 5 & 1 & -1 & 1 & -1 & -1 & -1 \end{pmatrix}. \quad (\text{A33})$$

Carrying out a series of similarity transformations for \tilde{F} ,

$$\tilde{F} \rightarrow \tilde{F}', \quad (\text{A34})$$

we arrive

$$\tilde{F}'\tilde{X} = 0, \quad (\text{A35})$$

where

$$\tilde{F}' = \begin{pmatrix} 1 & 0 & 0 & 0 & 0 & 0 & 0 & 1 & -1 & -1 & 2 & 1 \\ 0 & 1 & 0 & 0 & 0 & 0 & 0 & 1 & 1 & -1 & 0 & 1 \\ 0 & 0 & 1 & 0 & 0 & 0 & 0 & 0 & 1 & 0 & -1 & -1 \\ 0 & 0 & 0 & 1 & 0 & 0 & 0 & 1 & 1 & 1 & 0 & -1 \\ 0 & 0 & 0 & 0 & 1 & 0 & 0 & 1 & 0 & 0 & 1 & 1 \\ 0 & 0 & 0 & 0 & 0 & 1 & 0 & 1 & -1 & 1 & 0 & 1 \\ 0 & 0 & 0 & 0 & 0 & 0 & 1 & 0 & 0 & 1 & -1 & -1 \\ 0 & 0 & 0 & 0 & 0 & 0 & 0 & 0 & 0 & 0 & 0 & 0 \\ 0 & 0 & 0 & 0 & 0 & 0 & 0 & 0 & 0 & 0 & 0 & 0 \\ 0 & 0 & 0 & 0 & 0 & 0 & 0 & 0 & 0 & 0 & 0 & 0 \\ 0 & 0 & 0 & 0 & 0 & 0 & 0 & 0 & 0 & 0 & 0 & 0 \\ 0 & 0 & 0 & 0 & 0 & 0 & 0 & 0 & 0 & 0 & 0 & 0 \\ 0 & 0 & 0 & 0 & 0 & 0 & 0 & 0 & 0 & 0 & 0 & 0 \end{pmatrix}. \quad (\text{A36})$$

Equation (A35) can also be written as

$$\sum_{j=1}^2 (\bar{\Psi}\gamma_0\gamma_j\Psi)^2 = -(\bar{\Psi}\gamma_0\Psi)^2 + (\bar{\Psi}\Psi)^2 + (\bar{\Psi}\gamma_0\gamma_5\Psi)^2 - 2(\bar{\Psi}i\gamma_5\Psi)^2 - (\bar{\Psi}\gamma_0\gamma_3\Psi)^2, \quad (\text{A37})$$

$$\sum_{\langle\langle lk \rangle\rangle} (\bar{\Psi}i\gamma_l\gamma_k\Psi)^2 = -(\bar{\Psi}\gamma_0\Psi)^2 - (\bar{\Psi}\Psi)^2 + (\bar{\Psi}\gamma_0\gamma_5\Psi)^2 - (\bar{\Psi}\gamma_0\gamma_3\Psi)^2, \quad (\text{A38})$$

$$(\bar{\Psi}i\gamma_1\gamma_2\Psi)^2 = -(\bar{\Psi}\Psi)^2 + (\bar{\Psi}i\gamma_5\Psi)^2 + (\bar{\Psi}\gamma_0\gamma_3\Psi)^2, \quad (\text{A39})$$

$$\sum_{j=1}^2 (\bar{\Psi}i\gamma_5\gamma_j\Psi)^2 = -(\bar{\Psi}\gamma_0\Psi)^2 - (\bar{\Psi}\Psi)^2 - (\bar{\Psi}\gamma_0\gamma_5\Psi)^2 + (\bar{\Psi}\gamma_0\gamma_3\Psi)^2, \quad (\text{A40})$$

$$(\bar{\Psi}i\gamma_5\gamma_3\Psi)^2 = -(\bar{\Psi}\gamma_0\Psi)^2 - (\bar{\Psi}i\gamma_5\Psi)^2 - (\bar{\Psi}\gamma_0\gamma_3\Psi)^2, \quad (\text{A41})$$

$$\sum_{j=1}^2 (\bar{\Psi}i\gamma_j\Psi)^2 = -(\bar{\Psi}\gamma_0\Psi)^2 + (\bar{\Psi}\Psi)^2 - (\bar{\Psi}\gamma_0\gamma_5\Psi)^2 - (\bar{\Psi}\gamma_0\gamma_3\Psi)^2, \quad (\text{A42})$$

$$(\bar{\Psi}i\gamma_3\Psi)^2 = -(\bar{\Psi}\gamma_0\gamma_5\Psi)^2 + (\bar{\Psi}i\gamma_5\Psi)^2 + (\bar{\Psi}\gamma_0\gamma_3\Psi)^2. \quad (\text{A43})$$

APPENDIX B: MEAN-FIELD ANALYSIS

Here taking the short-range four-fermion interaction $g_2(\bar{\Psi}\Psi)^2$ as an example, we give the details of the derivation and calculation for the mean-field analysis. Analysis for other kinds of four-fermion interactions could be carried out similarly.

1. Derivation of the self-consistent equation

Under the influence of short-range four-fermion interaction $g_2(\bar{\Psi}\Psi)^2$, the expectation value

$$\Delta_2 = \langle \bar{\Psi}\Psi \rangle \quad (\text{B1})$$

could become finite. Considering the order parameter Δ_2 , the fermion propagator can be written as

$$G(i\omega, \mathbf{k}, \Delta_2) = [i\omega\gamma_0 + iv(k_1\gamma_1 + k_2\gamma_2) + iAk_3^2\gamma_3 + \Delta_2]^{-1}. \quad (\text{B2})$$

For finite temperature, we employ the propagator in Matsubara formalism as follows:

$$G(i\omega_n, \mathbf{k}, \Delta_2) = [i\omega_n\gamma_0 + iv(k_1\gamma_1 + k_2\gamma_2) + iAk_3^2\gamma_3 + \Delta_2]^{-1}, \quad (\text{B3})$$

where $\omega_n = (2n+1)\pi T$ with n being integers and T the temperature.

The partition function is given by

$$\begin{aligned} Z &= \int \mathcal{D}\bar{\Psi} \mathcal{D}\Psi e^{\mathcal{S}} \\ &= \prod_{\omega_n} \prod_{\mathbf{k}} \int \mathcal{D}\bar{\Psi} \mathcal{D}\Psi e^{\bar{\Psi}\omega_n\mathbf{k}\beta G^{-1}(i\omega_n, \mathbf{k}, \Delta_2)\Psi\omega_n\mathbf{k}} e^{-\int d\tau \int d^3\mathbf{x} \frac{\Delta_2^2}{2g_2}}, \end{aligned} \quad (\text{B4})$$

where $\beta = \frac{1}{T}$. Using the functional integral formula

$$\int \mathcal{D}\bar{\eta} \mathcal{D}\eta e^{\bar{\eta}K\eta} = \det K, \quad (\text{B5})$$

we get

$$Z = \prod_{\omega_n} \prod_{\mathbf{k}} \beta^4 \det[G^{-1}(i\omega_n, \mathbf{k}, \Delta_2)] e^{-\int d\tau \int d^3\mathbf{x} \frac{\Delta_2^2}{2g_2}}, \quad (\text{B6})$$

which leads to

$$\begin{aligned} \ln Z &= \sum_{\omega_n} \sum_{\mathbf{k}} \ln\{\beta^4 \det[G^{-1}(i\omega_n, \mathbf{k}, \Delta_2)]\} \\ &\quad - \int d\tau \int d^3\mathbf{x} \frac{\Delta_2^2}{2g_2}. \end{aligned} \quad (\text{B7})$$

It is easy to obtain

$$\det[G^{-1}(i\omega_n, \mathbf{k}, \Delta_2)] = (\omega_n^2 + E_{\mathbf{k}, \Delta_2}^2)^2, \quad (\text{B8})$$

where

$$E_{\mathbf{k}, \Delta_2} = \sqrt{v^2 k_\perp^2 + A^2 k_3^4 + \Delta_2^2}. \quad (\text{B9})$$

Thus we arrive at

$$\begin{aligned} \ln Z &= \sum_{\omega_n} \sum_{\mathbf{k}} \ln [\beta^4 (\omega_n^2 + E_{\mathbf{k}, \Delta_2}^2)^2] \\ &\quad - \int d\tau \int d^3 \mathbf{x} \frac{\Delta_2^2}{2g_2}. \end{aligned} \quad (\text{B10})$$

Carrying out the summarization of frequency, we get

$$\ln Z = 4 \sum_{\mathbf{k}} \ln \left[2 \cosh \left(\frac{E_{\mathbf{k}, \Delta_2}}{2T} \right) \right] - \beta \mathcal{V} \frac{\Delta_2^2}{2g_2}, \quad (\text{B11})$$

where \mathcal{V} is volume of sample.

The free energy density f and free energy F are defined as

$$\begin{aligned} f &= \frac{F}{\mathcal{V}} = -\frac{1}{\beta} \ln Z \\ &= -4T \frac{1}{\mathcal{V}} \sum_{\mathbf{k}} \ln \left[2 \cosh \left(\frac{E_{\mathbf{k}, \Delta_2}}{2T} \right) \right] + \frac{\Delta_2^2}{2g_2}. \end{aligned} \quad (\text{B12})$$

Taking the continuous limit by using the replacement

$$\frac{1}{\mathcal{V}} \sum_{\mathbf{k}} \rightarrow \int \frac{d^3 \mathbf{k}}{(2\pi)^3}, \quad (\text{B13})$$

we obtain

$$f = -4T \int \frac{d^3 \mathbf{k}}{(2\pi)^3} \ln \left[2 \cosh \left(\frac{E_{\mathbf{k}, \Delta_2}}{2T} \right) \right] + \frac{\Delta_2^2}{2g_2}. \quad (\text{B14})$$

The self-consistent equation for Δ_2 is determined by

$$\frac{\partial f}{\partial \Delta_2} = 0. \quad (\text{B15})$$

Concretely, the self-consistent equation is given by

$$1 = 2g_2 \int \frac{d^3 \mathbf{k}}{(2\pi)^3} \tanh \left(\frac{E_{\mathbf{k}, \Delta_2}}{2T} \right) \frac{1}{E_{\mathbf{k}, \Delta_2}}. \quad (\text{B16})$$

At zero temperature, the equation becomes

$$1 = 2g_2 \int \frac{d^3 \mathbf{k}}{(2\pi)^3} \frac{1}{E_{\mathbf{k}, \Delta_2}}. \quad (\text{B17})$$

2. Solving the self-consistent equation

a. Zero temperature

At zero temperature, the self-consistent equation can be written as

$$\begin{aligned} 1 &= 2g_2 \int \frac{d^3 \mathbf{k}}{(2\pi)^3} \frac{1}{\sqrt{v^2 k_\perp^2 + A^2 k_3^4 + \Delta_2^2}} \\ &= \frac{g_2}{\pi^2} \int dk_\perp d|k_3| k_\perp \frac{1}{\sqrt{v^2 k_\perp^2 + A^2 k_3^4 + \Delta_2^2}}. \end{aligned} \quad (\text{B18})$$

We employ the transformations

$$E = \sqrt{v^2 q_\perp^2 + A^2 q_3^4}, \quad \delta = \frac{Aq_3^2}{vq_\perp}, \quad (\text{B19})$$

which are equivalent to

$$q_\perp = \frac{E}{v\sqrt{1+\delta^2}}, \quad |q_3| = \frac{\sqrt{\delta}\sqrt{E}}{\sqrt{A}(1+\delta^2)^{\frac{1}{4}}}. \quad (\text{B20})$$

The integration measures satisfy the relation

$$dq_\perp d|q_3| = \frac{\sqrt{E}}{2v\sqrt{A}\sqrt{\delta}(1+\delta^2)^{\frac{3}{4}}} dE d\delta. \quad (\text{B21})$$

Utilizing the transformations Eqs. (B19)–(B21), we obtain

$$\begin{aligned} 1 &= \frac{g_2}{2\pi^2 v^2 \sqrt{A}} \int_0^\Lambda dE \frac{E^{\frac{3}{2}}}{\sqrt{E^2 + \Delta_2^2}} \int_0^{+\infty} d\delta \frac{1}{\sqrt{\delta}(1+\delta^2)^{\frac{5}{4}}} \\ &= \frac{g_2}{\pi^2 v^2 \sqrt{A}} \int_0^\Lambda dE \frac{E^{\frac{3}{2}}}{\sqrt{E^2 + \Delta_2^2}}. \end{aligned} \quad (\text{B22})$$

It can be further written as

$$1 = \frac{g_2 \Lambda^{\frac{3}{2}}}{\pi^2 v^2 \sqrt{A}} \left[\int_0^1 dx \left(\frac{x^{\frac{3}{2}}}{\sqrt{x^2 + \left(\frac{\Delta_2}{\Lambda}\right)^2}} - x^{\frac{1}{2}} \right) + \frac{2}{3} \right]. \quad (\text{B23})$$

Taking $\Delta_2 = 0$, we can get the critical coupling strength g_{2c} , which satisfies

$$g_{2c} = \frac{3\pi^2 v^2 \sqrt{A}}{2\Lambda^{\frac{3}{2}}}. \quad (\text{B24})$$

In the limit $\Delta_2 \ll \Lambda$, we have

$$\begin{aligned} 1 &\approx \frac{2g_2 \Lambda^{\frac{3}{2}}}{3\pi^2 v^2 \sqrt{A}} \left[1 - \frac{\Gamma(\frac{1}{4})\Gamma(\frac{5}{4})}{\sqrt{\pi}} \left(\frac{\Delta_2}{\Lambda} \right)^{\frac{3}{2}} \right] \\ &= \frac{g_2}{g_{2c}} \left[1 - \frac{\Gamma(\frac{1}{4})\Gamma(\frac{5}{4})}{\sqrt{\pi}} \left(\frac{\Delta_2}{\Lambda} \right)^{\frac{3}{2}} \right]. \end{aligned} \quad (\text{B25})$$

Thus Δ_2 is given by

$$\Delta_2 \approx c_1 \Lambda \frac{(g_2 - g_{2c})^{\frac{2}{3}}}{g_{2c}^{\frac{2}{3}}}, \quad (\text{B26})$$

where

$$c_1 = \left(\frac{\sqrt{\pi}}{\Gamma(\frac{1}{4})\Gamma(\frac{5}{4})} \right)^{\frac{2}{3}} \approx 0.662596. \quad (\text{B27})$$

b. Finite temperature

At finite temperature, the self-consistent equation can be written as

$$\begin{aligned} \frac{1}{g_2} &= \frac{1}{\pi^2} \int dk_\perp d|k_3| k_\perp \frac{1}{\sqrt{v^2 k_\perp^2 + A^2 k_3^4 + \Delta_2^2}} \\ &\quad \times \tanh \left(\frac{\sqrt{v^2 k_\perp^2 + A^2 k_3^4 + \Delta_2^2}}{2T} \right). \end{aligned} \quad (\text{B28})$$

TABLE III. Energy dispersions of fermion excitations considering different order parameters.

Order parameter	Expectation value	Energy dispersion
Δ_1	$\langle \bar{\Psi} \gamma_0 \Psi \rangle$	$E_{\mathbf{k}, \Delta_1}^\pm = \sqrt{v^2 k_\perp^2 + A^2 k_3^4} \pm \Delta_1$
Δ_2	$\langle \bar{\Psi} \Psi \rangle$	$E_{\mathbf{k}, \Delta_2} = \sqrt{v^2 k_\perp^2 + A^2 k_3^4} + \Delta_2^2$
$\Delta_{3\perp}$	$\sum_{j=1,2} \langle \bar{\Psi} \gamma_0 \gamma_j \Psi \rangle$	$E_{\mathbf{k}, \Delta_{3\perp}}^\pm = \sqrt{\frac{1}{2} v^2 (k_1 + k_2)^2 + 2[\Delta_{3\perp} \pm \frac{1}{2} \sqrt{v^2 (k_2 - k_1)^2 + 2A^2 k_3^4}]^2}$
Δ_{3z}	$\langle \bar{\Psi} \gamma_0 \gamma_3 \Psi \rangle$	$E_{\mathbf{k}, \Delta_{3z}}^\pm = \sqrt{(v k_\perp \pm \Delta_{3z})^2 + A^2 k_3^4}$
Δ_4	$\langle \bar{\Psi} \gamma_0 \gamma_5 \Psi \rangle$	$E_{\mathbf{k}, \Delta_4}^\pm = \sqrt{v^2 k_\perp^2 + A^2 k_3^4} \pm \Delta_4$
Δ_5	$\langle \bar{\Psi} i \gamma_5 \Psi \rangle$	$E_{\mathbf{k}, \Delta_5} = \sqrt{v^2 k_\perp^2 + A^2 k_3^4} + \Delta_5^2$
$\Delta_{6\perp}$	$\langle \bar{\Psi} (i \gamma_2 \gamma_3 + i \gamma_3 \gamma_1) \Psi \rangle$	$E_{\mathbf{k}, \Delta_{6\perp}}^\pm = \sqrt{\frac{1}{2} v^2 (k_1 + k_2)^2 + 2[\Delta_{6\perp} \pm \frac{1}{2} \sqrt{v^2 (k_2 - k_1)^2 + 2A^2 k_3^4}]^2}$
Δ_{6z}	$\langle \bar{\Psi} i \gamma_1 \gamma_2 \Psi \rangle$	$E_{\mathbf{k}, \Delta_{6z}}^\pm = \sqrt{(v k_\perp \pm \Delta_{6z})^2 + A^2 k_3^4}$
$\Delta_{7\perp}$	$\sum_{j=1,2} \langle \bar{\Psi} i \gamma_5 \gamma_j \Psi \rangle$	$E_{\mathbf{k}, \Delta_{7\perp}}^\pm = \sqrt{\frac{1}{2} (k_1 - k_2)^2 + A^2 k_3^4} + \frac{1}{2} (k_1 + k_2 \pm 2\Delta_{7\perp})^2$
Δ_{7z}	$\langle \bar{\Psi} i \gamma_5 \gamma_3 \Psi \rangle$	$E_{\mathbf{k}, \Delta_{7z}}^\pm = \sqrt{v^2 k_\perp^2 + (A k_3^2 \pm \Delta_{7z})^2}$
$\Delta_{8\perp}$	$\sum_{j=1,2} \langle \bar{\Psi} i \gamma_j \Psi \rangle$	$E_{\mathbf{k}, \Delta_{8\perp}} = \sqrt{(v k_\perp + \Delta_{8\perp})^2 + (v k_2 + \Delta_{8\perp})^2 + A^2 k_3^4}$
Δ_{8z}	$\langle \bar{\Psi} i \gamma_3 \Psi \rangle$	$E_{\mathbf{k}, \Delta_{8z}} = \sqrt{v^2 k_\perp^2 + (A k_3^2 + \Delta_{8z})^2}$

Employing the transformations, Eqs. (B19)–(B21), and carrying out the integration of δ , we obtain

$$\frac{1}{g_2} = \frac{1}{\pi^2 v^2 \sqrt{A}} \int_0^\Lambda dE \frac{E^{\frac{3}{2}}}{\sqrt{E^2 + \Delta_2^2}} \times \tanh\left(\frac{\sqrt{E^2 + \Delta_2^2}}{2T}\right). \quad (\text{B29})$$

T_c is determined by

$$\begin{aligned} \frac{1}{g_2} &= \frac{1}{\pi^2 v^2 \sqrt{A}} \int_0^\Lambda dE \sqrt{E} \tanh\left(\frac{E}{2T_c}\right) \\ &= \frac{2\sqrt{2} T_c^{\frac{3}{2}}}{\pi^2 v^2 \sqrt{A}} \left[\frac{2}{3} \left(\frac{\Lambda}{2T_c}\right)^{\frac{3}{2}} \tanh\left(\frac{\Lambda}{2T_c}\right) \right. \\ &\quad \left. - \frac{2}{3} \int_0^{\frac{\Lambda}{2T_c}} dx x^{\frac{3}{2}} \frac{1}{\cosh^2(x)} \right]. \quad (\text{B30}) \end{aligned}$$

If $T_c \ll \Lambda$, the equation can be approximated by

$$\begin{aligned} \frac{1}{g_2} &\approx \frac{2\sqrt{2} T_c^{\frac{3}{2}}}{\pi^2 v^2 \sqrt{A}} \left[\frac{2}{3} \left(\frac{\Lambda}{2T_c}\right)^{\frac{3}{2}} - \frac{2}{3} \int_0^{+\infty} dx x^{\frac{3}{2}} \frac{1}{\cosh^2(x)} \right] \\ &= \frac{1}{g_{2c}} - 2\sqrt{2} a \frac{1}{g_{2c}} \left(\frac{T_c}{\Lambda}\right)^{\frac{3}{2}}, \quad (\text{B31}) \end{aligned}$$

where

$$a = \int_0^{+\infty} dx x^{\frac{3}{2}} \frac{1}{\cosh^2(x)} \approx 0.719227. \quad (\text{B32})$$

Then T_c satisfies

$$T_c \approx c_2 \Lambda \frac{(g_2 - g_{2c})^{\frac{2}{3}}}{g_2^{\frac{3}{2}}}, \quad (\text{B33})$$

where $c_2 = 1/(2\sqrt{2}a)^{\frac{2}{3}} \approx 0.622863$.

3. Dispersion of fermions with finite order parameter

Mean-field analysis for other four-fermion couplings can be performed through similar procedures as subsections B 1 and B 2. For convenience, we show the fermion dispersions with various finite order parameters in Table III.

If $\Delta_1 > 0$, the original fermion dispersion $E_{\mathbf{k}} = \sqrt{v^2 k_\perp^2 + A^2 k_3^2}$ becomes two dispersions $E_{\mathbf{k}, \Delta_1}^+$ and $E_{\mathbf{k}, \Delta_1}^-$. $E_{\mathbf{k}, \Delta_1}^+$ is gapped, whereas, $E_{\mathbf{k}, \Delta_1}^-$ is gapless when $\sqrt{v^2 k_\perp^2 + A^2 k_3^2} = \Delta_1$. It indicates that the gapless nodal point becomes gapless on a surface. If $\Delta_2 > 0$, the fermion dispersion becomes $E_{\mathbf{k}, \Delta_2}$, which is gapped. If $\Delta_{3\perp} > 0$, there are two fermion dispersions $E_{\mathbf{k}, \Delta_{3\perp}}^+$ and $E_{\mathbf{k}, \Delta_{3\perp}}^-$. We find that $E_{\mathbf{k}, \Delta_{3\perp}}^+$ is gapped, but $E_{\mathbf{k}, \Delta_{3\perp}}^-$ is gapless along a nodal line which is determined by

$$k_1 + k_2 = 0, \quad (\text{B34})$$

$$\frac{1}{2} \sqrt{v^2 (k_2 - k_1)^2 + 2A^2 k_3^4} = \Delta_{3\perp}. \quad (\text{B35})$$

If $\Delta_{3z} > 0$, one dispersion $E_{\mathbf{k}, \Delta_{3z}}^+$ is gapped, but another dispersion $E_{\mathbf{k}, \Delta_{3z}}^-$ is gapless along a nodal line which is decided by $v k_\perp = \Delta_{3z}$ and $k_3 = 0$. If $\Delta_4 > 0$, the dispersion $E_{\mathbf{k}, \Delta_4}^+$ is gapped, whereas $E_{\mathbf{k}, \Delta_4}^-$ is gapless on the surface which satisfies $\sqrt{v^2 k_\perp^2 + A^2 k_3^2} = \Delta_4$. If $\Delta_5 > 0$, the corresponding fermion dispersion $E_{\mathbf{k}, \Delta_5}$ is gapped. If $\Delta_{6\perp} > 0$, the dispersion $E_{\mathbf{k}, \Delta_{6\perp}}^+$ is gapped, but the dispersion $E_{\mathbf{k}, \Delta_{6\perp}}^-$ is gapless along a nodal line which satisfies

$$k_1 + k_2 = 0, \quad (\text{B36})$$

$$\frac{1}{2} \sqrt{v^2 (k_2 - k_1)^2 + 2A^2 k_3^4} = \Delta_{6\perp}. \quad (\text{B37})$$

If $\Delta_{6z} > 0$, we can find that one dispersion $E_{\mathbf{k}, \Delta_{6z}}^+$ is gapped, but another dispersion $E_{\mathbf{k}, \Delta_{6z}}^-$ is gapless along a nodal line which is determined by $v k_\perp = \Delta_{6z}$ and $k_3 = 0$. If $\Delta_{7\perp} > 0$, there are two fermion dispersions $E_{\mathbf{k}, \Delta_{7\perp}}^+$ and $E_{\mathbf{k}, \Delta_{7\perp}}^-$. It is easy to verify that $E_{\mathbf{k}, \Delta_{7\perp}}^+$ is gapless at the point $(-\Delta_{7\perp}, -\Delta_{7\perp}, 0)$ and $E_{\mathbf{k}, \Delta_{7\perp}}^-$ is gapless at $(\Delta_{7\perp}, \Delta_{7\perp}, 0)$. At these two gapless

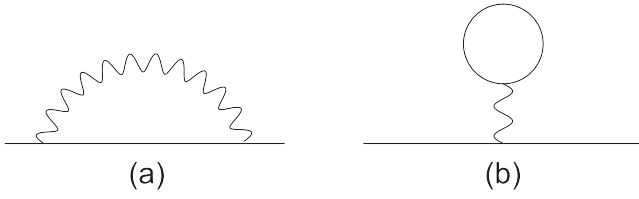


FIG. 6. Feynman diagrams for the self-energies of fermions induced by four-fermion interactions. Solid line represents the fermion propagator and wavy line stands for the four-fermion interaction.

points, the fermion dispersions are still linear within the xy plane and quadratic along the z axis. If $\Delta_{7z} > 0$, we can find that one dispersion $E_{\mathbf{k}, \Delta_{7z}}^+$ is gapped, but another dispersion $E_{\mathbf{k}, \Delta_{7z}}^-$ is gapless at two points

$$\mathbf{k}_a = \left(0, 0, \sqrt{\frac{\Delta_{7z}}{A}}\right), \quad \mathbf{k}_b = \left(0, 0, -\sqrt{\frac{\Delta_{7z}}{A}}\right). \quad (\text{B38})$$

At these two gapless points, the fermion dispersion can be written as

$$E_{\mathbf{k}, \Delta_{7z}} = \sqrt{v^2 K_{\perp}^2 + v_z^2 K_z^2}, \quad (\text{B39})$$

with $v_z = 2\sqrt{A\Delta_{7z}}$ and \mathbf{K} being the momentum relative to the point \mathbf{k}_a or \mathbf{k}_b . It is clear that this fermion dispersion is linear within the xy plane and also linear along the z axis. If $\Delta_{8\perp} > 0$, the fermion dispersion $E_{\mathbf{k}, \Delta_{8\perp}}$ is gapless at the point $(-\Delta_{8\perp}/v, -\Delta_{8\perp}/v, 0)$. If $\Delta_{8z} > 0$, the fermion dispersion $E_{\mathbf{k}, \Delta_{8z}} > 0$ is gapped.

APPENDIX C: DERIVATION OF THE RG EQUATIONS FOR THE STRENGTH OF FOUR-FERMION COUPLINGS

1. Self-energy of the fermions

The fermion propagator reads as

$$G_0(i\omega, \mathbf{k}) = -\frac{i\omega\gamma_0 + iv(k_1\gamma_1 + k_2\gamma_2) + iAk_3^2\gamma_3}{\omega^2 + E_{\mathbf{k}}^2}, \quad (\text{C1})$$

where $E_{\mathbf{k}} = \sqrt{v^2 k_{\perp}^2 + A^2 k_3^4}$ with $k_{\perp}^2 = k_1^2 + k_2^2$. The self-energy of fermions resulting from Fig. 6(a) takes the form

$$\Sigma_1 = \sum_a g_a \int_{-\infty}^{+\infty} \frac{d\omega}{2\pi} \int' \frac{d^3\mathbf{k}}{(2\pi)^3} \Gamma_a G_0(\omega, \mathbf{k}) \Gamma_a, \quad (\text{C2})$$

where

$$\sum_a \equiv \sum_{a=1,2,4,5,3z}. \quad (\text{C3})$$

\int' represents that a momentum shell will be properly taken. Figure 6(b) induces the self-energy of fermions as follows:

$$\Sigma_2 = \sum_a g_a \int_{-\infty}^{+\infty} \frac{d\omega}{2\pi} \int' \frac{d^3\mathbf{k}}{(2\pi)^3} \text{Tr}[G_0(\omega, \mathbf{k}) \Gamma_a]. \quad (\text{C4})$$

Substituting Eq. (C1) into Eqs. (C2) and (C4), we obtain

$$\Sigma_1 = 0, \quad (\text{C5})$$

$$\Sigma_2 = 0. \quad (\text{C6})$$

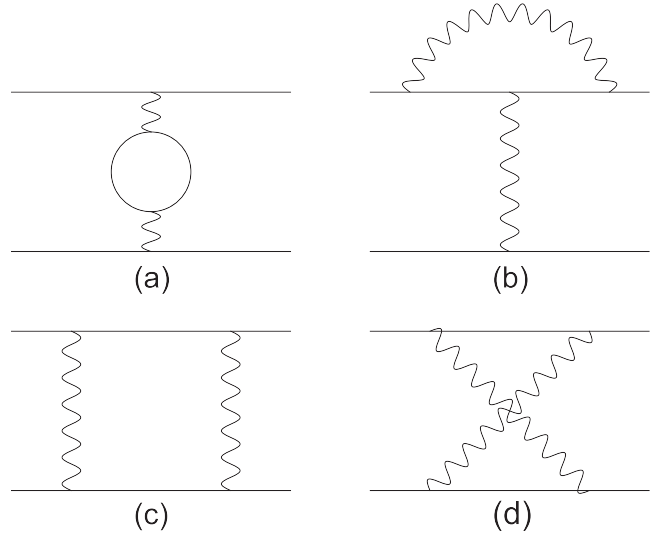


FIG. 7. One-loop Feynman diagrams for the corrections to the four-fermion couplings.

It should be noted that a generated constant term in Σ_1 has been discarded. The generated constant term in self-energy is also discarded in the study about long-range Coulomb interaction in 3D semi-DSM [38]. According to Eqs. (C5) and (C6), the fermion propagator is not renormalized by the four-fermion interactions to one-loop order.

For the five independent four-fermion interactions shown in Eq. (22), there is not a constant term in Σ_2 and Σ_2 always equals zero. If we consider the four-fermion interaction $(\bar{\Psi}i\gamma_3\Psi)^2$, we can find that there is a constant term in Σ_2 . This constant term is actually a correction for the chemical potential μ . This constant term could modify the chemical potential μ from zero to finite and thus drive the Fermi level away from the node. In this case, we assume that the system parameters (for example, gate voltage, pressure, etc.) are fine-tuned in such a way that effective chemical potential is zero. This way we can study the influence of interactions on 3D semi-DSM with zero chemical potential.

2. One-loop corrections for the four-fermion couplings

Figure 7(a) leads to the correction

$$V_a^{(1)} = -2g_a^2 (\bar{\Psi}\Gamma_a\Psi)^2 \int_{-\infty}^{+\infty} \frac{d\omega}{2\pi} \int' \frac{d^3\mathbf{k}}{(2\pi)^3} \times \text{Tr}[\Gamma_a G_0(i\omega, \mathbf{k}) \Gamma_a G_0(i\omega, \mathbf{k})]. \quad (\text{C7})$$

Figure 7(b) results in the correction

$$V_a^{(2)} = \sum_b V_{ab}^{(2)}, \quad (\text{C8})$$

where

$$V_{ab}^{(2)} = 4g_a g_b (\bar{\Psi}\Gamma_a\Psi) \int_{-\infty}^{+\infty} \frac{d\omega}{2\pi} \int' \frac{d^3\mathbf{k}}{(2\pi)^3} \times [\bar{\Psi}\Gamma_b G_0(i\omega, \mathbf{k}) \Gamma_a G_0(i\omega, \mathbf{k}) \Gamma_b \Psi]. \quad (\text{C9})$$

Figures 7(c) and 7(d) induce the correction

$$V^{(3)+(4)} = \sum_a \sum_{a \leq b} V_{ab}^{(3)+(4)}, \quad (\text{C10})$$

where

$$V_{ab}^{(3)+(4)} = 4g_a g_b \int_{-\infty}^{+\infty} \frac{d\omega}{2\pi} \int' \frac{d^3\mathbf{k}}{(2\pi)^3} [\bar{\Psi} \Gamma_a G_0(i\omega, \mathbf{k}) \Gamma_b \Psi] \bar{\Psi} \{[\Gamma_b G_0(i\omega, \mathbf{k}) \Gamma_a + \Gamma_a G_0(-i\omega, -\mathbf{k}) \Gamma_b]\} \Psi. \quad (\text{C11})$$

Substituting Eq. (C1) into Eq. (C7), we obtain

$$V_a^{(1)} = \delta g_a^{(1)} (\bar{\Psi} \Gamma_a \Psi)^2, \quad (\text{C12})$$

where

$$\delta g_1^{(1)} = 0, \quad (\text{C13})$$

$$\delta g_2^{(1)} = g_2^2 \frac{2\Lambda^{\frac{3}{2}}}{\pi^2 v^2 \sqrt{A}} \ell, \quad (\text{C14})$$

$$\delta g_4^{(1)} = 0, \quad (\text{C15})$$

$$\delta g_5^{(1)} = g_5^2 \frac{2\Lambda^{\frac{3}{2}}}{\pi^2 v^2 \sqrt{A}} \ell, \quad (\text{C16})$$

$$\delta g_{3z}^{(1)} = g_{3z}^2 \frac{2\Lambda^{\frac{3}{2}}}{5\pi^2 v^2 \sqrt{A}} \ell. \quad (\text{C17})$$

Substituting Eq. (C1) into Eqs. (C8) and (C9), we find that the contribution from Fig. 7(b) can be written as

$$V_a^{(2)} = \delta g_a^{(2)} (\bar{\Psi} \Gamma_a \Psi)^2, \quad (\text{C18})$$

where

$$\delta g_1^{(2)} = 0, \quad (\text{C19})$$

$$\delta g_2^{(2)} = (-g_2 g_1 - g_2^2 + g_2 g_4 + g_2 g_5 + g_2 g_{3z}) \frac{\Lambda^{\frac{3}{2}}}{\pi^2 v^2 \sqrt{A}} \ell, \quad (\text{C20})$$

$$\delta g_4^{(2)} = 0, \quad (\text{C21})$$

$$\delta g_5^{(2)} = (-g_5 g_1 + g_5 g_2 + g_5 g_4 - g_5^2 - g_5 g_{3z}) \frac{\Lambda^{\frac{3}{2}}}{\pi^2 v^2 \sqrt{A}} \ell, \quad (\text{C22})$$

$$\delta g_{3z}^{(2)} = (-g_{3z} g_1 + g_{3z} g_2 + g_{3z} g_4 - g_{3z} g_5 - g_{3z}^2) \frac{\Lambda^{\frac{3}{2}}}{5\pi^2 v^2 \sqrt{A}} \ell. \quad (\text{C23})$$

Substituting Eq. (C1) into Eq. (C11), the contribution from Figs. 7(c) and 7(d) can be written as

$$V_{1,1}^{(3)+(4)} = g_1^2 \frac{\Lambda^{\frac{3}{2}}}{5\pi^2 v^2 \sqrt{A}} \ell (\bar{\Psi} i\gamma_3 \Psi)^2, \quad (\text{C24})$$

$$V_{2,2}^{(3)+(4)} = g_2^2 \frac{\Lambda^{\frac{3}{2}}}{5\pi^2 v^2 \sqrt{A}} \ell (\bar{\Psi} i\gamma_3 \Psi)^2, \quad (\text{C25})$$

$$V_{4,4}^{(3)+(4)} = g_4^2 \frac{\Lambda^{\frac{3}{2}}}{5\pi^2 v^2 \sqrt{A}} \ell (\bar{\Psi} i\gamma_3 \Psi)^2, \quad (\text{C26})$$

$$V_{5,5}^{(3)+(4)} = g_5^2 \frac{\Lambda^{\frac{3}{2}}}{5\pi^2 v^2 \sqrt{A}} \ell (\bar{\Psi} i\gamma_3 \Psi)^2, \quad (\text{C27})$$

$$V_{3z,3z}^{(3)+(4)} = g_{3z}^2 \frac{\Lambda^{\frac{3}{2}}}{5\pi^2 v^2 \sqrt{A}} \ell (\bar{\Psi} i\gamma_3 \Psi)^2, \quad (\text{C28})$$

$$V_{1,2}^{(3)+(4)} = g_1 g_2 \frac{2\Lambda^{\frac{3}{2}}}{5\pi^2 v^2 \sqrt{A}} \ell \sum_{j=1}^2 (\bar{\Psi} \gamma_0 \gamma_j \Psi)^2, \quad (\text{C29})$$

$$V_{1,4}^{(3)+(4)} = g_1 g_4 \frac{\Lambda^{\frac{3}{2}}}{5\pi^2 v^2 \sqrt{A}} \ell (\bar{\Psi} i\gamma_5 \gamma_3 \Psi)^2, \quad (\text{C30})$$

$$V_{1,5}^{(3)+(4)} = g_1 g_5 \frac{2\Lambda^{\frac{3}{2}}}{5\pi^2 v^2 \sqrt{A}} \ell \sum_{\langle\langle lk \rangle\rangle} (\bar{\Psi} i \gamma_l \gamma_k \Psi)^2, \quad (\text{C31})$$

$$V_{1,3z}^{(3)+(4)} = 0, \quad (\text{C32})$$

$$V_{2,4}^{(3)+(4)} = -g_2 g_4 \frac{\Lambda^{\frac{3}{2}}}{\pi^2 v^2 \sqrt{A}} \ell (\bar{\Psi} i \gamma_5 \Psi)^2 + g_2 g_4 \frac{\Lambda^{\frac{3}{2}}}{5\pi^2 v^2 \sqrt{A}} \ell (\bar{\Psi} i \gamma_1 \gamma_2 \Psi)^2, \quad (\text{C33})$$

$$V_{2,5}^{(3)+(4)} = -g_2 g_5 \frac{\Lambda^{\frac{3}{2}}}{\pi^2 v^2 \sqrt{A}} \ell (\bar{\Psi} \gamma_0 \gamma_5 \Psi)^2 + g_2 g_5 \sum_{j=1}^2 \frac{2\Lambda^{\frac{3}{2}}}{5\pi^2 v^2 \sqrt{A}} \ell (\bar{\Psi} i \gamma_5 \gamma_j \Psi)^2, \quad (\text{C34})$$

$$V_{2,3z}^{(3)+(4)} = -g_2 g_{3z} \frac{\Lambda^{\frac{3}{2}}}{\pi^2 v^2 \sqrt{A}} \ell (\bar{\Psi} i \gamma_3 \Psi)^2, \quad (\text{C35})$$

$$V_{4,5}^{(3)+(4)} = -g_4 g_5 \frac{\Lambda^{\frac{3}{2}}}{\pi^2 v^2 \sqrt{A}} \ell (\bar{\Psi} \Psi)^2 + g_4 g_5 \frac{\Lambda^{\frac{3}{2}}}{5\pi^2 v^2 \sqrt{A}} \ell (\bar{\Psi} \gamma_0 \gamma_3 \Psi)^2, \quad (\text{C36})$$

$$V_{4,3z}^{(3)+(4)} = -g_4 g_{3z} \frac{\Lambda^{\frac{3}{2}}}{\pi^2 v^2 \sqrt{A}} \ell (\bar{\Psi} i \gamma_1 \gamma_2 \Psi)^2 + g_4 g_{3z} \sum_{j=1}^2 \frac{2\Lambda^{\frac{3}{2}}}{5\pi^2 v^2 \sqrt{A}} \ell (\bar{\Psi} \gamma_0 \gamma_j \Psi)^2 + g_4 g_{3z} \frac{\Lambda^{\frac{3}{2}}}{5\pi^2 v^2 \sqrt{A}} \ell (\bar{\Psi} i \gamma_5 \Psi)^2, \quad (\text{C37})$$

$$V_{5,3z}^{(3)+(4)} = g_5 g_{3z} \sum_{j=1}^2 \frac{2\Lambda^{\frac{3}{2}}}{5\pi^2 v^2 \sqrt{A}} \ell (\bar{\Psi} i \gamma_j \Psi)^2 + g_5 g_{3z} \frac{\Lambda^{\frac{3}{2}}}{5\pi^2 v^2 \sqrt{A}} \ell (\bar{\Psi} \gamma_0 \gamma_5 \Psi)^2. \quad (\text{C38})$$

Using the relations shown in Eqs. (A37)–(A43), we further get

$$V_{1,1}^{(3)+(4)} = g_0^2 \frac{\Lambda^{\frac{3}{2}}}{5\pi^2 v^2 \sqrt{A}} \ell [-(\bar{\Psi} \gamma_0 \gamma_5 \Psi)^2 + (\bar{\Psi} i \gamma_5 \Psi)^2 + (\bar{\Psi} \gamma_0 \gamma_3 \Psi)^2], \quad (\text{C39})$$

$$V_{2,2}^{(3)+(4)} = g_2^2 \frac{\Lambda^{\frac{3}{2}}}{5\pi^2 v^2 \sqrt{A}} \ell [-(\bar{\Psi} \gamma_0 \gamma_5 \Psi)^2 + (\bar{\Psi} i \gamma_5 \Psi)^2 + (\bar{\Psi} \gamma_0 \gamma_3 \Psi)^2], \quad (\text{C40})$$

$$V_{4,4}^{(3)+(4)} = g_4^2 \frac{\Lambda^{\frac{3}{2}}}{5\pi^2 v^2 \sqrt{A}} \ell [-(\bar{\Psi} \gamma_0 \gamma_5 \Psi)^2 + (\bar{\Psi} i \gamma_5 \Psi)^2 + (\bar{\Psi} \gamma_0 \gamma_3 \Psi)^2], \quad (\text{C41})$$

$$V_{5,5}^{(3)+(4)} = g_5^2 \frac{\Lambda^{\frac{3}{2}}}{5\pi^2 v^2 \sqrt{A}} \ell [-(\bar{\Psi} \gamma_0 \gamma_5 \Psi)^2 + (\bar{\Psi} i \gamma_5 \Psi)^2 + (\bar{\Psi} \gamma_0 \gamma_3 \Psi)^2], \quad (\text{C42})$$

$$V_{3z,3z}^{(3)+(4)} = g_{3z}^2 \frac{\Lambda^{\frac{3}{2}}}{5\pi^2 v^2 \sqrt{A}} \ell [-(\bar{\Psi} \gamma_0 \gamma_5 \Psi)^2 + (\bar{\Psi} i \gamma_5 \Psi)^2 + (\bar{\Psi} \gamma_0 \gamma_3 \Psi)^2], \quad (\text{C43})$$

$$V_{1,2}^{(3)+(4)} = g_1 g_2 \frac{2\Lambda^{\frac{3}{2}}}{5\pi^2 v^2 \sqrt{A}} \ell [-(\bar{\Psi} \gamma_0 \Psi)^2 + (\bar{\Psi} \Psi)^2 + (\bar{\Psi} \gamma_0 \gamma_5 \Psi)^2 - 2(\bar{\Psi} i \gamma_5 \Psi)^2 - (\bar{\Psi} \gamma_0 \gamma_3 \Psi)^2], \quad (\text{C44})$$

$$V_{1,4}^{(3)+(4)} = g_1 g_4 \frac{\Lambda^{\frac{3}{2}}}{5\pi^2 v^2 \sqrt{A}} \ell [-(\bar{\Psi} \gamma_0 \Psi)^2 - (\bar{\Psi} i \gamma_5 \Psi)^2 - (\bar{\Psi} \gamma_0 \gamma_3 \Psi)^2], \quad (\text{C45})$$

$$V_{1,5}^{(3)+(4)} = g_1 g_5 \frac{2\Lambda^{\frac{3}{2}}}{5\pi^2 v^2 \sqrt{A}} \ell [-(\bar{\Psi} \gamma_0 \Psi)^2 - (\bar{\Psi} \Psi)^2 + (\bar{\Psi} \gamma_0 \gamma_5 \Psi)^2 - (\bar{\Psi} \gamma_0 \gamma_3 \Psi)^2], \quad (\text{C46})$$

$$V_{1,3z}^{(3)+(4)} = 0, \quad (\text{C47})$$

$$V_{2,4}^{(3)+(4)} = g_2 g_4 \frac{\Lambda^{\frac{3}{2}}}{5\pi^2 v^2 \sqrt{A}} \ell [-(\bar{\Psi} \Psi)^2 - 4(\bar{\Psi} i \gamma_5 \Psi)^2 + (\bar{\Psi} \gamma_0 \gamma_3 \Psi)^2], \quad (\text{C48})$$

$$V_{2,5}^{(3)+(4)} = g_2 g_5 \frac{2\Lambda^{\frac{3}{2}}}{5\pi^2 v^2 \sqrt{A}} \ell \left[-(\bar{\Psi} \gamma_0 \Psi)^2 - (\bar{\Psi} \Psi)^2 - \frac{7}{2}(\bar{\Psi} \gamma_0 \gamma_5 \Psi)^2 + (\bar{\Psi} \gamma_0 \gamma_3 \Psi)^2 \right], \quad (\text{C49})$$

$$V_{2,3z}^{(3)+(4)} = -g_2 g_{3z} \frac{\Lambda^{\frac{3}{2}}}{\pi^2 v^2 \sqrt{A}} \ell [-(\bar{\Psi} \gamma_0 \gamma_5 \Psi)^2 + (\bar{\Psi} i \gamma_5 \Psi)^2 + (\bar{\Psi} \gamma_0 \gamma_3 \Psi)^2], \quad (\text{C50})$$

$$V_{4,5}^{(3)+(4)} = g_4 g_5 \frac{\Lambda^{\frac{3}{2}}}{5\pi^2 v^2 \sqrt{A}} \ell [-5(\bar{\Psi} \Psi)^2 + (\bar{\Psi} \gamma_0 \gamma_3 \Psi)^2], \quad (\text{C51})$$

$$V_{4,3z}^{(3)+(4)} = g_4 g_{3z} \frac{2\Lambda^{\frac{3}{2}}}{5\pi^2 v^2 \sqrt{A}} \ell \left[-(\bar{\Psi} \gamma_0 \Psi)^2 + \frac{7}{2}(\bar{\Psi} \Psi)^2 + (\bar{\Psi} \gamma_0 \gamma_5 \Psi)^2 - 4(\bar{\Psi} i \gamma_5 \Psi)^2 - \frac{7}{2}(\bar{\Psi} \gamma_0 \gamma_3 \Psi)^2 \right], \quad (\text{C52})$$

$$V_{5,3z}^{(3)+(4)} = g_5 g_{3z} \frac{2\Lambda^{\frac{3}{2}}}{5\pi^2 v^2 \sqrt{A}} \ell \left[-(\bar{\Psi} \gamma_0 \Psi)^2 + (\bar{\Psi} \Psi)^2 - \frac{1}{2}(\bar{\Psi} \gamma_0 \gamma_5 \Psi)^2 - (\bar{\Psi} \gamma_0 \gamma_3 \Psi)^2 \right]. \quad (\text{C53})$$

Thus the contribution from Figs. 7(c) and 7(d) is given by

$$V^{(3)+(4)} = \sum_{a=1,2,4,5,3z} \sum_{a \leq b} V_{ab}^{(3)+(4)} = \sum_{a=1,2,4,5,3z} \delta g_a^{(3)+(4)} (\bar{\Psi} \Gamma_a \Psi)^2, \quad (\text{C54})$$

where

$$\delta g_1^{(3)+(4)} = \left(-g_1 g_2 - \frac{1}{2} g_1 g_4 - g_1 g_5 - g_2 g_5 - g_4 g_{3z} - g_5 g_{3z} \right) \frac{2\Lambda^{\frac{3}{2}}}{5\pi^2 v^2 \sqrt{A}} \ell, \quad (\text{C55})$$

$$\delta g_2^{(3)+(4)} = \left(g_1 g_2 - g_1 g_5 - \frac{1}{2} g_2 g_4 - g_2 g_5 - \frac{5}{2} g_4 g_5 + \frac{7}{2} g_4 g_{3z} + g_5 g_{3z} \right) \frac{2\Lambda^{\frac{3}{2}}}{5\pi^2 v^2 \sqrt{A}} \ell, \quad (\text{C56})$$

$$\delta g_4^{(3)+(4)} = \left(-\frac{1}{2} g_1^2 - \frac{1}{2} g_2^2 - \frac{1}{2} g_4^2 - \frac{1}{2} g_5^2 - \frac{1}{2} g_{3z}^2 + g_1 g_2 + g_1 g_5 - \frac{7}{2} g_2 g_5 + \frac{5}{2} g_2 g_{3z} + g_4 g_{3z} - \frac{1}{2} g_5 g_{3z} \right) \frac{2\Lambda^{\frac{3}{2}}}{5\pi^2 v^2 \sqrt{A}} \ell, \quad (\text{C57})$$

$$\delta g_5^{(3)+(4)} = \left(\frac{1}{2} g_1^2 + \frac{1}{2} g_2^2 + \frac{1}{2} g_4^2 + \frac{1}{2} g_5^2 + \frac{1}{2} g_{3z}^2 - 2g_1 g_2 - \frac{1}{2} g_1 g_4 - 2g_2 g_4 - \frac{5}{2} g_2 g_{3z} - 4g_4 g_{3z} \right) \frac{2\Lambda^{\frac{3}{2}}}{5\pi^2 v^2 \sqrt{A}} \ell, \quad (\text{C58})$$

$$\delta g_{3z}^{(3)+(4)} = \left(\frac{1}{2} g_1^2 + \frac{1}{2} g_2^2 + \frac{1}{2} g_4^2 + \frac{1}{2} g_5^2 + \frac{1}{2} g_{3z}^2 - g_1 g_2 - \frac{1}{2} g_1 g_4 - g_1 g_5 + \frac{1}{2} g_2 g_4 + g_2 g_5 - \frac{5}{2} g_2 g_{3z} \right. \\ \left. + \frac{1}{2} g_4 g_5 - \frac{7}{2} g_4 g_{3z} - g_5 g_{3z} \right) \frac{2\Lambda^{\frac{3}{2}}}{5\pi^2 v^2 \sqrt{A}} \ell. \quad (\text{C59})$$

As shown above, the one-loop corrections are proportional to $\Lambda^{\frac{3}{2}}$. This characteristic actually is easy to see from the expressions of the one-loop corrections to four-fermion interactions. From Eqs. (C7) to (C11), we can find that the one-loop corrections should be proportional to

$$\frac{\Lambda^{\frac{z_{\perp} + z_3}{2}}}{\Lambda} = \Lambda^{\frac{3}{2}}, \quad (\text{C60})$$

where $z_{\perp} = 1$ and $z_3 = 2$. The numerator $\Lambda^{\frac{z_{\perp} + z_3}{2}} = \Lambda^{\frac{5}{2}}$ comes from the integral measure $\int' d^3 \mathbf{k}$. The denominator Λ results from the expression of integrand after the integration of energy ω is carried out.

From the above results, we obtain

$$\delta g_a = \delta g_a^{(1)} + \delta g_a^{(2)} + \delta g_a^{(3)+(4)}. \quad (\text{C61})$$

Concretely,

$$\delta g_1 = \left(-g_1 g_2 - \frac{1}{2} g_1 g_4 - g_1 g_5 - g_2 g_5 - g_4 g_{3z} - g_5 g_{3z} \right) \frac{2\Lambda^{\frac{3}{2}}}{5\pi^2 v^2 \sqrt{A}} \ell, \quad (\text{C62})$$

$$\delta g_2 = \left(\frac{5}{2} g_2^2 - \frac{3}{2} g_1 g_2 - g_1 g_5 + 2g_2 g_4 + \frac{3}{2} g_2 g_5 + \frac{5}{2} g_2 g_{3z} - \frac{5}{2} g_4 g_5 + \frac{7}{2} g_4 g_{3z} + g_5 g_{3z} \right) \frac{2\Lambda^{\frac{3}{2}}}{5\pi^2 v^2 \sqrt{A}} \ell, \quad (\text{C63})$$

$$\delta g_4 = \left(-\frac{1}{2} g_1^2 - \frac{1}{2} g_2^2 - \frac{1}{2} g_4^2 - \frac{1}{2} g_5^2 - \frac{1}{2} g_{3z}^2 + g_1 g_2 + g_1 g_5 - \frac{7}{2} g_2 g_5 + \frac{5}{2} g_2 g_{3z} + g_4 g_{3z} - \frac{1}{2} g_5 g_{3z} \right) \frac{2\Lambda^{\frac{3}{2}}}{5\pi^2 v^2 \sqrt{A}} \ell, \quad (\text{C64})$$

$$\delta g_5 = \left(\frac{1}{2} g_1^2 + \frac{1}{2} g_2^2 + \frac{1}{2} g_4^2 + 3g_5^2 + \frac{1}{2} g_{3z}^2 - 2g_1 g_2 - \frac{1}{2} g_1 g_4 - \frac{5}{2} g_1 g_5 - 2g_2 g_4 + \frac{5}{2} g_2 g_5 - \frac{5}{2} g_2 g_{3z} \right. \\ \left. + \frac{5}{2} g_4 g_5 - 4g_4 g_{3z} - \frac{5}{2} g_5 g_{3z} \right) \frac{2\Lambda^{\frac{3}{2}}}{5\pi^2 v^2 \sqrt{A}} \ell, \quad (\text{C65})$$

$$\delta g_{3z} = \left(\frac{1}{2} g_1^2 + \frac{1}{2} g_2^2 + \frac{1}{2} g_4^2 + \frac{1}{2} g_5^2 + g_{3z}^2 - g_1 g_2 - \frac{1}{2} g_1 g_4 - g_1 g_5 - \frac{1}{2} g_1 g_{3z} + \frac{1}{2} g_2 g_4 + g_2 g_5 - 2g_2 g_{3z} \right. \\ \left. + \frac{1}{2} g_4 g_5 - 3g_4 g_{3z} - \frac{3}{2} g_5 g_{3z} \right) \frac{2\Lambda^{\frac{3}{2}}}{5\pi^2 v^2 \sqrt{A}} \ell. \quad (\text{C66})$$

3. Scaling transformations

The free action of fermions is

$$S_{\Psi} = \int \frac{d\omega}{2\pi} \frac{d^3 \mathbf{k}}{(2\pi)^3} \bar{\Psi}(\omega, \mathbf{k}) (i\omega \gamma_0 + ivk_1 \gamma_1 + ivk_2 \gamma_2 + iAk_3^2 \gamma_3) \Psi(\omega, \mathbf{k}). \quad (\text{C67})$$

The fermion self-energy induced by four-fermion interactions to one-loop order vanishes. Thus the form of action S_Ψ is not changed. Employing the transformations

$$\omega = \omega' e^{-\ell}, \quad (\text{C68})$$

$$k_1 = k'_1 e^{-\ell}, \quad (\text{C69})$$

$$k_2 = k'_2 e^{-\ell}, \quad (\text{C70})$$

$$k_3 = k'_3 e^{-\frac{\ell}{2}}, \quad (\text{C71})$$

$$v = v', \quad (\text{C72})$$

$$A = A', \quad (\text{C73})$$

$$\Psi = \Psi' e^{\frac{3}{2}\ell}, \quad (\text{C74})$$

the action becomes

$$S_{\Psi'} = \int \frac{d\omega'}{2\pi} \frac{d^3\mathbf{k}'}{(2\pi)^3} \bar{\Psi}'(\omega', \mathbf{k}') (i\omega' \gamma_0 + iv' k'_1 \gamma_1 + iv' k'_2 \gamma_2 + iA' k'_3 \gamma_3) \Psi'(\omega', \mathbf{k}'), \quad (\text{C75})$$

which has the same form as the original action.

The original action of four-fermion interactions takes the form

$$S_{\Psi^4} = \sum_{a=1,2,4,5,3z} g_a \int \frac{d\omega_1}{2\pi} \frac{d^3\mathbf{k}_1}{(2\pi)^3} \frac{d\omega_2}{2\pi} \frac{d^3\mathbf{k}_2}{(2\pi)^3} \frac{d\omega_3}{2\pi} \frac{d^3\mathbf{k}_3}{(2\pi)^3} \bar{\Psi}(\omega_1, \mathbf{k}_1) \Gamma_a \Psi(\omega_2, \mathbf{k}_2) \bar{\Psi}(\omega_3, \mathbf{k}_3) \Gamma_a \Psi(\omega_1 - \omega_2 + \omega_3, \mathbf{k}_1 - \mathbf{k}_2 + \mathbf{k}_3). \quad (\text{C76})$$

Including the one-loop order correction, the action becomes

$$S_{\Psi^4} = \sum_{a=1,2,4,5,3z} (g_a + \delta g_a) \int \frac{d\omega_1}{2\pi} \frac{d^3\mathbf{k}_1}{(2\pi)^3} \frac{d\omega_2}{2\pi} \frac{d^3\mathbf{k}_2}{(2\pi)^3} \frac{d\omega_3}{2\pi} \frac{d^3\mathbf{k}_3}{(2\pi)^3} \bar{\Psi}(\omega_1, \mathbf{k}_1) \Gamma_a \Psi(\omega_2, \mathbf{k}_2) \bar{\Psi}(\omega_3, \mathbf{k}_3) \Gamma_a \times \Psi(\omega_1 - \omega_2 + \omega_3, \mathbf{k}_1 - \mathbf{k}_2 + \mathbf{k}_3). \quad (\text{C77})$$

Utilizing the transformations Eqs. (C68)–(C71) and (C74), we get

$$S_{\Psi^4} = \sum_{a=1,2,4,5,3z} (g_a + \delta g_a) e^{-\frac{3}{2}\ell} \int \frac{d\omega'_1}{2\pi} \frac{d^3\mathbf{k}'_1}{(2\pi)^3} \frac{d\omega'_2}{2\pi} \frac{d^3\mathbf{k}'_2}{(2\pi)^3} \frac{d\omega'_3}{2\pi} \frac{d^3\mathbf{k}'_3}{(2\pi)^3} \bar{\Psi}'(\omega'_1, \mathbf{k}'_1) \Gamma_a \Psi'(\omega'_2, \mathbf{k}'_2) \bar{\Psi}'(\omega'_3, \mathbf{k}'_3) \Gamma_a \times \Psi'(\omega'_1 - \omega'_2 + \omega'_3, \mathbf{k}'_1 - \mathbf{k}'_2 + \mathbf{k}'_3). \quad (\text{C78})$$

Letting

$$g'_a = (g_a + \delta g_a) e^{-\frac{3}{2}\ell} \approx g_a - \frac{3}{2} g_a \ell + \delta g_a, \quad (\text{C79})$$

we obtain

$$S_{\Psi^4} = \sum_{a=1,2,4,5,3z} g'_a \int \frac{d\omega'_1}{2\pi} \frac{d^3\mathbf{k}'_1}{(2\pi)^3} \frac{d\omega'_2}{2\pi} \frac{d^3\mathbf{k}'_2}{(2\pi)^3} \frac{d\omega'_3}{2\pi} \frac{d^3\mathbf{k}'_3}{(2\pi)^3} \bar{\Psi}'(\omega'_1, \mathbf{k}'_1) \Gamma_a \Psi'(\omega'_2, \mathbf{k}'_2) \bar{\Psi}'(\omega'_3, \mathbf{k}'_3) \Gamma_a \Psi'(\omega'_1 - \omega'_2 + \omega'_3, \mathbf{k}'_1 - \mathbf{k}'_2 + \mathbf{k}'_3), \quad (\text{C80})$$

which recovers the original form of the action.

From Eq. (C79), we get the RG equation for g_a as follows:

$$\frac{dg_a}{d\ell} = -\frac{3}{2} g_a + \frac{d\delta g_a}{d\ell}. \quad (\text{C81})$$

Substituting Eqs. (C62)–(C66) into Eq. (C81), we find

$$\frac{dg_1}{d\ell} = -\frac{3}{2}g_1 - \frac{2}{5}g_1\left(g_2 + \frac{1}{2}g_4 + g_5\right) - \frac{2}{5}(g_2g_5 + g_4g_{3z} + g_5g_{3z}), \quad (\text{C82})$$

$$\frac{dg_2}{d\ell} = -\frac{3}{2}g_2 + g_2^2 + g_2\left(-\frac{3}{5}g_1 + \frac{4}{5}g_4 + \frac{3}{5}g_5 + g_{3z}\right) - \frac{2}{5}g_1g_5 + g_4\left(-g_5 + \frac{7}{5}g_{3z}\right) + \frac{2}{5}g_5g_{3z}, \quad (\text{C83})$$

$$\frac{dg_4}{d\ell} = -\frac{3}{2}g_4 - \frac{1}{5}g_4^2 - \frac{1}{5}(g_1^2 + g_2^2 + g_5^2 + g_{3z}^2) + \frac{2}{5}g_4g_{3z} + \frac{2}{5}g_1(g_2 + g_5) + g_2\left(-\frac{7}{5}g_5 + g_{3z}\right) - \frac{1}{5}g_5g_{3z}, \quad (\text{C84})$$

$$\frac{dg_5}{d\ell} = -\frac{3}{2}g_5 + \frac{6}{5}g_5^2 + \frac{1}{5}(g_1^2 + g_2^2 + g_4^2 + g_{3z}^2) + g_5(-g_1 + g_2 + g_4 - g_{3z}) - \frac{2}{5}g_1\left(2g_2 + \frac{1}{2}g_4\right) - g_2\left(\frac{4}{5}g_4 + g_{3z}\right) - \frac{8}{5}g_4g_{3z}, \quad (\text{C85})$$

$$\begin{aligned} \frac{dg_{3z}}{d\ell} &= -\frac{3}{2}g_{3z} + \frac{2}{5}g_{3z}^2 + \frac{1}{5}(g_1^2 + g_2^2 + g_4^2 + g_5^2) - \frac{2}{5}g_{3z}\left(\frac{1}{2}g_1 + 2g_2 + 3g_4 + \frac{3}{2}g_5\right) - \frac{2}{5}g_1\left(g_2 + \frac{1}{2}g_4 + g_5\right) \\ &+ \frac{2}{5}g_2\left(\frac{1}{2}g_4 + g_5\right) + \frac{1}{5}g_4g_5. \end{aligned} \quad (\text{C86})$$

The redefinition

$$\frac{\Lambda^{\frac{3}{2}}g_a}{\pi^2v^2\sqrt{A}} \rightarrow g_a \quad (\text{C87})$$

has been employed.

APPENDIX D: SUSCEPTIBILITY OF SOURCE TERMS

We consider the Lagrangian for the source terms as follows:

$$\begin{aligned} \mathcal{L}_s &= \Delta_1\bar{\Psi}\gamma_0\Psi + \Delta_2\bar{\Psi}\Psi + \Delta_{3\perp}\sum_{j=1}^2\bar{\Psi}\gamma_0\gamma_j\Psi \\ &+ \Delta_{3z}\bar{\Psi}\gamma_0\gamma_3\Psi + \Delta_4\bar{\Psi}\gamma_0\gamma_5\Psi + \Delta_5\bar{\Psi}i\gamma_5\Psi \\ &+ \Delta_{6\perp}\sum_{\langle\langle lk\rangle\rangle}(\bar{\Psi}i\gamma_l\gamma_k\Psi) + \Delta_{6z}\bar{\Psi}i\gamma_1\gamma_2\Psi \\ &+ \Delta_{7\perp}\sum_{j=1}^2\bar{\Psi}i\gamma_5\gamma_j\Psi + \Delta_{7z}\bar{\Psi}i\gamma_5\gamma_3\Psi \\ &+ \Delta_{8\perp}\sum_{j=1}^2\bar{\Psi}i\gamma_j\Psi + \Delta_{8z}\bar{\Psi}i\gamma_3\Psi + \Delta_5\Psi^\dagger i\gamma_0\gamma_5\gamma_2\Psi^* \\ &+ \Delta_{op}\Psi^\dagger i\gamma_0\gamma_2\Psi^* + \Delta_{v,1}\Psi^\dagger\gamma_3\Psi^* + \Delta_{v,2}\Psi^\dagger i\gamma_0\gamma_5\Psi^* \\ &+ \Delta_{v,3}\Psi^\dagger\gamma_1\Psi^* + \Delta_{v,0}\Psi^\dagger i\gamma_0\gamma_2\gamma_3\Psi^*. \end{aligned} \quad (\text{D1})$$

1. One-loop order corrections for source terms in particle-hole channels

There are two one-loop Feynman diagrams leading to the corrections for source terms in particle-hole channels. The one-loop correction for the source term Δ_X from Fig. 8(a) is given by

$$\begin{aligned} W_{\Delta_X}^{(1)} &= -2\Delta_X g_X(\bar{\Psi}\Gamma_X\Psi) \sum_{a=1,2,4,5,3z} g_a \int_{-\infty}^{+\infty} \frac{d\omega}{2\pi} \\ &\times \int' \frac{d^3\mathbf{k}}{(2\pi)^3} \text{Tr}[\Gamma_X G_0(i\omega, \mathbf{k})\Gamma_a G_0(i\omega, \mathbf{k})]. \end{aligned} \quad (\text{D2})$$

The one-loop correction for the source term Δ_X resulting from Fig. 8(b) can be written as

$$\begin{aligned} W_{\Delta_X}^{(2)} &= 2\Delta_X \sum_{a=1,2,4,5,3z} g_a \int_{-\infty}^{+\infty} \frac{d\omega}{2\pi} \int' \frac{d^3\mathbf{k}}{(2\pi)^3} \\ &\times [\bar{\Psi}\Gamma_a G_0(i\omega, \mathbf{k})\Gamma_X G_0(i\omega, \mathbf{k})\Gamma_a\Psi]. \end{aligned} \quad (\text{D3})$$

Substituting Eq. (C1) into Eq. (D2), we find

$$W_{\Delta_1}^{(1)} = 0, \quad (\text{D4})$$

$$W_{\Delta_2}^{(1)} = \Delta_2 g_2 \frac{2\Lambda^{\frac{3}{2}}}{\pi^2 v^2 \sqrt{A}} \ell(\bar{\Psi}\Psi), \quad (\text{D5})$$

$$W_{\Delta_{3\perp}}^{(1)} = 0, \quad (\text{D6})$$

$$W_{3z}^{(1)} = \Delta_{3z} g_{3z} \frac{2\Lambda^{\frac{3}{2}}}{5\pi^2 v^2 \sqrt{A}} \ell(\bar{\Psi}\gamma_0\gamma_3\Psi), \quad (\text{D7})$$

$$W_{\Delta_4}^{(1)} = 0, \quad (\text{D8})$$

$$W_{\Delta_5}^{(1)} = \Delta_5 g_5 \frac{2\Lambda^{\frac{3}{2}}}{\pi^2 v^2 \sqrt{A}} \ell(\bar{\Psi}i\gamma_5\Psi), \quad (\text{D9})$$

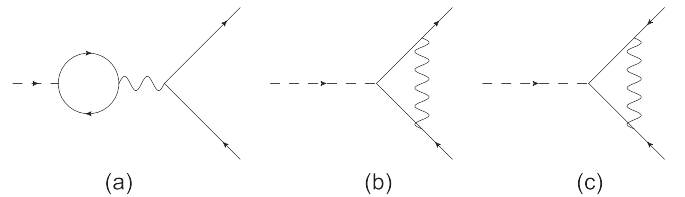


FIG. 8. (a),(b) One-loop Feynman diagrams for the corrections to the source terms in particle-hole channels. (c) One-loop Feynman diagram for the corrections to the source terms in particle-particle channels.

$$W_{\Delta_{6\perp}}^{(1)} = 0, \quad (\text{D10})$$

$$W_{\Delta_{6z}}^{(1)} = 0, \quad (\text{D11})$$

$$W_{\Delta_{7\perp}}^{(1)} = 0, \quad (\text{D12})$$

$$W_{\Delta_{7z}}^{(1)} = 0, \quad (\text{D13})$$

$$W_{\Delta_{8\perp}}^{(1)} = 0, \quad (\text{D14})$$

$$W_{\Delta_{8z}}^{(1)} = 0. \quad (\text{D15})$$

Substituting Eq. (C1) into Eq. (D3), we obtain

$$W_{\Delta_1}^{(2)} = 0, \quad (\text{D16})$$

$$W_{\Delta_2}^{(2)} = \frac{1}{2} \Delta_2 (-g_1 - g_2 + g_4 + g_5 + g_{3z}) \frac{\Lambda^{\frac{3}{2}}}{\pi^2 v^2 \sqrt{A}} \ell(\bar{\Psi} \Psi), \quad (\text{D17})$$

$$W_{\Delta_{3\perp}}^{(2)} = \Delta_{3\perp} (-g_1 + g_2 + g_4 - g_5 + g_{3z}) \frac{\Lambda^{\frac{3}{2}}}{5\pi^2 v^2 \sqrt{A}} \ell \sum_{j=1}^2 (\bar{\Psi} \gamma_0 \gamma_j \Psi), \quad (\text{D18})$$

$$W_{\Delta_{3z}}^{(2)} = \Delta_{3z} (-g_1 + g_2 + g_4 - g_5 - g_{3z}) \frac{\Lambda^{\frac{3}{2}}}{10\pi^2 v^2 \sqrt{A}} \ell(\bar{\Psi} \gamma_0 \gamma_3 \Psi), \quad (\text{D19})$$

$$W_{\Delta_4}^{(2)} = 0, \quad (\text{D20})$$

$$W_{\Delta_5}^{(2)} = \Delta_5 (-g_1 + g_2 + g_4 - g_5 - g_{3z}) \frac{\Lambda^{\frac{3}{2}}}{2\pi^2 v^2 \sqrt{A}} \ell(\bar{\Psi} i \gamma_5 \Psi), \quad (\text{D21})$$

$$W_{\Delta_{6\perp}}^{(2)} = \Delta_{6\perp} (-g_1 - g_2 + g_4 + g_5 - g_{3z}) \frac{\Lambda^{\frac{3}{2}}}{5\pi^2 v^2 \sqrt{A}} \ell \sum_{\langle l k \rangle} (\bar{\Psi} i \gamma_l \gamma_k \Psi), \quad (\text{D22})$$

$$W_{\Delta_{6z}}^{(2)} = \Delta_{6z} (-g_1 - g_2 + g_4 + g_5 + g_{3z}) \frac{\Lambda^{\frac{3}{2}}}{10\pi^2 v^2 \sqrt{A}} \ell(\bar{\Psi} i \gamma_1 \gamma_2 \Psi), \quad (\text{D23})$$

$$W_{\Delta_{7\perp}}^{(2)} = \Delta_{7\perp} (-g_1 - g_2 - g_4 - g_5 + g_{3z}) \frac{3\Lambda^{\frac{3}{2}}}{10\pi^2 v^2 \sqrt{A}} \ell \sum_{j=1}^2 (\bar{\Psi} i \gamma_5 \gamma_j \Psi), \quad (\text{D24})$$

$$W_{\Delta_{7z}}^{(2)} = -\Delta_{7z} (g_1 + g_2 + g_4 + g_5 + g_{3z}) \frac{2\Lambda^{\frac{3}{2}}}{5\pi^2 v^2 \sqrt{A}} \ell(\bar{\Psi} i \gamma_5 \gamma_3 \Psi), \quad (\text{D25})$$

$$W_{\Delta_{8\perp}}^{(2)} = \Delta_{8\perp} (-g_1 + g_2 - g_4 + g_5 - g_{3z}) \frac{3\Lambda^{\frac{3}{2}}}{10\pi^2 v^2 \sqrt{A}} \ell \sum_{j=1}^2 (\bar{\Psi} i \gamma_j \Psi), \quad (\text{D26})$$

$$W_{\Delta_{8z}}^{(2)} = \Delta_{8z} (-g_1 + g_2 - g_4 + g_5 + g_{3z}) \frac{2\Lambda^{\frac{3}{2}}}{5\pi^2 v^2 \sqrt{A}} \ell(\bar{\Psi} i \gamma_3 \Psi). \quad (\text{D27})$$

From

$$W_{\Delta_X} = W_{\Delta_X}^{(1)} + W_{\Delta_X}^{(2)}, \quad (\text{D28})$$

we arrive at

$$W_{\Delta_X} = \delta \Delta_X (\bar{\Psi} \Gamma_X \Psi). \quad (\text{D29})$$

The parameters $\delta \Delta_X$ are given by

$$\delta \Delta_1 = 0, \quad (\text{D30})$$

$$\delta \Delta_2 = \Delta_2 (-g_1 + 3g_2 + g_4 + g_5 + g_{3z}) \frac{\Lambda^{\frac{3}{2}}}{2\pi^2 v^2 \sqrt{A}} \ell, \quad (\text{D31})$$

$$\delta \Delta_{3\perp} = \Delta_{3\perp} (-g_1 + g_2 + g_4 - g_5 + g_{3z}) \frac{\Lambda^{\frac{3}{2}}}{5\pi^2 v^2 \sqrt{A}} \ell, \quad (\text{D32})$$

$$\delta\Delta_{3z} = \Delta_{3z}(-g_1 + g_2 + g_4 - g_5 + 3g_{3z}) \frac{\Lambda^{\frac{3}{2}}}{10\pi^2 v^2 \sqrt{A}} \ell, \quad (\text{D33})$$

$$\delta\Delta_4 = 0, \quad (\text{D34})$$

$$\delta\Delta_5 = \Delta_5(-g_1 + g_2 + g_4 + 3g_5 - g_{3z}) \frac{\Lambda^{\frac{3}{2}}}{2\pi^2 v^2 \sqrt{A}} \ell, \quad (\text{D35})$$

$$\delta\Delta_{6\perp} = \Delta_{6\perp}(-g_1 - g_2 + g_4 + g_5 - g_{3z}) \frac{\Lambda^{\frac{3}{2}}}{5\pi^2 v^2 \sqrt{A}} \ell, \quad (\text{D36})$$

$$\delta\Delta_{6z} = \Delta_{6z}(-g_1 - g_2 + g_4 + g_5 + g_{3z}) \frac{\Lambda^{\frac{3}{2}}}{10\pi^2 v^2 \sqrt{A}} \ell, \quad (\text{D37})$$

$$\delta\Delta_{7\perp} = \Delta_{7\perp}(-g_1 - g_2 - g_4 - g_5 + g_{3z}) \frac{3\Lambda^{\frac{3}{2}}}{10\pi^2 v^2 \sqrt{A}} \ell, \quad (\text{D38})$$

$$\delta\Delta_{7z} = \Delta_{7z}(-g_1 - g_2 - g_4 - g_5 - g_{3z}) \frac{2\Lambda^{\frac{3}{2}}}{5\pi^2 v^2 \sqrt{A}} \ell, \quad (\text{D39})$$

$$\delta\Delta_{8\perp} = \Delta_{8\perp}(-g_1 + g_2 - g_4 + g_5 - g_{3z}) \frac{3\Lambda^{\frac{3}{2}}}{10\pi^2 v^2 \sqrt{A}} \ell, \quad (\text{D40})$$

$$\delta\Delta_{8z} = \Delta_{8z}(-g_1 + g_2 - g_4 + g_5 + g_{3z}) \frac{2\Lambda^{\frac{3}{2}}}{5\pi^2 v^2 \sqrt{A}} \ell. \quad (\text{D41})$$

2. One-loop order corrections for source terms in particle-particle channels

In particle-particle channels, to one-loop order, there is one Feynman diagram as shown in Fig. 8(c) resulting in the corrections to source terms. The correction can be expressed as

$$W_{\Delta_Y} = 2\Delta_Y \sum_{a=1,2,4,5,3z} g_a \int_{-\infty}^{+\infty} \frac{d\omega}{2\pi} \int' \frac{d^3\mathbf{k}}{(2\pi)^3} [\Psi^\dagger \Gamma_a^T G_0^T(i\omega, \mathbf{k}) \Gamma_Y G_0(-i\omega, -\mathbf{k}) \Gamma_a \Psi^*], \quad (\text{D42})$$

where T represents transposition. Substituting Eq. (C1) into Eq. (D42), we get

$$W_{\Delta_Y} = \delta\Delta_Y (\Psi^\dagger \Gamma_Y \Psi^*), \quad (\text{D43})$$

where

$$\delta\Delta_S = \Delta_S(g_1 - g_2 + g_4 + g_5 - g_{3z}) \frac{2\Lambda^{\frac{3}{2}}}{5\pi^2 v^2 \sqrt{A}} \ell, \quad (\text{D44})$$

$$\delta\Delta_{op} = \Delta_{op}(g_1 + g_2 + g_4 - g_5 + g_{3z}) \frac{2\Lambda^{\frac{3}{2}}}{5\pi^2 v^2 \sqrt{A}} \ell, \quad (\text{D45})$$

$$\delta\Delta_{V,1} = \Delta_{V,1}(g_1 + g_2 - g_4 + g_5 + g_{3z}) \frac{\Lambda^{\frac{3}{2}}}{5\pi^2 v^2 \sqrt{A}} \ell, \quad (\text{D46})$$

$$\delta\Delta_{V,2} = \Delta_{V,2}(g_1 + g_2 - g_4 + g_5 + g_{3z}) \frac{\Lambda^{\frac{3}{2}}}{5\pi^2 v^2 \sqrt{A}} \ell, \quad (\text{D47})$$

$$\delta\Delta_{V,3} = \Delta_{V,3}(g_1 + g_2 - g_4 + g_5 - g_{3z}) \frac{\Lambda^{\frac{3}{2}}}{2\pi^2 v^2 \sqrt{A}} \ell, \quad (\text{D48})$$

$$\delta\Delta_{V,0} = \Delta_{V,0}(g_1 - g_2 - g_4 - g_5 + g_{3z}) \frac{\Lambda^{\frac{3}{2}}}{20\pi^2 v^2 \sqrt{A}} \ell. \quad (\text{D49})$$

3. Derivation of the RG equations for source terms

In particle-hole channels, the bare action for the source terms is

$$S_s = \Delta_X \int \frac{d\omega}{2\pi} \frac{d^3\mathbf{k}}{(2\pi)^3} \bar{\Psi}(\omega, \mathbf{k}) \Gamma_X \Psi(\omega, \mathbf{k}). \quad (\text{D50})$$

Considering the one-loop order corrections, we obtain

$$S_s = (\Delta_X + \delta\Delta_X) \int \frac{d\omega}{2\pi} \frac{d^3\mathbf{k}}{(2\pi)^3} \bar{\Psi}(\omega, \mathbf{k}) \Gamma_X \Psi(\omega, \mathbf{k}). \quad (\text{D51})$$

Using the transformations Eqs. (C68)–(C71) and (C74), we can get

$$\begin{aligned} S_s &= (\Delta_X + \delta\Delta_X) e^\ell \int \frac{d\omega'}{2\pi} \frac{d^3\mathbf{k}'}{(2\pi)^3} \bar{\Psi}'(\omega', \mathbf{k}') \Gamma_X \Psi'(\omega', \mathbf{k}') \\ &\approx (\Delta_X + \Delta_X \ell + \delta\Delta_X) \int \frac{d\omega'}{2\pi} \frac{d^3\mathbf{k}'}{(2\pi)^3} \bar{\Psi}'(\omega', \mathbf{k}') \Gamma_X \Psi'(\omega', \mathbf{k}'). \end{aligned} \quad (\text{D52})$$

Letting

$$\Delta'_X = \Delta_X + \Delta_X \ell + \delta\Delta_X, \quad (\text{D53})$$

the action can be further written as

$$S_s = \Delta'_X \int \frac{d\omega'}{2\pi} \frac{d^3\mathbf{k}'}{(2\pi)^3} \bar{\Psi}'(\omega', \mathbf{k}') \Gamma_X \Psi'(\omega', \mathbf{k}'), \quad (\text{D54})$$

which recovers the form of the original action. We can easily find that the RG equation for Δ_X is

$$\frac{d\Delta_X}{d\ell} = \Delta_X + \frac{d\delta\Delta_X}{d\ell}. \quad (\text{D55})$$

Performing similar rescaling transformations, we can get the RG equation for source terms in particle-particle channels

$$\frac{d\Delta_Y}{d\ell} = \Delta_Y + \frac{d\delta\Delta_Y}{d\ell}. \quad (\text{D56})$$

Substituting Eqs. (D30)–(D41) into Eq. (D55), and substituting Eqs. (D44)–(D49) into Eq. (D56), we get the RG equations

$$\bar{\beta}_1 = 0, \quad (\text{D57})$$

$$\bar{\beta}_2 = \frac{1}{2}(-g_1 + 3g_2 + g_4 + g_5 + g_{3z}), \quad (\text{D58})$$

$$\bar{\beta}_{3\perp} = \frac{1}{5}(-g_1 + g_2 + g_4 - g_5 + g_{3z}), \quad (\text{D59})$$

$$\bar{\beta}_{3z} = \frac{1}{10}(-g_1 + g_2 + g_4 - g_5), \quad (\text{D60})$$

$$\bar{\beta}_4 = 0, \quad (\text{D61})$$

$$\bar{\beta}_5 = \frac{1}{2}(-g_1 + g_2 + g_4 + 3g_5 - g_{3z}), \quad (\text{D62})$$

$$\bar{\beta}_{6\perp} = \frac{1}{5}(-g_1 - g_2 + g_4 + g_5 - g_{3z}), \quad (\text{D63})$$

$$\bar{\beta}_{6z} = \frac{1}{10}(-g_1 - g_2 + g_4 + g_5 + g_{3z}), \quad (\text{D64})$$

$$\bar{\beta}_{7\perp} = \frac{3}{10}(-g_1 - g_2 - g_4 - g_5 + g_{3z}), \quad (\text{D65})$$

$$\bar{\beta}_{7z} = \frac{2}{5}(-g_1 - g_2 - g_4 - g_5 - g_{3z}), \quad (\text{D66})$$

$$\bar{\beta}_{8\perp} = \frac{3}{10}(-g_1 + g_2 - g_4 + g_5 - g_{3z}), \quad (\text{D67})$$

$$\bar{\beta}_{8z} = \frac{2}{5}(-g_1 + g_2 - g_4 + g_5 + g_{3z}), \quad (\text{D68})$$

$$\bar{\beta}_S = \frac{2}{5}(g_1 - g_2 + g_4 + g_5 - g_{3z}), \quad (\text{D69})$$

$$\bar{\beta}_{op} = \frac{2}{5}(g_1 + g_2 + g_4 - g_5 + g_{3z}), \quad (\text{D70})$$

$$\bar{\beta}_{V,1} = \frac{1}{5}(g_1 + g_2 - g_4 + g_5 + g_{3z}), \quad (\text{D71})$$

$$\bar{\beta}_{V,2} = \frac{1}{5}(g_1 + g_2 - g_4 + g_5 + g_{3z}), \quad (\text{D72})$$

$$\bar{\beta}_{V,3} = \frac{1}{2}(g_1 + g_2 - g_4 + g_5 - g_{3z}), \quad (\text{D73})$$

$$\bar{\beta}_{V,0} = \frac{1}{20}(g_1 - g_2 - g_4 - g_5 + g_{3z}), \quad (\text{D74})$$

where

$$\bar{\beta}_{X,Y} = \frac{d \ln(\Delta_{X,Y})}{d\ell} - 1. \quad (\text{D75})$$

For convenience, we show the physical meaning of different order parameters and corresponding fermion bilinears in Table IV.

TABLE IV. Physical meaning of different order parameters and the corresponding fermion bilinears.

Order parameter	Fermion bilinear	Physical meaning
Δ_1	$\bar{\Psi} \gamma_0 \Psi$	Chemical potential
Δ_2	$\bar{\Psi} \Psi$	Scalar mass
$\Delta_{3\perp}$	$\sum_{j=1,2} \bar{\Psi} \gamma_0 \gamma_j \Psi$	Spin-orbit coupling within xy plane
Δ_{3z}	$\bar{\Psi} \gamma_0 \gamma_3 \Psi$	Spin-orbit coupling along z axis
Δ_4	$\bar{\Psi} \gamma_0 \gamma_5 \Psi$	Axial chemical potential
Δ_5	$\bar{\Psi} i \gamma_5 \Psi$	Pseudoscalar mass
$\Delta_{6\perp}$	$\bar{\Psi} (i \gamma_2 \gamma_3 + \gamma_3 \gamma_1) \Psi$	Magnetization within xy plane
Δ_{6z}	$\bar{\Psi} i \gamma_1 \gamma_2 \Psi$	Magnetization along z axis
$\Delta_{7\perp}$	$\sum_{j=1,2} \bar{\Psi} i \gamma_5 \gamma_j \Psi$	Axial magnetization within xy plane
Δ_{7z}	$\bar{\Psi} i \gamma_5 \gamma_3 \Psi$	Axial magnetization along z axis
$\Delta_{8\perp}$	$\sum_{j=1,2} \bar{\Psi} i \gamma_j \Psi$	Current within xy plane
Δ_{8z}	$\bar{\Psi} i \gamma_3 \Psi$	Current along z axis
Δ_S	$\Psi^\dagger i \gamma_0 \gamma_5 \gamma_2 \Psi^*$	s -wave pairing
Δ_{op}	$\Psi^\dagger i \gamma_0 \gamma_2 \Psi^*$	Odd-parity pairing
$\Delta_{V,1}$	$\Psi^\dagger \gamma_3 \Psi^*$	Vector pairing along x axis
$\Delta_{V,2}$	$\Psi^\dagger i \gamma_0 \gamma_5 \Psi^*$	Vector pairing along y axis
$\Delta_{V,3}$	$\Psi^\dagger \gamma_1 \Psi^*$	Vector pairing along z axis
$\Delta_{V,0}$	$\Psi^\dagger i \gamma_0 \gamma_1 \gamma_3 \Psi^*$	Temporal vector pairing

APPENDIX E: NUMERICAL RESULTS

1. Fixed points and their properties

Solving the RG equations for g_a as shown in Eqs. (C82)–(C86), we obtained the real roots as follows:

$$\text{FP0: } (g_1^*, g_2^*, g_4^*, g_5^*, g_{3z}^*) = (0, 0, 0, 0, 0), \quad (\text{E1})$$

$$\text{FP1: } (g_1^*, g_2^*, g_4^*, g_5^*, g_{3z}^*) = (0.152019, 1.25444, 0.459247, -0.561711, 0.0551435), \quad (\text{E2})$$

$$\text{FP2: } (g_1^*, g_2^*, g_4^*, g_5^*, g_{3z}^*) = (0.140905, -0.585585, 0.418385, 1.34668, 0.06996), \quad (\text{E3})$$

$$\text{FP3: } (g_1^*, g_2^*, g_4^*, g_5^*, g_{3z}^*) = (-0.100015, 0.575751, -0.61003, 0.775675, 0.199924), \quad (\text{E4})$$

$$\text{FP4: } (g_1^*, g_2^*, g_4^*, g_5^*, g_{3z}^*) = (-2.33263, 0, -0.610178, -1.72246, -1.72246), \quad (\text{E5})$$

$$\text{FP5: } (g_1^*, g_2^*, g_4^*, g_5^*, g_{3z}^*) = (0.126936, -0.463077, -0.854005, 0.769245, 1.23232), \quad (\text{E6})$$

$$\text{FP6: } (g_1^*, g_2^*, g_4^*, g_5^*, g_{3z}^*) = (0.0860014, 1.37623, 0.236822, -0.304132, 0.0941005), \quad (\text{E7})$$

$$\text{FP7: } (g_1^*, g_2^*, g_4^*, g_5^*, g_{3z}^*) = (0.103947, -0.465334, 0.29293, 1.43995, 0.0944817), \quad (\text{E8})$$

$$\text{FP8: } (g_1^*, g_2^*, g_4^*, g_5^*, g_{3z}^*) = (-3.33745, -1.22097, -1.28072, -1.32395, -0.102973), \quad (\text{E9})$$

$$\text{FP9: } (g_1^*, g_2^*, g_4^*, g_5^*, g_{3z}^*) = (-2.68181, 1.06255, -1.97657, -1.35604, -2.41859), \quad (\text{E10})$$

$$\text{FP10: } (g_1^*, g_2^*, g_4^*, g_5^*, g_{3z}^*) = (0, 0, -1.25, 1.25, 1.25), \quad (\text{E11})$$

$$\text{FP11: } (g_1^*, g_2^*, g_4^*, g_5^*, g_{3z}^*) = (-5.16737, 0, -4.38982, -0.777544, -0.777544). \quad (\text{E12})$$

FP0 is the trivial Gaussian fixed point. FP1–FP11 are nontrivial fixed points.

Expanding the RG equations (C82)–(C86) in the vicinity of a fixed point $(g_1^*, g_2^*, g_4^*, g_5^*, g_{3z}^*)$, we find that

$$\frac{dG}{d\ell} = MG, \quad (\text{E13})$$

where

$$G = \begin{pmatrix} \delta g_1 \\ \delta g_2 \\ \delta g_4 \\ \delta g_5 \\ \delta g_{3z} \end{pmatrix}, \quad (\text{E14})$$

with $\delta g_a = g_a - g_a^*$. The matrix M is given by

$$M = \begin{pmatrix} M_{11} & M_{12} & M_{13} & M_{14} & M_{15} \\ M_{21} & M_{22} & M_{23} & M_{24} & M_{25} \\ M_{31} & M_{32} & M_{33} & M_{34} & M_{35} \\ M_{41} & M_{42} & M_{43} & M_{44} & M_{45} \\ M_{51} & M_{52} & M_{53} & M_{54} & M_{55} \end{pmatrix}, \quad (\text{E15})$$

where

$$M_{11} = -\left(\frac{3}{2} + \frac{2}{5}g_2^* + \frac{1}{5}g_4^* + \frac{2}{5}g_5^*\right), \quad (\text{E16})$$

$$M_{12} = -\frac{2}{5}(g_1^* + g_5^*), \quad (\text{E17})$$

$$M_{13} = -\left(\frac{1}{5}g_1^* + \frac{2}{5}g_{3z}^*\right), \quad (\text{E18})$$

$$M_{14} = -\frac{2}{5}(g_1^* + g_2^* + g_{3z}^*), \quad (\text{E19})$$

$$M_{15} = -\frac{2}{5}(g_4^* + g_5^*), \quad (\text{E20})$$

$$M_{21} = -\frac{3}{5}g_2^* - \frac{2}{5}g_5^*, \quad (\text{E21})$$

$$M_{22} = -\frac{3}{2} + 2g_2^* - \frac{3}{5}g_1^* + \frac{4}{5}g_4^* + \frac{3}{5}g_5^* + g_{3z}^*, \quad (\text{E22})$$

$$M_{23} = \frac{4}{5}g_2^* - g_5^* + \frac{7}{5}g_{3z}^*, \quad (\text{E23})$$

$$M_{24} = \frac{3}{5}g_2^* - \frac{2}{5}g_1^* - g_4^* + \frac{2}{5}g_{3z}^*, \quad (\text{E24})$$

$$M_{25} = g_2^* + \frac{7}{5}g_4^* + \frac{2}{5}g_5^*, \quad (\text{E25})$$

$$M_{31} = -\frac{2}{5}g_1^* + \frac{2}{5}g_2^* + \frac{2}{5}g_5^*, \quad (\text{E26})$$

$$M_{32} = -\frac{2}{5}g_2^* + \frac{2}{5}g_1^* - \frac{7}{5}g_5^* + g_{3z}^*, \quad (\text{E27})$$

$$M_{33} = -\frac{3}{2} - \frac{2}{5}g_4^* + \frac{2}{5}g_{3z}^*, \quad (\text{E28})$$

$$M_{34} = -\frac{2}{5}g_5^* + \frac{2}{5}g_1^* - \frac{7}{5}g_2^* - \frac{1}{5}g_{3z}^*, \quad (\text{E29})$$

$$M_{35} = -\frac{2}{5}g_{3z}^* + \frac{2}{5}g_4^* + g_2^* - \frac{1}{5}g_5^*, \quad (\text{E30})$$

$$M_{41} = \frac{2}{5}g_1^* - g_5^* - \frac{4}{5}g_2^* - \frac{1}{5}g_4^*, \quad (\text{E31})$$

$$M_{42} = \frac{2}{5}g_2^* + g_5^* - \frac{4}{5}g_1^* - \frac{4}{5}g_4^* - g_{3z}^*, \quad (\text{E32})$$

TABLE V. Eigenvalues of matrix M at different fixed points.

FP0	FP1	FP2	FP3	FP4	FP5	FP6	FP7	FP8	FP9	FP10	FP11
-1.5	-3.12277	-3.05426	-2.11269	-4.19874	-2.50996	-2.98441	-2.99224	-5.70333	-5.29866	-2.25	-9.30126
-1.5	-2.7634	-2.48233	-1.42791	-2.79748	-2.05542	-2.77106	-2.49091	-3.26902	-3.36509	-2.25	-1.69424
-1.5	-1.77432	-1.76197	-1.26511	-2.46863	-1.41052	-1.80787	-1.77301	-1.46547	-1.38636	-1.47474	1.5
-1.5	-0.412398	-0.231803	-1.18664	-0.848268	-1.06884	0.390411	0.224733	1.5	1.5	0.974745	3.33999
-1.5	1.5	1.5	1.5	1.5	1.5	1.5	1.5	2.47601	2.17557	1.5	5.46863

$$M_{43} = \frac{2}{5}g_4^* + g_5^* - \frac{1}{5}g_1^* - \frac{4}{5}g_2^* - \frac{8}{5}g_{3z}^*, \quad (\text{E33})$$

$$M_{44} = -\frac{3}{2} + \frac{12}{5}g_5^* - g_1^* + g_2^* + g_4^* - g_{3z}^*, \quad (\text{E34})$$

$$M_{45} = \frac{2}{5}g_{3z}^* - g_5^* - g_2^* - \frac{8}{5}g_4^*, \quad (\text{E35})$$

$$M_{51} = \frac{2}{5}g_1^* - \frac{1}{5}g_{3z}^* - \frac{2}{5}g_2^* - \frac{1}{5}g_4^* - \frac{2}{5}g_5^*, \quad (\text{E36})$$

$$M_{52} = \frac{2}{5}g_2^* - \frac{4}{5}g_{3z}^* - \frac{2}{5}g_1^* + \frac{1}{5}g_4^* + \frac{2}{5}g_5^*, \quad (\text{E37})$$

$$M_{53} = \frac{2}{5}g_4^* - \frac{6}{5}g_{3z}^* - \frac{1}{5}g_1^* + \frac{1}{5}g_2^* + \frac{1}{5}g_5^*, \quad (\text{E38})$$

$$M_{54} = \frac{2}{5}g_5^* - \frac{3}{5}g_{3z}^* - \frac{2}{5}g_1^* + \frac{2}{5}g_2^* + \frac{1}{5}g_4^*, \quad (\text{E39})$$

$$M_{55} = -\frac{3}{2} + \frac{4}{5}g_{3z}^* - \frac{1}{5}g_1^* - \frac{4}{5}g_2^* - \frac{6}{5}g_4^* - \frac{3}{5}g_5^*. \quad (\text{E40})$$

From eigenvalues of M at a fixed point ($g_1^*, g_2^*, g_4^*, g_5^*, g_{3z}^*$), we can get the properties of the fixed point. A negative (positive) eigenvalue is corresponding to a stable (unstable) eigendirection [32,34]. For quantum critical point (QCP), bicritical point (BCP), and tricritical point (TCP), there is/are one, two, and three unstable direction(s), respectively. For a QCP, the correlation length exponent is determined by the inverse of the corresponding positive eigenvalue.

Substituting the values of g_a^* at each fixed point into the expression M , we calculate the corresponding eigenvalues of M . The eigenvalues for the fixed points are shown in Table V. For FP0, the eigenvalues of M are always negative; thus FP0 is a stable fixed point. We can find that there is one positive eigenvalue for FP1, FP2, FP3, FP4, and FP5, and there are two positive eigenvalues for FP6, FP7, FP8, FP9, and FP10, and three positive eigenvalues for FP11. Thus FP1, FP2, FP3, FP4, and FP5 are QCPs, FP6, FP7, FP8, FP9, and FP10 are BCPs, and FP11 is a TCP.

It is easy to find that the correlation length exponents at the QCPs FP1, FP2, FP3, FP4, and FP5 all satisfy

$$\nu^{-1} = 1.5. \quad (\text{E41})$$

Substituting the values of g_a^* with $i = 1, 2, 4, 5, 3z$ into Eqs. (D57)–(D74), we can get values of $\tilde{\beta}_{X,Y}$ for different $\Delta_{X,Y}$, which are shown in Table VI. For a QCP, the largest value of $\tilde{\beta}_{X,Y}$ is marked by the bold style. It represents that the fixed point is a QCP to the new state in which $\Delta_{X,Y}$ acquires finite value. FP1, FP2, FP4, and FP5 are corresponding to QCPs to a state in which Δ_2 , Δ_5 , Δ_{7z} , and Δ_{8z} acquire finite value, respectively. For FP3, it stands for a QCP to a state in which both Δ_2 and Δ_5 become finite generally. This state represents an axionic insulator whose order parameter can be written as $\langle \bar{\Psi}[\cos(\theta) + i\gamma_5 \sin(\theta)]\Psi \rangle$ [33].

APPENDIX F: INTERPLAY OF FOUR-FERMION INTERACTION AND LONG-RANGE COULOMB INTERACTION

The Coulomb interaction between fermions can be described by the coupling between fermion field Ψ and boson field ϕ as the following action:

$$S_{\psi\phi} = i\lambda \int \frac{d\omega_1}{2\pi} \frac{d^3\mathbf{k}_1}{(2\pi)^3} \frac{d\omega_2}{2\pi} \frac{d^3\mathbf{k}_2}{(2\pi)^3} \bar{\Psi}(\omega_1, \mathbf{k}_1)\gamma_0\Psi(\omega_2, \mathbf{k}_2) \times \phi(\omega_1 - \omega_2, \mathbf{k}_1 - \mathbf{k}_2), \quad (\text{F1})$$

where $\lambda = \frac{e}{\sqrt{\epsilon}}$ with e the elementary charge and ϵ the dielectric constant. The free action of ϕ is given by

$$S_\phi^0 = \int \frac{d\omega}{2\pi} \frac{d^3\mathbf{k}}{(2\pi)^3} \phi(\omega, \mathbf{k}) \left(\frac{1}{\sqrt{\eta}} k_\perp^2 + \sqrt{\eta} k_z^2 \right) \phi(\omega, \mathbf{k}). \quad (\text{F2})$$

1. Interaction corrections related to Coulomb interaction

a. Fermion self-energy induced by Coulomb interaction

As shown in Fig. 9(a), the fermion self-energy induced by long-range Coulomb interaction is given by

$$\Sigma_C(i\omega, \mathbf{k}) = -\lambda^2 \int_{-\infty}^{+\infty} \frac{d\Omega}{2\pi} \int' \frac{d^3\mathbf{q}}{(2\pi)^3} \gamma_0 G_0(i\Omega, \mathbf{q}) \gamma_0 \times D_0(i\omega - i\Omega, \mathbf{k} - \mathbf{q}), \quad (\text{F3})$$

where

$$D_0(i\Omega, \mathbf{q}) = \frac{\sqrt{\eta}}{q_\perp^2 + \eta q_3^2}. \quad (\text{F4})$$

Substituting Eqs. (C1) and (F4) into Eq. (F3), we obtain

$$\Sigma_C(i\omega, \mathbf{k}) = -iv(k_1\gamma_1 + k_2\gamma_2)\Sigma_{C,\perp} - iAk_3^2\gamma_3\Sigma_{C,3}, \quad (\text{F5})$$

where

$$\Sigma_{C,\perp} = \frac{\lambda^2\sqrt{\eta}}{4\pi^2} \int' dq_\perp d|q_3|q_\perp \frac{q_\perp^2}{\sqrt{v^2q_\perp^2 + A^2q_3^4}} \times \frac{1}{(q_\perp^2 + \eta q_3^2)^2}, \quad (\text{F6})$$

$$\Sigma_{C,3} = \frac{\lambda^2\eta^{\frac{3}{2}}}{4\pi^2} \int' dq_\perp d|q_3|q_\perp \frac{q_3^2(-q_\perp^2 + 3\eta q_3^2)}{\sqrt{v^2q_\perp^2 + A^2q_3^4}} \times \frac{1}{(q_\perp^2 + \eta q_3^2)^3}. \quad (\text{F7})$$

TABLE VI. $\beta_{X,Y}$ at different fixed points. The largest value at a QCP is marked by the bold style. Notice that FP1, FP2, FP3, FP4, and FP5 are QCPs.

	FP1	FP2	FP3	FP4	FP5	FP6	FP7	FP8	FP9	FP10	FP11
$\tilde{\beta}_1$	0	0	0	0	0	0	0	0	0	0	0
$\tilde{\beta}_2$	1.78199	-0.0313166	1.09642	-0.861228	-0.184302	2.03474	0.163708	-1.51656	0.0591369	0.625	-0.388772
$\tilde{\beta}_{3\perp}$	0.435705	-0.316965	-0.102003	0.344491	-0.196188	0.385057	-0.324365	0.411346	0.141049	-0.25	0.155509
$\tilde{\beta}_{3z}$	0.212338	-0.165478	-0.070994	0.344491	-0.221326	0.183119	-0.171631	0.21597	0.312383	-0.25	0.155509
$\tilde{\beta}_4$	0	0	0	0	0	0	0	0	0	0	0
$\tilde{\beta}_5$	-0.0893033	1.83099	1.09642	-0.861228	-0.184302	0.260278	1.97451	-1.51656	0.0591369	0.625	-0.388772
$\tilde{\beta}_{6\perp}$	-0.312814	0.427957	-0.102003	0.344491	-0.196188	-0.324729	0.399958	0.411346	0.141049	-0.25	0.155509
$\tilde{\beta}_{6z}$	-0.145378	0.227971	-0.0110167	-0.172246	0.14837	-0.143544	0.218875	0.185078	-0.413193	0.125	-0.0777544
$\tilde{\beta}_{7\perp}$	-0.374656	-0.375128	-0.132437	0.882843	0.495967	-0.390247	-0.383104	2.11804	0.759982	0.375	2.86716
$\tilde{\beta}_{7z}$	-0.543656	-0.556138	-0.336522	2.55509	-0.324568	-0.59561	-0.586391	2.90643	2.94818	-0.5	4.44491
$\tilde{\beta}_{8\perp}$	0.00789679	0.0395537	0.558464	0.882843	-0.0597252	0.196553	0.144978	0.652867	2.03504	0.375	2.86716
$\tilde{\beta}_{8z}$	0.0546439	0.108706	0.904558	-0.20084	0.906224	0.337352	0.26889	0.788112	0.778521	1.5	3.20084
$\tilde{\beta}_S$	-0.504013	0.968638	-0.284018	-1.17712	-0.290828	-0.580657	0.883073	-1.84727	-1.86335	-0.5	-3.82288
$\tilde{\beta}_{op}$	0.993025	-0.521206	-0.284018	-1.17712	-0.290828	0.838916	-0.565572	-1.84727	-1.86335	-0.5	-3.82288
$\tilde{\beta}_{V,1}$	0.0881294	0.110715	0.412273	-1.03347	0.503886	0.203076	0.176024	-0.940925	-0.683464	0.75	-0.466527
$\tilde{\beta}_{V,2}$	0.0881294	0.110715	0.412273	-1.03347	0.503886	0.203076	0.176024	-0.940925	-0.683464	0.75	-0.466527
$\tilde{\beta}_{V,3}$	0.16518	0.206828	0.830758	-0.861228	0.027394	0.41359	0.345578	-2.24934	0.709928	0.625	-0.388772
$\tilde{\beta}_{V,0}$	-0.0472408	-0.0484308	-0.0320743	-0.0861228	0.0953547	-0.0564411	-0.053456	0.019261	-0.141517	0.0625	-0.0388772

A constant term that does not depend on energy and momenta has been discarded.

Utilizing the transformations, Eqs. (B19)–(B21), and carrying out the integrations of E and δ within the ranges $b\Lambda < E < \Lambda$ and $0 < \delta < +\infty$, we get

$$\Sigma_{C,\perp} \approx C_1 \ell, \quad \Sigma_{C,3} = C_2 \ell, \quad (\text{F8})$$

where

$$C_1 = \frac{\lambda^2 \zeta^{\frac{3}{2}}}{8\pi^2 v} \int_0^{+\infty} d\delta \frac{1}{\sqrt{\delta(1+\delta^2)^{\frac{1}{4}}} (\zeta + \delta(1+\delta^2)^{\frac{1}{2}})^2}, \quad (\text{F9})$$

$$C_2 = \frac{\lambda^2 \zeta^{\frac{1}{2}}}{8\pi^2 v} \int_0^{+\infty} d\delta \sqrt{\delta(1+\delta^2)^{\frac{1}{4}}} \frac{(-\zeta + 3\delta(1+\delta^2)^{\frac{1}{2}})}{(\zeta + \delta(1+\delta^2)^{\frac{1}{2}})^3}, \quad (\text{F10})$$

with $\zeta = \frac{A\Lambda}{v^2\eta}$.

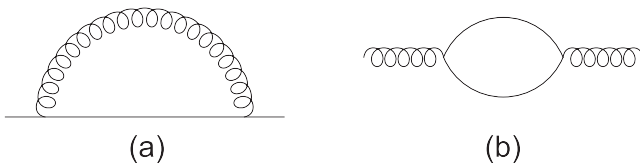


FIG. 9. (a) Feynman diagram for the self-energy of fermions induced by long-range Coulomb interaction; (b) Feynman diagram for self-energy of the boson field. The solid line represents the fermion propagator and the spiral line stands for the boson field which is equivalent to the long-range Coulomb interaction.

b. Boson self-energy

As depicted in Fig. 9(b), the boson self-energy is given by

$$\Pi(i\Omega, \mathbf{q}) = -\lambda^2 \int \frac{d\omega}{2\pi} \int' \frac{d^3\mathbf{k}}{(2\pi)^3} \text{Tr}[\gamma_0 G_0(i\omega, \mathbf{k}) \gamma_0 \times G_0(i\omega + i\Omega, \mathbf{k} + \mathbf{q})]. \quad (\text{F11})$$

Substituting Eq. (C1) into Eq. (F11) and expanding to quadratic order of Ω and q_i , we arrive at

$$\Pi(i\Omega, \mathbf{q}) = \lambda^2 v^2 q_{\perp}^2 \frac{1}{8\pi^2} \int' dk_{\perp} d|k_3| k_{\perp} \left(\frac{2}{E_{\mathbf{k}}^3} - \frac{v^2 k_{\perp}^2}{E_{\mathbf{k}}^5} \right) + \lambda^2 v^2 A^2 q_3^2 \frac{1}{\pi^2} \int' dk_{\perp} d|k_3| k_{\perp} \frac{k_3^2 k_{\perp}^2}{E_{\mathbf{k}}^5}. \quad (\text{F12})$$

Employing the transformations, Eqs. (B19)–(B21), and performing the integrations of E and δ , Π can be expressed as

$$\Pi(i\Omega, \mathbf{q}) = C_{\perp} q_{\perp}^2 \ell + C_z q_3^2 \ell, \quad (\text{F13})$$

where

$$C_{\perp} = \frac{3\lambda^2}{20\pi^2 \sqrt{A} \sqrt{\Lambda}}, \quad (\text{F14})$$

$$C_z = \frac{4\lambda^2 \sqrt{A} \Lambda^{\frac{1}{2}}}{21\pi^2 v^2}. \quad (\text{F15})$$

c. Corrections to fermion-boson coupling

As displayed in Fig. 10(a), the correction to fermion-boson coupling induced by Coulomb interaction takes the form

$$V_C^{(1)} = -i\lambda^3 \int \frac{d\Omega}{2\pi} \frac{d^3\mathbf{q}}{(2\pi)^3} \gamma_0 G_0(i\Omega, \mathbf{q}) \gamma_0 G_0(i\Omega, \mathbf{q}) \gamma_0 \times D_0(i\Omega, \mathbf{q}). \quad (\text{F16})$$

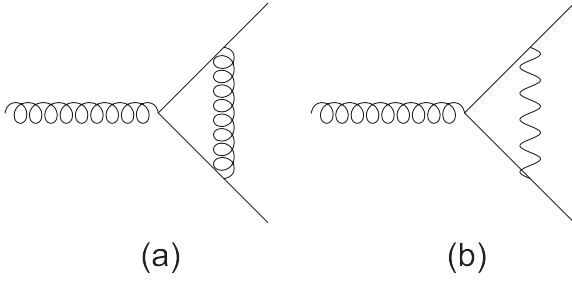


FIG. 10. Feynman diagrams for the vertex corrections to fermion-boson coupling due to (a) long-range Coulomb interaction and (b) four-fermion interaction.

Substituting Eqs. (C1) and (F4) into Eq. (F16), we find

$$V_C^{(1)} = -i\lambda^3 \gamma_0 \int' \frac{d^3 \mathbf{q}}{(2\pi)^3} \int_{-\infty}^{+\infty} \frac{d\Omega}{2\pi} \frac{-\Omega^2 + E_{\mathbf{q}}^2}{(\Omega^2 + E_{\mathbf{q}}^2)^2} \times \frac{\sqrt{\eta}}{q_{\perp}^2 + \eta q_z^2} = 0, \quad (\text{F17})$$

which means

$$\delta\lambda^{(1)} = 0. \quad (\text{F18})$$

As presented in Fig. 10(b), the correction to fermion-boson coupling generated by four-fermion interactions can be written as

$$V_C^{(2)} = i\lambda^3 \sum_{a=1,2,4,5,3z} g_a^2 \int' \frac{d\Omega}{2\pi} \frac{d^3 \mathbf{q}}{(2\pi)^3} \Gamma_a G_0(i\Omega, \mathbf{q}) \gamma_0 \times G_0(i\Omega, \mathbf{q}) \Gamma_a. \quad (\text{F19})$$

Substituting Eq. (C1) into Eq. (F19), one can obtain

$$V_C^{(2)} = i\lambda^3 \sum_{a=1,2,4,5,3z} g_a^2 \int' \frac{d^3 \mathbf{q}}{(2\pi)^3} \int_{-\infty}^{+\infty} \frac{d\Omega}{2\pi} \Gamma_a \gamma_0 \times \frac{-\Omega^2 + E_{\mathbf{q}}^2}{(\Omega^2 + E_{\mathbf{q}}^2)^2} \Gamma_a = 0. \quad (\text{F20})$$

Thus $\delta\lambda^{(2)}$ is given by

$$\delta\lambda^{(2)} = 0. \quad (\text{F21})$$

The total correction to fermion-boson coupling is

$$\delta\lambda = \delta\lambda^{(1)} + \delta\lambda^{(2)} = 0. \quad (\text{F22})$$

d. Corrections to four-fermion couplings induced by long-range Coulomb interaction

The correction from Fig. 11(a) is

$$V_a^{(5)} = 2\lambda^2 g_a (\bar{\Psi} \Gamma_a \Psi)^2 \int' \frac{d\omega}{2\pi} \frac{d^3 \mathbf{k}}{(2\pi)^3} \text{Tr}[\gamma_0 G_0(i\omega, \mathbf{k}) \Gamma_a \times G_0(i\omega + i\Omega, \mathbf{k} + \mathbf{q})] D_0(i\Omega, \mathbf{q}). \quad (\text{F23})$$

Figure 11(b) leads to the correction

$$V_a^{(6)} = -4\lambda^2 g_a (\bar{\Psi} \Gamma_a \Psi) \int' \frac{d\Omega}{2\pi} \frac{d^3 \mathbf{q}}{(2\pi)^3} [\bar{\Psi} \gamma_0 G_0(i\Omega, \mathbf{q}) \Gamma_a \times G_0(i\Omega, \mathbf{q}) \gamma_0 \Psi] D_0(i\Omega, \mathbf{q}). \quad (\text{F24})$$

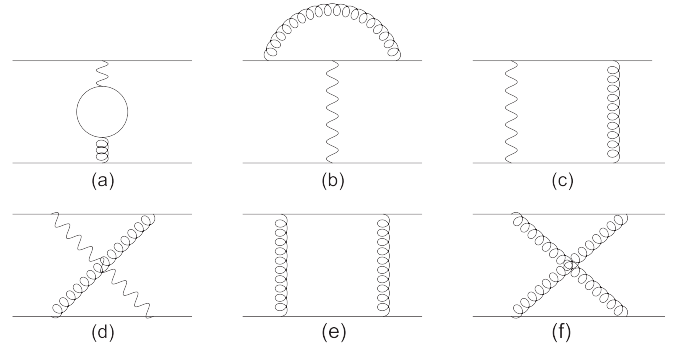


FIG. 11. Feynman diagrams for the vertex corrections to four-fermion interaction induced by long-range Coulomb interaction.

The correction from Figs. 11(c) and 11(d) takes the form

$$V_a^{(7)+(8)} = -4\lambda^2 g_a \int' \frac{d\Omega}{2\pi} \frac{d^3 \mathbf{q}}{(2\pi)^3} [\bar{\Psi} \Gamma_a G_0(i\Omega, \mathbf{q}) \gamma_0 \Psi] \times \{ \bar{\Psi} [\gamma_0 G_0(i\Omega, \mathbf{q}) \Gamma_a + \Gamma_a G_0(-i\Omega, -\mathbf{q}) \gamma_0] \Psi \} D_0(i\Omega, \mathbf{q}). \quad (\text{F25})$$

Figures 11(e) and 11(f) generate the correction

$$V_a^{(9)+(10)} = 4\lambda^4 \int' \frac{d\Omega}{2\pi} \frac{d^3 \mathbf{q}}{(2\pi)^3} [\bar{\Psi} \gamma_0 G_0(i\Omega, \mathbf{q}) \gamma_0 \Psi] \times D_0(i\Omega, \mathbf{q}) \{ \bar{\Psi} [\gamma_0 G_0(i\Omega, \mathbf{q}) \gamma_0 + \gamma_0 G_0(-i\Omega, -\mathbf{q}) \gamma_0] \Psi \} D_0(i\Omega, \mathbf{q}). \quad (\text{F26})$$

Substituting Eqs. (C1) and (F4) into Eq. (F23), we get

$$V_a^{(5)} = \delta g_a^{(5)} (\bar{\Psi} \Gamma_a \Psi)^2, \quad (\text{F27})$$

where

$$\delta g_1^{(5)} = -2g_1 \left(\sqrt{\eta} C_{\perp} + \frac{C_z}{\sqrt{\eta}} \right) \ell, \quad (\text{F28})$$

$$\delta g_2^{(5)} = 0, \quad (\text{F29})$$

$$\delta g_4^{(5)} = 0, \quad (\text{F30})$$

$$\delta g_5^{(5)} = 0, \quad (\text{F31})$$

$$\delta g_{3z}^{(5)} = 0. \quad (\text{F32})$$

Substituting Eqs. (C1) and (F4) into Eq. (F24), we arrive at

$$V_a^{(6)} = \delta g_a^{(6)} (\bar{\Psi} \Gamma_a \Psi)^2, \quad (\text{F33})$$

where

$$\delta g_1^{(6)} = 0, \quad (\text{F34})$$

$$\delta g_2^{(6)} = g_2 C_3 \ell, \quad (\text{F35})$$

$$\delta g_4^{(6)} = 0, \quad (\text{F36})$$

$$\delta g_5^{(6)} = g_5 C_3 \ell, \quad (\text{F37})$$

$$\delta g_{3z}^{(6)} = -g_{3z} C_4 \ell, \quad (\text{F38})$$

with

$$C_3 = \frac{\lambda^2 \sqrt{\zeta}}{2\pi^2 v} \int_0^{+\infty} d\delta \frac{1}{\sqrt{\delta}(1+\delta^2)^{\frac{1}{4}}} \frac{1}{\zeta + \delta(1+\delta^2)^{\frac{1}{2}}}, \quad (\text{F39})$$

$$C_4 = \frac{\lambda^2 \sqrt{\zeta}}{2\pi^2 v} \int_0^{+\infty} d\delta \frac{\delta^{\frac{3}{2}}}{(1+\delta^2)^{\frac{5}{4}}} \frac{1}{\zeta + \delta(1+\delta^2)^{\frac{1}{2}}}. \quad (\text{F40})$$

Substituting Eqs. (C1) and (F4) into Eq. (F25), $V_a^{(7)+(8)}$ can be written as

$$V_1^{(7)+(8)} = -(\bar{\Psi}i\gamma_3\Psi)^2 g_1 C_4 \ell, \quad (\text{F41})$$

$$V_2^{(7)+(8)} = \sum_{j=1}^2 (\bar{\Psi}\gamma_0\gamma_j\Psi)^2 g_2 C_5 \ell, \quad (\text{F42})$$

$$V_4^{(7)+(8)} = -(\bar{\Psi}i\gamma_5\gamma_3\Psi)^2 g_4 C_4 \ell, \quad (\text{F43})$$

$$V_5^{(7)+(8)} = -\sum_{\langle\langle lk \rangle\rangle} (\bar{\Psi}\gamma_l\gamma_k\Psi)^2 g_5 C_5 \ell, \quad (\text{F44})$$

$$V_{3z}^{(7)+(8)} = 0, \quad (\text{F45})$$

where

$$C_5 = \frac{\lambda^2 \sqrt{\zeta}}{4\pi^2 v} \int_0^{+\infty} d\delta \frac{1}{\sqrt{\delta}(1+\delta^2)^{\frac{5}{4}}} \frac{1}{\zeta + \delta(1+\delta^2)^{\frac{1}{2}}}. \quad (\text{F46})$$

Through the relations Eqs. (A37), (A38), (A41), and (A43), we obtain

$$V_1^{(7)+(8)} = [(\bar{\Psi}\gamma_0\gamma_5\Psi)^2 - (\bar{\Psi}i\gamma_5\Psi)^2 - (\bar{\Psi}\gamma_0\gamma_3\Psi)^2] g_1 C_4 \ell, \quad (\text{F47})$$

$$V_2^{(7)+(8)} = [-(\bar{\Psi}\gamma_0\Psi)^2 + (\bar{\Psi}\Psi)^2 + (\bar{\Psi}\gamma_0\gamma_5\Psi)^2 - 2(\bar{\Psi}i\gamma_5\Psi)^2 - (\bar{\Psi}\gamma_0\gamma_3\Psi)^2] g_2 C_5 \ell, \quad (\text{F48})$$

$$V_4^{(7)+(8)} = [(\bar{\Psi}\gamma_0\Psi)^2 + (\bar{\Psi}i\gamma_5\Psi)^2 + (\bar{\Psi}\gamma_0\gamma_3\Psi)^2] g_4 C_4 \ell, \quad (\text{F49})$$

$$V_5^{(7)+(8)} = [(\bar{\Psi}\gamma_0\Psi)^2 + (\bar{\Psi}\Psi)^2 - (\bar{\Psi}\gamma_0\gamma_5\Psi)^2 + (\bar{\Psi}\gamma_0\gamma_3\Psi)^2] g_5 C_5 \ell. \quad (\text{F50})$$

Thus the total correction from Figs. 11(c) and 11(d) can be expressed as

$$\begin{aligned} V^{(7)+(8)} &= \sum_{a=1,2,4,5,3z} V_a^{(7)+(8)} \\ &= \sum_{a=1,2,4,5,3z} \delta g_a^{(7)+(8)} (\bar{\Psi}\Gamma_a\Psi)^2, \end{aligned} \quad (\text{F51})$$

where

$$\delta g_1^{(7)+(8)} = (-g_2 C_5 + g_2 C_4 + g_5 C_5) \ell, \quad (\text{F52})$$

$$\delta g_2^{(7)+(8)} = (g_2 C_5 + g_5 C_5) \ell, \quad (\text{F53})$$

$$\delta g_4^{(7)+(8)} = (g_1 C_4 + g_2 C_5 - g_5 C_5) \ell, \quad (\text{F54})$$

$$\delta g_5^{(7)+(8)} = (-g_1 C_4 - 2g_2 C_5 + g_4 C_4) \ell, \quad (\text{F55})$$

$$\delta g_{3z}^{(7)+(8)} = (-g_1 C_4 - g_2 C_5 + g_4 C_4 + g_5 C_5) \ell. \quad (\text{F56})$$

Substituting Eqs. (C1) and (F4) into Eq. (F26), one can get

$$V^{(9)+(10)} = (\bar{\Psi}i\gamma_3\Psi)^2 \frac{\pi^2 v^2 A^{\frac{1}{2}}}{\Lambda^{\frac{3}{2}}} C_6 \ell, \quad (\text{F57})$$

where

$$C_6 = \frac{\lambda^4 \zeta}{2\pi^4 v^2} \int_0^{+\infty} d\delta \frac{\delta^{\frac{3}{2}}}{(1+\delta^2)^{\frac{1}{4}}} \frac{1}{[\zeta + \delta(1+\delta^2)^{\frac{1}{2}}]^2}. \quad (\text{F58})$$

Using Eq. (A43), we can get

$$\begin{aligned} V_{3z}^{(9)+(10)} &= [-(\bar{\Psi}\gamma_0\gamma_5\Psi)^2 + (\bar{\Psi}i\gamma_5\Psi)^2 \\ &\quad + (\bar{\Psi}\gamma_0\gamma_3\Psi)^2] \frac{\pi^2 v^2 A^{\frac{1}{2}}}{\Lambda^{\frac{3}{2}}} C_6 \ell. \end{aligned} \quad (\text{F59})$$

It indicates that

$$\delta g_1^{(9)+(10)} = 0, \quad (\text{F60})$$

$$\delta g_2^{(9)+(10)} = 0, \quad (\text{F61})$$

$$\delta g_4^{(9)+(10)} = -\frac{\pi^2 v^2 A^{\frac{1}{2}}}{\Lambda^{\frac{3}{2}}} C_6 \ell, \quad (\text{F62})$$

$$\delta g_5^{(9)+(10)} = \frac{\pi^2 v^2 A^{\frac{1}{2}}}{\Lambda^{\frac{3}{2}}} C_6 \ell, \quad (\text{F63})$$

$$\delta g_{3z}^{(9)+(10)} = \frac{\pi^2 v^2 A^{\frac{1}{2}}}{\Lambda^{\frac{3}{2}}} C_6 \ell. \quad (\text{F64})$$

2. RG equations

Considering the correction of interactions, the action of fermions becomes

$$\begin{aligned} S_\Psi &= \int \frac{d\omega}{2\pi} \frac{d^3\mathbf{k}}{(2\pi)^3} \bar{\Psi}(\omega, \mathbf{k}) [i\omega\gamma_0 + ivk_1\gamma_1 + ivk_2\gamma_2 \\ &\quad + iAk_3^2\gamma_3 - \Sigma_C(i\omega, \mathbf{k})] \Psi(\omega, \mathbf{k}) \\ &\approx \int \frac{d\omega}{2\pi} \frac{d^3\mathbf{k}}{(2\pi)^3} \bar{\Psi}(\omega, \mathbf{k}) (i\omega\gamma_0 + ivk_1\gamma_1 + ivk_2\gamma_2 \\ &\quad \times e^{C_1\ell} + iAk_3^2\gamma_3 e^{C_2\ell}) \Psi(\omega, \mathbf{k}). \end{aligned} \quad (\text{F65})$$

Employing the transformations, Eqs. (C68)–(C71), (C74), and

$$v = v' e^{-C_1\ell}, \quad (\text{F66})$$

$$A = A' e^{-C_2\ell}, \quad (\text{F67})$$

the action becomes

$$\begin{aligned} S_{\Psi'} &= \int \frac{d\omega'}{2\pi} \frac{d^3\mathbf{k}'}{(2\pi)^3} \bar{\Psi}'(\omega', \mathbf{k}') (i\omega'\gamma_0 + iv'k'_1\gamma_1 + iv'k'_2\gamma_2 \\ &\quad + iA'k_3'^2\gamma_3) \Psi'(\omega', \mathbf{k}'), \end{aligned} \quad (\text{F68})$$

which recovers the original form of the fermion action.

Including the correction of boson self-energy, the action of ϕ can be written as

$$\begin{aligned} S_\phi &= \int \frac{d\omega}{2\pi} \frac{d^3\mathbf{k}}{(2\pi)^3} \phi(\omega, \mathbf{k}) \left(\frac{1}{\sqrt{\eta}} k_\perp^2 + \sqrt{\eta} k_z^2 + \Pi(\mathbf{k}) \right) \phi(\omega, \mathbf{k}) \\ &\approx \int \frac{d\omega}{2\pi} \frac{d^3\mathbf{k}}{(2\pi)^3} \phi(\omega, \mathbf{k}) \left(\frac{1}{\sqrt{\eta}} k_\perp^2 e^{\sqrt{\eta} C_\perp \ell} + \sqrt{\eta} k_z^2 e^{\frac{C_z}{\sqrt{\eta}} \ell} \right) \\ &\quad \times \phi(\omega, \mathbf{k}). \end{aligned} \quad (\text{F69})$$

Utilizing the transformations, Eqs. (C68)–(C71), and

$$\phi = \phi' e^{\left(\frac{5}{2} - \frac{\sqrt{\eta}c_{\perp} + \frac{c_{\parallel}}{\sqrt{\eta}}}{4}\right)\ell}, \quad (\text{F70})$$

$$\eta = \eta' e^{\left(-1 + \sqrt{\eta}c_{\perp} - \frac{c_{\parallel}}{\sqrt{\eta}}\right)\ell}, \quad (\text{F71})$$

the action can be expressed as

$$S_{\phi'} = \int \frac{d\omega'}{2\pi} \frac{d^3\mathbf{k}'}{(2\pi^3)} \phi'(\omega', \mathbf{k}') \left(\frac{1}{\sqrt{\eta'}} k_{\perp}'^2 + \sqrt{\eta'} k_{\parallel}'^2 \right) \phi'(\omega', \mathbf{k}'), \quad (\text{F72})$$

which has the same form as the original action of boson.

Including the correction of one-loop Feynman diagrams, the action of fermion-boson couplings can be written as

$$\begin{aligned} S_{\psi\phi} &= i(\lambda + \delta\lambda) \int \frac{d\omega_1}{2\pi} \frac{d^3\mathbf{k}_1}{(2\pi^3)} \frac{d\omega_2}{2\pi} \frac{d^3\mathbf{k}_2}{(2\pi^3)} \bar{\Psi}(\omega_1, \mathbf{k}_1) \gamma_0 \\ &\quad \times \Psi(\omega_2, \mathbf{k}_2) \phi(\omega_1 - \omega_2, \mathbf{k}_1 - \mathbf{k}_2) \\ &= i\lambda \int \frac{d\omega_1}{2\pi} \frac{d^3\mathbf{k}_1}{(2\pi^3)} \frac{d\omega_2}{2\pi} \frac{d^3\mathbf{k}_2}{(2\pi^3)} \bar{\Psi}(\omega_1, \mathbf{k}_1) \gamma_0 \Psi(\omega_2, \mathbf{k}_2) \\ &\quad \times \phi(\omega_1 - \omega_2, \mathbf{k}_1 - \mathbf{k}_2), \end{aligned} \quad (\text{F73})$$

since $\delta\lambda = 0$. Employing the transformations, Eqs. (C68)–(C71), (C74), (F70), and

$$\lambda = \lambda' e^{\left(\frac{\sqrt{\eta}c_{\perp} + \frac{c_{\parallel}}{\sqrt{\eta}}}{4}\right)\ell}, \quad (\text{F74})$$

the action becomes

$$\begin{aligned} S_{\psi'\phi'} &= i\lambda' \int \frac{d\omega'_1}{2\pi} \frac{d^3\mathbf{k}'_1}{(2\pi^3)} \frac{d\omega'_2}{2\pi} \frac{d^3\mathbf{k}'_2}{(2\pi^3)} \bar{\Psi}'(\omega'_1, \mathbf{k}'_1) \gamma_0 \\ &\quad \times \Psi'(\omega'_2, \mathbf{k}'_2) \phi'(\omega'_1 - \omega'_2, \mathbf{k}'_1 - \mathbf{k}'_2), \end{aligned} \quad (\text{F75})$$

which recovers the original form of the action of fermion-boson coupling.

Including the corrections of one-loop Feynman diagrams, the action of four-fermion interaction becomes

$$\begin{aligned} S_{\Psi^4} &= \sum_{a=1,2,4,5,3z} (g_a + \delta g_a) \int \frac{d\omega_1}{2\pi} \frac{d^3\mathbf{k}_1}{(2\pi^3)} \frac{d\omega_2}{2\pi} \frac{d^3\mathbf{k}_2}{(2\pi^3)} \\ &\quad \times \frac{d\omega_3}{2\pi} \frac{d^3\mathbf{k}_3}{(2\pi^3)} \bar{\Psi}(\omega_1, \mathbf{k}_1) \Gamma_a \Psi(\omega_2, \mathbf{k}_2) \bar{\Psi}(\omega_3, \mathbf{k}_3) \Gamma_a \\ &\quad \times \Psi(\omega_1 - \omega_2 + \omega_3, \mathbf{k}_1 - \mathbf{k}_2 + \mathbf{k}_3). \end{aligned} \quad (\text{F76})$$

Using the transformations, Eqs. (C68)–(C71), (C74), and

$$g'_a = (g_a + \delta g_a) e^{-\frac{3}{2}\ell} \approx g_a - \frac{3}{2}g_a\ell + \delta g_a, \quad (\text{F77})$$

we get

$$\begin{aligned} S_{\Psi^4} &= \sum_{a=1,2,4,5,3z} g'_a \int \frac{d\omega'_1}{2\pi} \frac{d^3\mathbf{k}'_1}{(2\pi^3)} \frac{d\omega'_2}{2\pi} \frac{d^3\mathbf{k}'_2}{(2\pi^3)} \frac{d\omega'_3}{2\pi} \frac{d^3\mathbf{k}'_3}{(2\pi^3)} \\ &\quad \times \bar{\Psi}'(\omega'_1, \mathbf{k}'_1) \Gamma_a \Psi'(\omega'_2, \mathbf{k}'_2) \bar{\Psi}'(\omega'_3, \mathbf{k}'_3) \Gamma_a \\ &\quad \times \Psi'(\omega'_1 - \omega'_2 + \omega'_3, \mathbf{k}'_1 - \mathbf{k}'_2 + \mathbf{k}'_3), \end{aligned} \quad (\text{F78})$$

which recovers the original form of the action.

From the transformations as shown in Eqs. (F66), (F67), (F71), (F74), and (F77), we can get the RG equations

$$\frac{dv}{d\ell} = C_1 v, \quad (\text{F79})$$

$$\frac{dA}{d\ell} = C_2 A, \quad (\text{F80})$$

$$\frac{d\eta}{d\ell} = (1 - \beta + \gamma)\eta, \quad (\text{F81})$$

$$\frac{dg}{d\ell} = -\frac{\beta + \gamma}{4}g, \quad (\text{F82})$$

$$\frac{d\bar{A}}{d\ell} = \left(-\frac{1}{2} + \frac{1}{2}C_2 - C_1 + \frac{1}{2}\beta - \frac{1}{2}\gamma \right) \bar{A}, \quad (\text{F83})$$

$$\frac{d\alpha}{d\ell} = \left(-C_1 - \frac{1}{2}\beta - \frac{1}{2}\gamma \right) \alpha, \quad (\text{F84})$$

$$\frac{d\beta}{d\ell} = \left(\frac{1}{2} - \frac{1}{2}C_2 - \beta \right) \beta, \quad (\text{F85})$$

$$\frac{d\gamma}{d\ell} = \left(-\frac{1}{2} + \frac{1}{2}C_2 - 2C_1 - \gamma \right) \gamma, \quad (\text{F86})$$

$$\begin{aligned} \frac{dg_1}{d\ell} &= -\frac{3}{2}g_1 - \frac{2}{5}g_1 \left(g_2 + \frac{1}{2}g_4 + g_5 \right) - \frac{2}{5}(g_2g_5 \\ &\quad + g_4g_{3z} + g_5g_{3z}) - 2g_1(\beta + \gamma) + \left(-2g_1C_1 \right. \\ &\quad \left. - \frac{1}{2}g_1C_2 - g_2C_5 + g_2C_4 + g_5C_5 \right), \end{aligned} \quad (\text{F87})$$

$$\begin{aligned} \frac{dg_2}{d\ell} &= -\frac{3}{2}g_2 + g_2^2 + g_2 \left(-\frac{3}{5}g_1 + \frac{4}{5}g_4 + \frac{3}{5}g_5 + g_{3z} \right) \\ &\quad - \frac{2}{5}g_1g_5 + g_4 \left(-g_5 + \frac{7}{5}g_{3z} \right) + \frac{2}{5}g_5g_{3z} \\ &\quad + \left(-2g_2C_1 - \frac{1}{2}g_2C_2 + g_2C_3 + g_2C_5 + g_5C_5 \right), \end{aligned} \quad (\text{F88})$$

$$\begin{aligned} \frac{dg_4}{d\ell} &= -\frac{3}{2}g_4 - \frac{1}{5}g_4^2 - \frac{1}{5}(g_1^2 + g_2^2 + g_5^2 + g_{3z}^2) \\ &\quad + \frac{2}{5}g_4g_{3z} + \frac{2}{5}g_1(g_2 + g_5) + g_2 \left(-\frac{7}{5}g_5 + g_{3z} \right) \\ &\quad - \frac{1}{5}g_5g_{3z} + \left(g_1C_4 + g_2C_5 - 2g_4C_1 - \frac{1}{2}g_4C_2 \right. \\ &\quad \left. - g_5C_5 \right) - \frac{2}{5}C_6, \end{aligned} \quad (\text{F89})$$

$$\begin{aligned} \frac{dg_5}{d\ell} &= -\frac{3}{2}g_5 + \frac{6}{5}g_5^2 + \frac{1}{5}(g_1^2 + g_2^2 + g_4^2 + g_{3z}^2) \\ &\quad + g_5(-g_1 + g_2 + g_4 - g_{3z}) - \frac{2}{5}g_1 \left(2g_2 + \frac{1}{2}g_4 \right) \\ &\quad - g_2 \left(\frac{4}{5}g_4 + g_{3z} \right) - \frac{8}{5}g_4g_{3z} + \left(-g_1C_4 - 2g_2C_5 \right. \\ &\quad \left. + g_4C_4 - 2g_5C_1 - \frac{1}{2}g_5C_2 + g_5C_3 \right) + \frac{2}{5}C_6, \end{aligned} \quad (\text{F90})$$

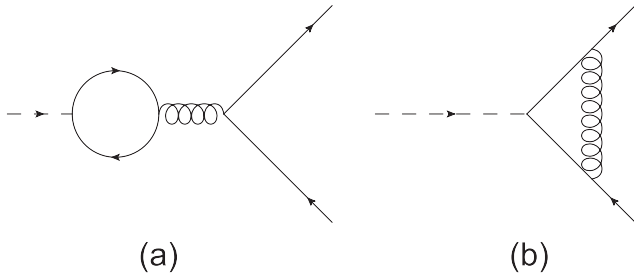


FIG. 12. One-loop Feynman diagrams for the corrections to the source terms in particle-hole channels induced by long-range Coulomb interaction.

$$\begin{aligned} \frac{dg_{3z}}{d\ell} = & -\frac{3}{2}g_{3z} + \frac{2}{5}g_{3z}^2 + \frac{1}{5}(g_1^2 + g_2^2 + g_4^2 + g_5^2) \\ & - \frac{2}{5}g_{3z}\left(\frac{1}{2}g_1 + 2g_2 + 3g_4 + \frac{3}{2}g_5\right) \\ & - \frac{2}{5}g_1\left(g_2 + \frac{1}{2}g_4 + g_5\right) + \frac{2}{5}g_2\left(\frac{1}{2}g_4 + g_5\right) \\ & + \frac{1}{5}g_4g_5 + \left(-g_1C_4 - g_2C_5 + g_4C_4 + g_5C_5\right. \\ & \left. - 2g_{3z}C_1 - \frac{1}{2}g_{3z}C_2 - g_{3z}C_4\right) + \frac{2}{5}C_6, \end{aligned} \quad (\text{F91})$$

where

$$\alpha = \frac{\lambda^2}{4\pi v}, \quad (\text{F92})$$

$$\bar{A} = \frac{\sqrt{A}\sqrt{\Lambda}}{v\sqrt{\eta}}, \quad (\text{F93})$$

$$\beta = \sqrt{\eta}C_{\perp} = \frac{3}{5\pi}\frac{\alpha}{\bar{A}}, \quad (\text{F94})$$

$$\gamma = \frac{C_z}{\sqrt{\eta}} = \frac{16}{21\pi}\alpha\bar{A}, \quad (\text{F95})$$

and redefinition

$$\frac{\Lambda^{\frac{3}{2}}g_a}{\pi^2v^2\sqrt{A}} \rightarrow g_a \quad (\text{F96})$$

has been employed.

3. Source terms

The one loop correction for the source term Δ_X in particle-hole channels induced by long-range Coulomb interaction as shown in Fig. 12(a) can be written as

$$\begin{aligned} W_{\Delta_X}^{(3)} = & 2\Delta_X\lambda^2(\bar{\Psi}\Gamma_X\Psi) \int_{-\infty}^{+\infty} d\omega \int' \frac{d^3\mathbf{k}}{(2\pi)^3} \\ & \times \text{Tr}[\Gamma_X G_0(i\omega + i\Omega, \mathbf{k} + \mathbf{q})\gamma_0 G_0(i\omega, \mathbf{k})] \\ & \times D_0(i\Omega, \mathbf{q}). \end{aligned} \quad (\text{F97})$$

In particle-hole channels, the one-loop correction for the source term Δ_X from Fig. 12(b) is given by

$$\begin{aligned} W_{\Delta_X}^{(4)} = & -2\Delta_X\lambda^2 \int_{-\infty}^{+\infty} \frac{d\Omega}{2\pi} \int' \frac{d^3\mathbf{q}}{(2\pi)^3} [\bar{\Psi}\gamma_0 G_0(i\Omega, \mathbf{q})\Gamma_X \\ & \times G_0(i\Omega, \mathbf{q})\gamma_0\Psi] D_0(i\Omega, \mathbf{q}). \end{aligned} \quad (\text{F98})$$

It should be noted that long-range Coulomb interaction does not induce correction for the source terms in particle-particle channels.

Calculating the corrections for source terms in particle-hole channels induced by long-range Coulomb interaction through Eqs. (F97) and (F98), and rederiving the RG equations for Δ_X , we finally obtain

$$\bar{\beta}_{\Delta_1} = -2(\beta + \gamma), \quad (\text{F99})$$

$$\bar{\beta}_{\Delta_2} = \frac{1}{2}(-g_1 + 3g_2 + g_4 + g_5 + g_{3z}) + \frac{1}{2}C_3, \quad (\text{F100})$$

$$\bar{\beta}_{\Delta_{3\perp}} = \frac{1}{5}(-g_1 + g_2 + g_4 - g_5 + g_{3z}) + \frac{1}{2}C_5, \quad (\text{F101})$$

$$\bar{\beta}_{\Delta_{3z}} = \frac{1}{10}(-g_1 + g_2 + g_4 - g_5 + 3g_{3z}) + \frac{1}{2}C_4, \quad (\text{F102})$$

$$\bar{\beta}_{\Delta_4} = 0, \quad (\text{F103})$$

$$\bar{\beta}_{\Delta_5} = \frac{1}{2}(-g_1 + g_2 + g_4 + 3g_5 - g_{3z}) + \frac{1}{2}C_3, \quad (\text{F104})$$

$$\bar{\beta}_{\Delta_{6\perp}} = \frac{1}{5}(-g_1 - g_2 + g_4 + g_5 - g_{3z}) + \frac{1}{2}C_5\ell, \quad (\text{F105})$$

$$\bar{\beta}_{\Delta_{6z}} = \frac{1}{10}(-g_1 - g_2 + g_4 + g_5 + g_{3z}) + \frac{1}{2}C_4\ell, \quad (\text{F106})$$

$$\bar{\beta}_{\Delta_{7\perp}} = \frac{3}{10}(-g_1 - g_2 - g_4 - g_5 + g_{3z}) + \frac{1}{2}(C_4 + C_5), \quad (\text{F107})$$

$$\bar{\beta}_{\Delta_{7z}} = \frac{2}{5}(-g_1 - g_2 - g_4 - g_5 - g_{3z}) + C_5, \quad (\text{F108})$$

$$\bar{\beta}_{\Delta_{8\perp}} = \frac{3}{10}(-g_1 + g_2 - g_4 + g_5 - g_{3z}) + \frac{1}{2}(C_4 + C_5), \quad (\text{F109})$$

$$\bar{\beta}_{\Delta_{8z}} = \frac{2}{5}(-g_1 + g_2 - g_4 + g_5 + g_{3z}) + C_5, \quad (\text{F110})$$

where β and γ are given by Eqs. (F94) and (F95) and C_3 , C_4 , and C_5 are given by Eqs. (F39), (F40), and (F46), respectively. The RG equations for source terms in particle-particle channels are still given by Eqs. (D69)–(D74).

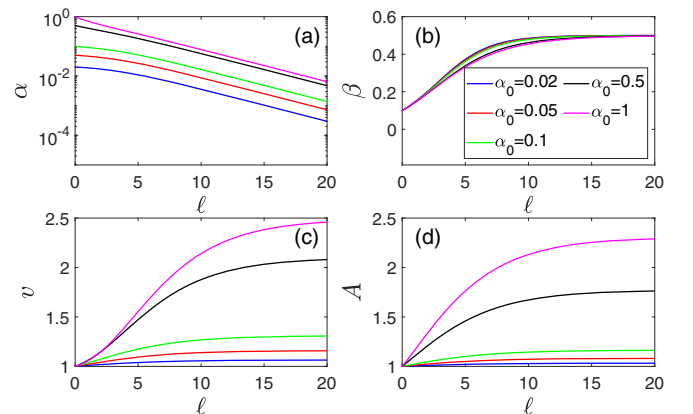


FIG. 13. Flows of α , β , v , and A with different initial values of Coulomb strength α_0 : 0.02 (blue), 0.05 (red), 0.1 (green), 0.5 (black), and 1.0 (magenta). $\beta_0 = 0.1$ is taken.

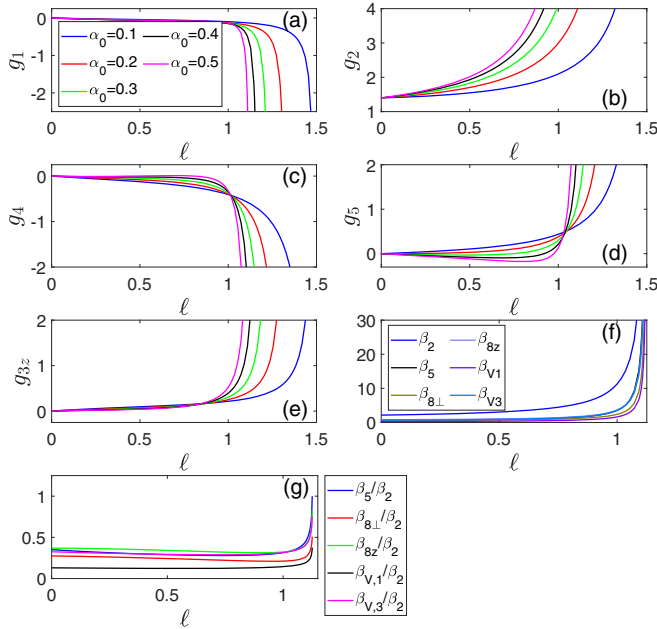


FIG. 14. Flows of g_1 , g_2 , g_4 , g_5 , and g_{3z} are shown in (a)–(e) with different values of Coulomb strength α_0 : 0.1 (blue), 0.2 (red), 0.3 (green), 0.4 (black), and 0.5 (magenta). (f),(g) Flows of $\tilde{\beta}_{X,Y}$ which approach positive infinity and ratios between $\tilde{\beta}_{X,Y}$. In (a)–(g) $g_{1,0} = 0$, $g_{2,0} = 1.4$, $g_{4,0} = 0$, $g_{5,0} = 0$, $g_{3z,0} = 0$, and $\beta_0 = 0.1$ are taken. $\alpha_0 = 0.5$ is taken in (f) and (g).

4. Numerical results

The flows of α , β , v , and A are shown in Figs. 13(a)–13(d), respectively. We can find that α approaches zero quickly in the lowest energy limit. It represents that long-range Coulomb interaction becomes irrelevant in the lowest energy regime. As shown in Fig. 13(b), $\beta \rightarrow \frac{1}{2}$, which indicates the anisotropic screening of Coulomb interaction. According to Figs. 13(c) and 13(d), v and A approach constant values in the lowest energy limit. Thus the fermion dispersion is not changed qualitatively by long-range Coulomb interaction.

According to Fig. 14, the four-fermion interactions become divergent more quickly with the increase of the initial

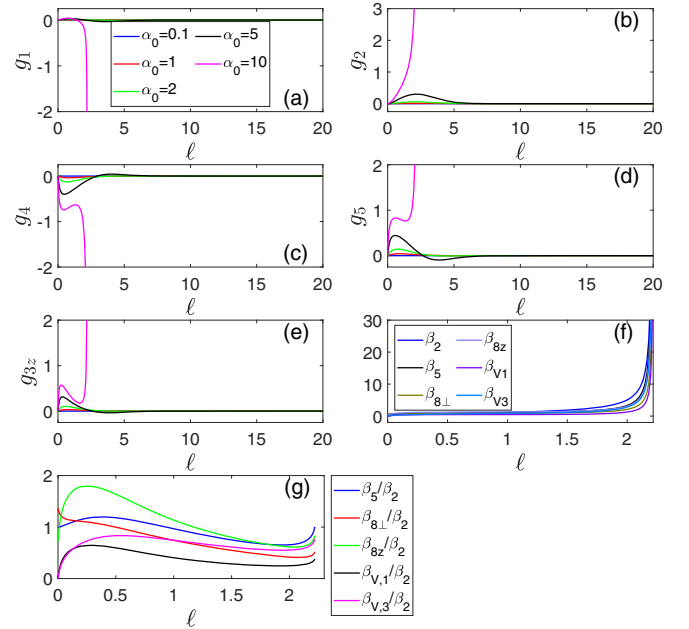


FIG. 15. Flows of g_1 , g_2 , g_4 , g_5 , and g_{3z} are shown in (a)–(e) with different initial values of Coulomb strength α_0 : 0.1 (blue), 1 (red), 2 (green), 5 (black), and 10 (magenta). (f),(g) Flows of $\tilde{\beta}_{X,Y}$ which approach positive infinity and ratios between $\tilde{\beta}_{X,Y}$. In (a)–(g) $g_{1,0} = 0$, $g_{2,0} = 0$, $g_{4,0} = 0$, $g_{5,0} = 0$, $g_{3z,0} = 0$, and $\beta_0 = 0.1$ are taken. $\alpha_0 = 10$ is taken in (f) and (g).

value of Coulomb strength. This result reveals that the long-range Coulomb interaction can enhance the instabilities in particle-hole channels, although it becomes irrelevant in the low energy regime. As shown in Figs. 15(a)–15(e), if the initial value of the Coulomb strength is large enough, we can find that, even if the initial values of the four-fermion interactions all vanish, the four-fermion interactions can be generated and become divergent finally at a finite energy scale. According to Figs. 15(f) and 15(g), the axionic insulating phase is generated if the initial value of Coulomb interaction is strong enough.

- [1] O. Vafek and A. Vishwanath, Dirac fermions in solids: From high- T_c cuprates and graphene to topological insulators and Weyl semimetals, *Annu. Rev. Condens. Matter Phys.* **5**, 83 (2014).
- [2] T. O. Wehling, A. M. Black-Schaffer, and A. V. Balatsky, Dirac materials, *Adv. Phys.* **63**, 1 (2014).
- [3] B. Yan and C. Felser, Topological materials: Weyl semimetals, *Annu. Rev. Condens. Matter Phys.* **8**, 337 (2017).
- [4] M. Z. Hasan, S.-Y. Xu, I. Belopolski, and S.-M. Huang, Discovery of Weyl fermion semimetals and topological Fermi arc states, *Annu. Rev. Condens. Matter Phys.* **8**, 289 (2017).
- [5] N. P. Armitage, E. J. Mele, and A. Vishwanath, Weyl and Dirac semimetals in three-dimensional solids, *Rev. Mod. Phys.* **90**, 015001 (2018).
- [6] J. Kruthoff, J. de Boer, J. van Wezel, C. L. Kane, and R.-J. Slager, Topological Classification of Crystalline Insulators through Band Structure Combinatorics, *Phys. Rev. X* **7**, 041069 (2017).
- [7] F. Tang, H. C. Po, A. Vishwanath, and X. Wan, Comprehensive search for topological materials using symmetry indicators, *Nature (London)* **566**, 486 (2019).
- [8] T. Zhang, Y. Jiang, Z. Song, H. Huang, Y. He, Z. Fang, H. Weng, and C. Fang, Catalogue of topological electronic materials, *Nature (London)* **566**, 475 (2019).
- [9] M. G. Vergniory, L. Elcoro, C. Felser, N. Regnault, B. A. Bernevig, and Z. Wang, A complete catalogue of high-quality topological materials, *Nature (London)* **566**, 480 (2019).
- [10] B. Lv, T. Qian, and H. Ding, Angle-resolved photoemission spectroscopy and its application to topological materials, *Nat. Rev. Phys.* **1**, 609 (2019).
- [11] G. Xu, H. Weng, Z. Wang, X. Dai, and Z. Fang, Chern Semimetal and the Quantized Anomalous Hall Effect in HgCr_2Se_4 , *Phys. Rev. Lett.* **107**, 186806 (2011).
- [12] C. Fang, M. J. Gilbert, X. Dai, and B. A. Bernevig, Multi-Weyl Topological Semimetals Stabilized by Point Group Symmetry, *Phys. Rev. Lett.* **108**, 266802 (2012).

- [13] P. Dietl, F. Piéchon, and G. Montambaux, New Magnetic Field Dependence of Landau Levels in a Graphenelike Structure, *Phys. Rev. Lett.* **100**, 236405 (2008).
- [14] B.-J. Yang and N. Nagaosa, Classification of stable three-dimensional Dirac semimetals with nontrivial topology, *Nat. Commun.* **5**, 4898 (2014).
- [15] B. Bradlyn, J. Cano, Z. Wang, M. G. Vergniory, R. J. Cava, and B. A. Bernevig, Beyond Dirac and Weyl fermions: Unconventional quasiparticles in conventional crystals, *Science* **353**, aaf5037 (2016).
- [16] P. Tang, Q. Zhou, and S.-C. Zhang, Multiple Types of Topological Fermions in Transition Metal Silicides, *Phys. Rev. Lett.* **119**, 206402 (2017).
- [17] T. Zhang, Z. Song, A. Alexandradinata, H. Weng, C. Fang, L. Lu, and Z. Fang, Double-Weyl Phonons in Transition-Metal Monosilicides, *Phys. Rev. Lett.* **120**, 016401 (2018).
- [18] D. Takane, Z. Wang, S. Souma, K. Nakayama, T. Nakamura, H. Oinuma, Y. Nakata, H. Iwasawa, C. Cacho, T. Kim, K. Horiba, H. Kumigashira, T. Takahashi, Y. Ando, and T. Sato, Observation of Chiral Fermions with a Large Topological Charge and Associated Fermi-Arc Surface States in CoSi, *Phys. Rev. Lett.* **122**, 076402 (2019).
- [19] Z. Rao, H. Li, T. Zhang, S. Tian, C. Li, B. Fu, C. Tang, L. Wang, Z. Li, W. Fan, J. Li, Y. Huang, Z. Liu, Y. Long, C. Fang, H. Weng, Y. Shi, H. Lei, Y. Sun, T. Qian *et al.*, Observation of unconventional chiral fermions with long Fermi arcs in CoSi, *Nature (London)* **567**, 496 (2019).
- [20] D. S. Sanchez, I. Belopolski, T. A. Cochran, X. Xu, J.-X. Yin, G. Chang, W. Xie, K. Manna, V. Süß, C.-Y. Huang, N. Alidoust, D. Multer, S. S. Zhang, N. Shumiya, X. Wang, G.-Q. Wang, T.-R. Chang, C. Felser, S.-Y. Xu, S. Jia, H. Lin, and M. Z. Hasan, Topological chiral crystals with helicoid-arc quantum states, *Nature (London)* **567**, 500 (2019).
- [21] N. B. M. Schröter, D. Pei, M. G. Vergniory, Y. Sun, K. Manna, F. de Juan, J. A. Krieger, V. Süß, M. Schmidt, P. Dudin, B. Bradlyn, T. K. Kim, T. Schmitt, C. Cacho, C. Felser, V. N. Strocov, and Y. Chen, Chiral topological semimetal with multifold band crossings and long Fermi arcs, *Nat. Phys.* **15**, 759 (2019).
- [22] N. B. M. Schröter, S. Stolz, K. Manna, F. de Juan, M. G. Vergniory, J. A. Krieger, D. Pei, T. Schmitt, P. Dudin, T. K. Kim, C. Cacho, B. Bradlyn, H. Borrmann, M. Schmidt, R. Widmer, V. N. Strocov, and C. Felser, Observation and control of maximal Chern numbers in a chiral topological semimetal, *Science* **369**, 179 (2020).
- [23] V. N. Kotov, B. Uchoa, V. M. Pereira, F. Guinea, and A. H. Castro Neto, Electron-electron interactions in graphene: Current status and perspectives, *Rev. Mod. Phys.* **84**, 1067 (2012).
- [24] J.-R. Wang and G.-Z. Liu, Absence of dynamical gap generation in suspended graphene, *New J. Phys.* **14**, 043036 (2012).
- [25] J. Hofmann, E. Barnes, and S. Das Sarma, Why Does Graphene Behave as a Weakly Interacting System?, *Phys. Rev. Lett.* **113**, 105502 (2014).
- [26] P. Goswami and S. Chakravarty, Quantum Criticality between Topological and Band Insulators in 3+1 Dimensions, *Phys. Rev. Lett.* **107**, 196803 (2011).
- [27] P. Hosur, S. A. Parameswaran, and A. Vishwanath, Charge Transport in Weyl Semimetals, *Phys. Rev. Lett.* **108**, 046602 (2012).
- [28] H.-K. Tang, J. N. Leaw, J. N. B. Rodrigues, I. F. Herbut, P. Sengupta, F. F. Assaad, and S. Adam, The role of electron-electron interactions in two-dimensional Dirac fermions, *Science* **361**, 570 (2018).
- [29] J. N. Leaw, H.-K. Tang, M. Trushin, F. F. Assaad, and S. Adam, Universal Fermi-surface anisotropy renormalization for interacting Dirac fermions with long-range interactions, *Proc. Natl. Acad. Sci. USA* **116**, 26431 (2019).
- [30] I. F. Herbut, Interactions and Phase Transitions on Graphene's Honeycomb Lattice, *Phys. Rev. Lett.* **97**, 146401 (2006).
- [31] I. F. Herbut, V. Juričić, and B. Roy, Theory of interacting electrons on the honeycomb lattice, *Phys. Rev. B* **79**, 085116 (2009).
- [32] J. Maciejko and R. Nandkishore, Weyl semimetals with short-range interactions, *Phys. Rev. B* **90**, 035126 (2014).
- [33] B. Roy and S. Das Sarma, Quantum phases of interacting electrons in three-dimensional dirty Dirac semimetals, *Phys. Rev. B* **94**, 115137 (2016).
- [34] A. L. Szabó and B. Roy, Emergent chiral symmetry in a three-dimensional interacting Dirac liquid, *J. High Energy Phys.* **01** (2021) 004.
- [35] E.-G. Moon, C. Xu, Y. B. Kim, and L. Balents, Non-Fermi-Liquid and Topological States with Strong Spin-Orbit Coupling, *Phys. Rev. Lett.* **111**, 206401 (2013).
- [36] I. F. Herbut and L. Janssen, Topological Mott Insulator in Three-Dimensional Systems with Quadratic Band Touching, *Phys. Rev. Lett.* **113**, 106401 (2014).
- [37] B.-J. Yang, E.-G. Moon, H. Isobe, and N. Nagaosa, Quantum criticality of topological phase transitions in three-dimensional interacting electronic systems, *Nat. Phys.* **10**, 774 (2014).
- [38] A. A. Abrikosov, Gapless state of bismuth-type semimetals, *J. Low. Temp. Phys.* **8**, 315 (1972).
- [39] H. Isobe, B.-J. Yang, A. Chubukov, J. Schmalian, and N. Nagaosa, Emergent Non-Fermi-Liquid at the Quantum Critical Point of a Topological Phase Transition in Two Dimensions, *Phys. Rev. Lett.* **116**, 076803 (2016).
- [40] G. Y. Cho and E.-G. Moon, Novel quantum criticality in two dimensional topological phase transitions, *Sci. Rep.* **6**, 19198 (2016).
- [41] J.-R. Wang, G.-Z. Liu, and C.-J. Zhang, Excitonic pairing and insulating transition in two-dimensional semi-Dirac semimetals, *Phys. Rev. B* **95**, 075129 (2017).
- [42] H.-H. Lai, Correlation effects in double-Weyl semimetals, *Phys. Rev. B* **91**, 235131 (2015).
- [43] S.-K. Jian and H. Yao, Correlated double-Weyl semimetals with Coulomb interactions: Possible applications to HgCr₂Se₄ and SrSi₂, *Phys. Rev. B* **92**, 045121 (2015).
- [44] J.-R. Wang, G.-Z. Liu, and C.-J. Zhang, Quantum phase transition and unusual critical behavior in multi-Weyl semimetals, *Phys. Rev. B* **96**, 165142 (2017).
- [45] S.-X. Zhang, S.-K. Jian, and H. Yao, Correlated triple-Weyl semimetals with Coulomb interactions, *Phys. Rev. B* **96**, 241111(R) (2017).
- [46] J.-R. Wang, G.-Z. Liu, and C.-J. Zhang, Breakdown of Fermi liquid theory in topological multi-Weyl semimetals, *Phys. Rev. B* **98**, 205113 (2018).
- [47] J.-R. Wang, G.-Z. Liu, and C.-J. Zhang, Topological quantum critical point in a triple-Weyl semimetal: Non-Fermi-liquid behavior and instabilities, *Phys. Rev. B* **99**, 195119 (2019).

- [48] S. Han, C. Lee, E.-G. Moon, and H. Min, Emergent Anisotropic Non-Fermi Liquid at a Topological Phase Transition in Three Dimensions, *Phys. Rev. Lett.* **122**, 187601 (2019).
- [49] S.-X. Zhang, S.-K. Jian, and H. Yao, Quantum criticality preempted by nematicity, *Phys. Rev. B* **103**, 165129 (2021).
- [50] B. Roy, M. P. Kennett, K. Yang, and V. Juričić, From Birefringent Electrons to a Marginal or Non-Fermi Liquid of Relativistic Spin-1/2 Fermions: An Emergent Superuniversality, *Phys. Rev. Lett.* **121**, 157602 (2018).
- [51] V. N. Kotov, B. Uchoa, and O. P. Sushov, Coulomb interactions and renormalization of semi-Dirac fermions near a topological Lifshitz transition, *Phys. Rev. B* **103**, 045403 (2021).
- [52] O. Vafek, Interacting fermions on the honeycomb bilayer: From weak to strong coupling, *Phys. Rev. B* **82**, 205106 (2010).
- [53] B. Roy, P. Goswami, and V. Juričić, Interacting Weyl fermions: Phases, phase transitions, and global phase diagram, *Phys. Rev. B* **95**, 201102(R) (2017).
- [54] B. Roy and M. S. Foster, Quantum Multicriticality near the Dirac-Semimetal to Band-Insulator Critical Point in Two Dimensions: A Controlled Ascent from One Dimension, *Phys. Rev. X* **8**, 011049 (2018).
- [55] J. Wang, Role of four-fermion interaction and impurity in the states of two-dimensional semi-Dirac materials, *J. Phys.: Condens. Matter* **30**, 125401 (2018).
- [56] A. L. Szabó, R. Moessner, and B. Roy, Interacting spin-3/2 fermions in a Luttinger (semi)metal: Competing phases and their selection in the global phase diagram, *Phys. Rev. B* **103**, 165139 (2021).
- [57] I. Boettcher, Interplay of Topology and Electron-Electron Interactions in Rarita-Schwinger-Weyl Semimetals, *Phys. Rev. Lett.* **124**, 127602 (2020).
- [58] L. Savary, E.-G. Moon, and L. Balents, New Type of Quantum Criticality in the Pyrochlore Iridates, *Phys. Rev. X* **4**, 041027 (2014).
- [59] M. D. Uryszek, E. Christou, A. Jaefari, F. Krüger, and B. Uchoa, Quantum criticality of semi-Dirac fermions in $2 + 1$ dimensions, *Phys. Rev. B* **100**, 155101 (2019).
- [60] S. Sur and B. Roy, Unifying Interacting Nodal Semimetals: A New Route to Strong Coupling, *Phys. Rev. Lett.* **123**, 207601 (2019).
- [61] M. D. Uryszek, F. Krüger, and E. Christou, Fermionic criticality of anisotropic nodal point semimetals away from the upper critical dimension: Exact exponents to leading order in $\frac{1}{N_f}$, *Phys. Rev. Res.* **2**, 043265 (2020).
- [62] R. Shankar, Renormalization-group approach to interacting fermions, *Rev. Mod. Phys.* **66**, 129 (1994).
- [63] X. Yuan, C. Zhang, Y. Liu, A. Narayan, C. Song, S. Shen, X. Sui, J. Xu, H. Yu, Z. An, J. Zhao, S. Sanvito, H. Yan, and F. Xiu, Observation of quasi-two-dimensional Dirac fermions in ZrTe₅, *NPG Asia Mater.* **8**, e325 (2016).
- [64] J. L. Zhang, C. Y. Guo, X. D. Zhu, L. Ma, G. L. Zheng, Y. Q. Wang, L. Pi, Y. Chen, H. Q. Yuan, and M. L. Tian, Disruption of the Accidental Dirac Semimetal State in ZrTe₅ under Hydrostatic Pressure, *Phys. Rev. Lett.* **118**, 206601 (2017).
- [65] E. Martino, I. Crassee, G. Eguchi, D. Santos-Cottin, R. D. Zhong, G. D. Gu, H. Berger, Z. Rukelj, M. Orlita, C. C. Homes, and A. Akrap, Two-Dimensional Conical Dispersion in ZrTe₅ Evidenced by Optical Spectroscopy, *Phys. Rev. Lett.* **122**, 217402 (2019).
- [66] D. Santos-Cottin, M. Padleski, E. Martino, S. Ben David, F. Le Mardelé, F. Capitani, F. Borondics, M. D. Bachmann, C. Putzke, P. J. W. Moll, R. D. Zhong, G. D. Gu, H. Berger, M. Orlita, C. C. Homes, Z. Rukelj, and A. Akrap, Probing intraband excitations in ZrTe₅: A high-pressure infrared and transport study, *Phys. Rev. B* **101**, 125205 (2020).
- [67] C. Zhang, J. Sun, F. Liu, A. Narayan, N. Li, X. Yuan, Y. Liu, J. Dai, Y. Long, Y. Uwatoko, J. Shen, S. Sanvito, W. Yang, J. Cheng, and F. Xiu, Evidence for pressure-induced node-pair annihilation in Cd₃As₂, *Phys. Rev. B* **96**, 155205 (2017).
- [68] N. Mohanta, J. M. Ok, J. Zhang, H. Miao, E. Dagotto, H. N. Lee, and S. Okamoto, Semi-Dirac and Weyl fermions in transition metal oxides, *Phys. Rev. B* **104**, 235121 (2021).